Mathematical models of RNA interference in plants

Giannis Neofytou

Thesis submitted for the degree of Doctor of Philosophy

August 2016

Declaration

I hereby declare that this thesis has not been and will not be submitted in whole or in part to another University for the award of any other degree.

Signature:

Giannis Neofytou

Dedication

To my family, who have always stood by my side and supported me.

Acknowledgements

First, I would like to express my sincere gratitude to my supervisors Dr. Konstantin Blyuss and Dr. Yuliya Kyrychko for their continuous support of my Ph.D study and related research, for their unrelenting patience and inspiration, as well as being a continuous source of motivation and knowledge that kept me pushing forward with my work

Also, I am indebted to my current and former postgraduate colleagues: Muhammad Abdullahi Yau, Andy Chung, Konstantinos Blazakis, Nima Sharoozi, Rahman Bootan, Martin Richie, Kiresh Parmar, Christof Heuer, Gary Pool, Philip Townsend and Erin Pichanick for their useful comments and friendship.

Finally, I would like to thank my family, especially my parents and siblings for providing me with all the support I needed.

Abstract

RNA interference (RNAi), or *Post-Transcriptional Gene Silencing* (PTGS), is a biological process which uses small RNAs to regulate gene expression on a cellular level, typically by causing the destruction of specific mRNA molecules. This biological pathway is found in both plants and animals, and can be used as an effective strategy in defending cells against parasitic nucleotide sequences, viruses and transposons. In the case of plants, it also constitutes a major component of the adaptive immune system. RNAi is characterised by the ability to induce sequence-specific degradation of target messenger RNA (mRNAs) and methylation of target gene sequences. The small interfering RNA produced within the initiated cell is not only used locally but can also be transported into neighbouring cells, thus acting as a mobile warning signal.

In the first part of the thesis I develop and analyse a new mathematical model of the plant immune response to a viral infection, with particular emphasis on the role of RNA interference. The model explicitly includes two different time delays, one to represent the maturation period of undifferentiated cells, and another to account for the time required for the RNAi propagating signal to reach other parts of the plant, resulting in either recovery or warning of susceptible cells. Analytical and numerical bifurcation theory is used to identify

parameter regions associated with recovery and resistant plant phenotypes, as well as possible chronic infections. The analysis shows that the maturation time plays an important role in determining the dynamics, and that long-term host recovery does not depend on the speed of the warning signal but rather on the strength of local recovery. At best, the warning signal can amplify and hasten recovery, but by itself it is not competent at eradicating the infection.

In the second part of the thesis I derive and analyse a new mathematical model of plant viral co-infection with particular account for RNA-mediated cross-protection in a single plant host. The model exhibits four non-trivial steady states, i.e. a disease-free steady state, two one-virus endemic equilibria, and a co-infected steady state. I obtained the basic reproduction number for each of the two viral strains and performed extensive numerical bifurcation analysis to investigate the stability of all steady states and identified parameter regions where the system exhibits synergistic or antagonistic interactions between viral strains, as well as different types of host recovery. The results indicate that the propagating component of RNA interference plays a significant role in determining whether both viruses can persist simultaneously, and as such, it controls whether the plant is able to support some constant level of both infections. If the two viruses are sufficiently immunologically related, the least harmful of the two viruses becomes dominant, and the plant experiences cross-protection.

In the third part of the thesis I investigate the properties of intracellular dynamics of RNA interference and its capacity as a gene regulator by extending a well known model of RNA interference with time delays. For each of the two amplification pathways of the model, I consider the cumulative effects of delay

in dsRNA-primed synthesis associated with the non-instantaneous nature of chemical signals and component transportation delay. An extensive bifurcation analysis is performed to demonstrate the significance of different parameters, and to investigate how time delays can affect the bi-stable regime in the model.

Contents

List of Tables

List of Figures

Notations and basic definitions

Anti-sense transcript: single-stranded RNA that is complementary to an mRNA strand transcribed within a cell.

Bistability: In a dynamical system, bistability means the system has two stable equilibrium states.

DNA: Deoxyribonucleic acid.

Cross-reactive: reaction between two different species or molecules as opposed to the self-reactivity.

dsRNA: Double-stranded RNA.

Eukaryote: an organism with a complex cell or cells, in which the genetic material is organized into a membrane-bound nucleus or nuclei.

Encapsidation: the process where the genome of a virus in encased in a rigid protein shell during viral assembly.

Garbage RNA: Abberant RNA that has lost its regular function.

Gene Expression: the process by which information from a gene is used in the synthesis of a functional gene product.

Hypersensitive Response: a mechanism, used by plants, to prevent the spread of infection by microbial pathogens and is characterized by the rapid death of cells in the local region surrounding an infection.

Immunological relation between viruses signifies the relationship and the degree of similarity or association between the host's immune response for each virus. In the context of this thesis, viruses that are immunologically related either share similar genetic traits or are perceived by the plant immune system in such a way that they trigger a similar immune response. In this case, both viral infections are affected whereas, immunologically unrelated means the opposite.

Inverted-repeat: a sequence of nucleotides followed downstream by its reverse complement.

Leukocytic defence: immune defence mediated by white blood cells.

Methylation: a form of alkylation in which methyl groups are added to DNA segments.

mRNA: messenger RNA, a large family of RNA molecules that convey genetic information from DNA to the protein synthesizers of a cell.

nt: nucleotide, the basic structural unit and building block for DNA and RNA.

Phenotype: the set of observable characteristics of an individual resulting from the interaction of its genotype with the environment.

RdRP: RNA-dependent RNA polymerase, an enzyme that catalyzes the replication of RNA from an RNA template.

RISC: RNA-induced silencing complex, specialized compound that can degrade target RNAs.

RNA: Ribonucleic Acid.

RNAi: RNA interference, a biological process in which RNA molecules inhibit gene expression.

Systemic: something that is spread throughout, system-wide, affecting a group or system.

Transcription: the first step of gene expression, in which a particular segment of DNA is copied into RNA (especially mRNA) by the enzyme RNA polymerase.

Transposon: DNA sequence that can change its position within a genome, sometimes creating or reversing mutations and altering the cell's genome size.

Viral Coat-protein: proteins used in forming the shell of a virus.

Chapter 1

Introduction

An *RNA interference* (RNAi) type phenomenon was first reported by Napoli and Jorgensen in 1990 [**Nap90**]. By introducing a chimeric transgene in petunias, they hoped that the intentional over-expression of the enzyme responsible for the violet pigmentation, would generate flowers of a violet colour. However, to their surprise, this resulted in producing flowers with white pigmentation instead. To account for this, it was hypothesized that the introduced transgene was instead "cossupressin" the corresponding endogenous gene. A similar phenomenon was later observed by Romano and Macino in 1992 when studying a type of bread mold [**Rom92**], and it was first documented in animals by Guo and Kempheus who worked with the nematode (roundworm) *C.elegans* [**Guo95**].

Elucidation of the RNAi mechanism did not occur until in 1998 [**Fir98**], when it was hailed as one of the greatest scientific breakthroughs since the discovery of the double-helix structure of DNA in the 1950s. As an incredibly powerful molecular tool, the discovery was awarded with a Nobel prize and consequently inspired a new area of research that had a profound effect on

our ability to develop treatments and control strategies against a variety of diseases for both animals and plants. This is, of course, a matter of the utmost importance for a number of reasons.

With a projected number of 9.7 billion people by the year 2050, the world population is rapidly growing to a size that cannot be easily sustained by existing agricultural methods. Human societies are heavily dependent on a steady agricultural output in order to provide a sustainable food source, as well as various forms of renewable fuel such as ethanol and biodiesel. In light of the agricultural stagnation experienced in the last decade, further fuelled by the public opposition to controversial newer practices [**Kun14**], securing an adequate and reliable food source has never been more relevant.

Despite the technological advances of the last century, it is estimated that up to 40% of the global crop production is still lost due to pathogens, animals and weeds [**Sav12**]. The necessity to minimize these losses, while also maximizing production, has long been an important task. As such, the fight for efficiency has been shaping the way we view and practise farming most likely since our species first successfully domesticated a variety of crops, an event known as the Neolithic revolution which paved the way for creating the first human settlements and thus defined world history. This inevitably led to the development of different agricultural practices throughout the centuries and gave birth to more contemporary methods including the use of various pesticides, and ultimately genetic engineering. It would, therefore, seem logical that successfully eliminating the problem of food supply could be one of the requirements for the next step of human advancement and development. Although significant efforts are constantly made to secure and increase crop production, usually with

a good degree of success, perhaps, a more effective or environmentally safe way to address this problem lies in better investigating and understanding some of the current methods. In this respect, mathematical modelling can provide invaluable insights into the dynamics of plant infections and, to some extent, be either a viable alternative, or contribute to the original laboratory work, as the latter might sometimes suffer from prohibitive costs and other limitations. As such, a mathematical approach is useful in establishing practical and theoretical frameworks in which both existing and experimental strategies can be safely and efficiently evaluated.

Unlike the mammalian immune system, a plant does not possess any type of specialized mobile cells with the ability to protect against infectious diseases or foreign invaders. Therefore, in the absence of a leukocytic defence, it has to rely solely on the cellular innate immunity to deal with possible infections. Moreover, the plant immune system also exhibits many plant-specific characteristics [**Jon06**], which arguably makes any attempts to derive complete mathematical models, able to account for the perceived variety of immune response among different species, a seemingly unrealistic task.

However, one can generally separate how plants respond to disease into three distinct phenotypes. The distinction is simply based on the plant's disease resistance which is usually pathogen-specific and describes the reduction of pathogen growth once the host has been infected, namely susceptible, resistant and a type of recovery phenotype. Susceptible plants, as the name suggests, offer little to no resistance to a particular disease and are often completely overwhelmed to the point where severe host damage is observed, which sometimes can even lead to death. On the other hand, resistant plants, are able to prevent the systemic

spread of a disease by successfully isolating the infection to the initiating sites at an early stage. Since this strategy dramatically reduces the growth of the pathogen, resistant plants are usually able to make a rapid recovery and experience minimal to no damage. The plants showing a recovery phenotype, for example, to a specific viral infection, initially become affected but later experience new growth that is progressively more resistant to the virus until they finally produce new virus-free leaves with complete immunity. In addition to these three categories, plants can be further separated into disease-tolerant or disease-intolerant types of host. For the former of these two, despite experiencing substantial pathogen levels, the plant will only exhibit minuscule damage compared to the latter type with no tolerance. An example of the resistant phenotype starts with the plant going into hypersensitive resistance, triggering the self-destruction of infected cells, with necrotic tissue forming at and around the infection site. The cells surrounding these necrotic lesions are usually found in an antiviral (resistant) state. Although some of them may contain traces of the virus, the virus is unable to replicate [**Ger06**, **Fri07**]. This can be explained by a phenomenon previously known as *post-transcriptional gene silencing* (PTGS), or using a more contemporary and widely used term, RNA interference.

Another reason for the significance of RNA interference, as a complex biological mechanism that occurs naturally in many eukaryotes, lies in its regulatory role within each individual cell [**Wat99**, **Esc00**, **Vau01**, **Wat01**]. This process follows a number of different steps while at the same time enabling some level of cooperation between affected cells. As such, it allows control over gene expression while also providing an effective immune response against viruses (virus-induced gene silencing) and tranposons through its ability to induce sequence-

specific degradation of target messenger RNAs (mRNAs) and methylation of target gene sequences perceived to be harmful or undesired by the immune system. Therefore, taking advantage of this mechanism, one can, therefore, induce an artificial response by introducing specific therapeutic molecules into targeted cells to trigger the process. Consequently, RNAi can be used for gene therapy whereby undesired or harmful genes can, with astonishing accuracy, be targeted and essentially deactivated through the same natural mechanism.

It has been demonstrated that RNAi is mediated by long, perfect or imperfect double-stranded RNAs (dsRNA) produced from either an inverted-repeat transgene or a replicating virus. The core pathway can be described as follows, When the viral or transgenic dsRNA is injected into the cell, it is targeted by up to four different dicer-like enzymes (DLC), which divide it into short 21-26 nucleotide (nt) long molecules. These molecules, known as small or short interfering RNAs (siRNA), are used as the building blocks for assembling a special protein complex called RNA-induced-silencing complex (RISC). This specialized compound can recognise and degrade RNAs containing complementary sequences to the short RNAs forming its structure. The degraded RNA pieces, labelled as garbage RNA, can no longer be translated into functioning proteins, which leads to the translational arrest of the viral or transgenic RNA. [**Esc00**, **Elb01**]. In the case of viruses, the process can prohibit viral replication within the host cell and thus prevent the infection from spreading to other cells [**Cos13**, **Ham00**, **Ber01b**], whereas in the case of transgenic dsRNA, it can be used to silence the expression of corresponding genes. While the core pathway might be sufficient to describe RNA interference in mammals, for other organisms it is possible that the process is not strictly limited to the siRNA at the initiating

site but can spread systemically [**Pal97**, **Mel11**, **Zha12b**].

In a study of RNA interference in the nematode *Caenorhabditis elegans*, it was observed that a notable proportion of the produced siRNA was not derived directly from the initializing dsRNA, suggesting the presence of a mechanism in which some additional dsRNA can be generated [**Sij01**]. To account for this discovery, a primed and an unprimed amplification pathway were proposed in which an RNA-dependent RNA polymerase (RdRp) or RNA replicase could synthesize the additional dsRNA [**Lip01**, **Mak02**]. In the case of primed amplification it is postulated that when assisted by RdRp, the siRNA that binds on mRNA can itself initialize dsRNA synthesis, thus, generating a new round of dsRNAs ready to be used in the process. On the other hand, unprimed amplification describes the situation where dsRNA synthesis occurs without the assistance of the primer RdRp, but instead relies on the presence of garbage RNA to facilitate synthesis.

As in most complex biological processes, RNA interference carries risks and is prone to different errors, as it relies on the host's ability to correctly discriminate between endogenous and exogenous mRNA [**Gio02**]. Thus, any invading viral sequences with cross-reactive similarities or the host's accidental production of anti-sense transcripts corresponding to self genes can result in a self-reactive response that can be extremely damaging to the host. To limit the self-damage caused by the feed-forward amplification in RNA interference, a protection mechanism has been proposed in [**Pak12**].

Another important aspect of plant immunology concerns the interactions that occur between different viruses and their hosts. According to the principle of competitive exclusion, two species occupying the same niche cannot

co-exist indefinitely but may, however, co-exist if they occupy sufficiently different niches. Hence, species whose life cycles take place at different periods of time and at host locations that are mutually exclusive with each other, or even require distinct host resources, can lead to sufficient biological and epidemiological differences that result in the species co-existence and have significant implications for viral evolution [**Fit06**]. A good example lies in the tomato yellow leaf curl virus outbreak in 1997, when it was observed that two different isolates of the virus had successfully spread in the main tomato-growing regions in Spain and could co-exist. What was even more astonishing was that this disease could also be transmitted to the common bean, and that one of the viral isolates was the causal factor of the newly emerged bean leaf crumple disease [**Cas99**]. Mixed infections are indeed common and are, in fact, a prerequisite for viral recombination to occur; the genetic exchange and re-assortment of viral genomic segments can lead to the creation of new species or strains that are better adapted to the host and, therefore, represent a natural evolutionary pathway [**Gar06**].

One very efficient way of protecting a plant against a disease can be found in the phenomenon of *cross-protection*, and describes the process by which prior infection of the plant with a primary virus can prevent or interfere with the subsequent infection with a secondary virus of the same family [**Zho12**]. In such a case, deliberately infecting the plant with a less virulent strain can offer partial or full protection against a much more virulent isolate of the virus. Although this natural phenomenon was first demonstrated more than 80 years ago, its precise mechanisms are still not fully understood, and several hypotheses have been put forward to explain how cross-protection works [**Pen01**]. It has been

suggested that the primary infection can trigger the formation of specific antibodies which prevent the subsequent infection by a similar virus. Another possibility is the coat-protein mediated resistance that is usually demonstrated by transgenic plants encoding viral coat-proteins. However, in the case of competing viral strains, the coat protein of the primary strain can also interfere with the encapsidation process of the secondary strain, thus rendering it ineffective for a cell-to-cell transmission [**Bea99**, **Ben97**]. Additionally, if the two viruses are closely related, they can very well be competing for the same components which are essential for viral replication, or that the occupation of replication sites by the primary strain could cause a spatial exclusion of the secondary strain [**Lee05**, **Tak04**, **Gal06**].

A very promising explanation of cross-protection can be found in the RNAi pathway [**Rat99**]. It is very important to note that in addition to the amplification pathways discussed earlier, the secondary generation of siRNA derived during the amplification process, can also be transported into neighbouring cells, thus acting as a mobile warning signal. This warning signal spreads systemically in a way that resembles the movement of viral particles, and can potentially fortify and prepare other cells by enabling them to express the antiviral components even before they become infected [**Zha12a**, **Was00**, **Zha12b**].

The ability to induce a propagating warning signal can most likely be attributed to the evolutionary race between the plant and the viruses that afflict them, as it has been demonstrated that viruses can suppress different stages of the RNA-interference pathway [**Cos13**, **Pum13**, **Raj08**]. In some cases the virus can prevent degradation of its genome by either suppressing cellular innate immune response or by simply managing to successfully spread before

being detected. The latter can be achieved by moving into another cell before a specific threshold of viral dsRNA has accumulated, which is necessary to initiate a cellular response. In other cases, the virus can only suppress the propagating warning signal, therefore, depending on which component of the immune response is targeted by viral suppressors, one can expect a different phenotype of recovery.

It is important to note that in the studies of plant pathology, single-host interactions between different viruses are highly important, as they can often produce distinct types of host immune response. Therefore, while some viral pairs are able to facilitate each other and engage in a synergistic relationship, others will compete with each other for dominance [**Mal09**, **Weg07**, **Pru97**]. Contrary to cross-protection, enhanced symptom display occurs when plants co-infected with two or more viral strains exhibit symptoms that are more severe when compared to the single-strain infections and this is often accompanied by an elevated viral load for one or multiple viruses. Therefore, depending on the level of competition between the viruses and the corresponding immune response, a different degree of cross-protection or cross-enhancement can be observed.

It is quite unlikely that any synergistic or antagonistic outcome of a viral co-infection in a single host, associated with cross-protection or enhanced symptom display, can be fully explained by one single mechanism. This is due to the wide variety of plants with an immune system that, as mentioned earlier, is highly specific to the plant, and the fact that different viruses can often produce unique patterns of interactions [**Gal06**, **Roo05**, **Tak05**, **Ber14**]. However, if one takes different hypotheses into consideration, depending on the sequence homology of

the two viruses and their specificity, one of them could inadvertently trigger an immune response or establish a set of host conditions that could either prevent the secondary infection from taking place or allow it to manifest more aggressively [**Mal09**, **Red12**].

1.1 Literature review

From a mathematical perspective, significant efforts have been made at qualitative and quantitative analysis of plant disease dynamics, including the environmental impact and its effects on the global yield of crops. Jeger *et al.* [**Jeg04**] give an overview of some of the quantitative approaches employed in plant virus epidemiology throughout the 20th century. Many mathematical models have focused on the spread of infection by considering populations of healthy and infected plants, with disease transmission occurring through some intermediary. Since disease propagation in plants is mainly carried out by insect vectors [**Pur05**], many of these models incorporate a vector population either explicitly or through empirically derived relationships between the two populations, done in a manner that is easily comparable to epidemic models of mosquito-borne diseases in humans [**Pur05**]. Other models have investigated the effects of traditional disease controls, such as roguing and replanting, where any plants carrying a disease are simply removed and replaced with healthy new plants [**Cha94**, **Van96**, **Zha12a**]. Due to the significant role played by vectors in plant disease transmission, some work has been done on the analysis of various behavioural aspects, vector aggregation, and the existence of helper viruses that mediate viral transmission [**Zha00a**, **Zha00b**].

In the 1970s, the increase of computing power allowed the development of models capable of simulating vector population under the consideration of weather variables [**Gut74**, **Fra77**, **Kir78**, **Irw00**]. Despite their simple structure, these models enabled the integration of various disease control options, thus creating a framework where such methods could be analysed and evaluated. Madden *et al.* [**Mad00**] have performed a detailed analysis of the transitional dynamics of plant diseases taking into account the effects of vector emigration. Depending on the way they are transmitted, plant viruses are classified as non-persistent, semi-persistent and persistent, and Madden *et al.* [**Mad00**] demonstrated which of these three classes were more susceptible to changes in vector longevity and inoculation, acquisition rates and vector mobility. Subsequent models have looked into the transmission dynamics of a pair of "helper" and helper-dependent viruses. Zhang *et al.* [**Zha00b**] provided insights into the commonly observed phenomenon where infecting a host with only a helper virus would cause minimal or no damage to the host, whereas, additionally introducing the helper-dependent virus would produce far more devastating symptoms.

In the last few decades it was discovered that viruses employ a wide antigenic diversity as an effective strategy to survive within the host population [**Fra02**, **Lip07**]. By employing a variety of antigenically distinct strains, viruses are able to adapt sufficiently fast to evade the host's immune system. Antigenic variation is known to be effective for a large number of pathogens affecting humans, including malaria [**Gup94**, **Fer04**], meningitis [**Gup96**, **Gup99**], dengue fever [**Gog02**], and influenza [**Fer03**]. The interactions between multiple strains are generally classified as either an ecological interference, or an immunological

interference. The first type of interactions describes a simple case where individual hosts can only be infected with a single strain, and are subsequently removed from the population susceptible to other strains [**Lev04**]. Immunological interference corresponds to situations where infection with one strain may cause partial or full immunity to the remaining strains [**Gup99**], or sometimes it can even augment the susceptibility of the host and the transmissibility of other strains [**Rec09**].

To better understand the dynamics of multi-strain diseases, a large number of mathematical models have been developed that can be divided into individual-based and equation-based models. In individual-based models, all pathogen strains are treated as individuals interacting according to a fixed set of rules [**Fer03**, **Buc04**, **Buc10**, **Cis04**], whereas in equation-based models, hosts are categorised either according to preceding exposure to individual strains [**And97**, **Gom02**], or based on their immunity to specific strains [**Gog02**, **Kry07**].

A number of mathematical models have considered different aspects of RNAi in its roles of immune guard against viral infections, as well as an attractive tool for targeted gene silencing that is important for gene therapies. One of the earliest models was developed and analysed by Bergstrom *et al.* [**Ber03**]. The

basic model takes the following form

$$\begin{aligned}
\dot{D}(t) &= -aD(t) + gC(t), \\
\dot{R}(t) &= anD(t) - d_R R(t) - bR(t)M(t), \\
\dot{C}(t) &= bR(t)M(t) - (g + d_C)C(t), \\
\dot{M}(t) &= h - d_M M(t) - bR(t)M(t),
\end{aligned} \tag{1.1}$$

where $D(t),\ R(t),\ C(t),\ M(t)$ denote the concentrations of dsRNA, the RNA-induced silencing complex (RISC), the RISC-mRNA complex, and mRNA at time t, respectively. The presence of dsRNA initializes the RNAi mechanism with the Dicer enzyme cleaving the available dsRNA at the rate a into n short fragments which form the RISC complex. The RISC modules bind at targeted mRNA at rate b to form the complex $C(t)$, and naturally degrade at the average rate d_R. The RISC-mRNA complex $C(t)$ is then consumed during dsRNA synthesis at the rate gC to produce 1 dsRNA per complex, and naturally degrades at the rate d_C. There is a constant production of mRNA given by h with some background loss modelled by the non-specific degradation term $d_M M$.

The authors focused on the issue of avoiding self-directed gene silencing during RNAi and hypothesised that this can be achieved via *unidirectional amplification*, whereby silencing only persists in the presence of a continuing input of dsRNA, thus acting as a safeguard against a sustained self-damaging reaction, or, in the case of viral infection, ending the process once the infection is cleared. This was achieved by introducing some additional assumptions and modifying the basic model (1.1). Suppose that each targeted dsRNA is cleaved

into n siRNA pieces labelled $1, 2, ...n$, respectively. Then, the secondary generation of siRNA produced through primed amplification can only occur for segments upstream of the original siRNA primer, meaning that if dsRNA synthesis is primed by the kth siRNA fragment, the new dsRNA to be produced will only be carrying the $1, 2, ...k$ segments. Thus, although the silencing reaction can initially take off and be rapidly amplified, the unidirectional nature of the amplification process will, given enough time, affect the distribution of the siRNA population. In the absence of a continuing dsRNA input, the population of siRNA will eventually be mainly composed of upstream siRNAs unable to prime further RNA polymerization, and the silencing reaction will subsequently stop. Based on these new assumptions, the model takes the following form.

$$\dot{D}_i(t) = -aD_i(t) + gC_i(t),$$

$$\dot{R}_i(t) = a\sum_{j=1}^{n} nD(t) - d_R R_i(t) - bR_i(t)M(t),$$

$$\dot{C}_i(t) = bR_i(t)M(t) - (g + d_C)C_i(t),$$

$$\dot{M}(t) = h - d_M M(t) - b\sum_{j=1}^{n} R_j(t)M(t).$$

This is a system of $3n+1$ differential equations where D_k represents the dsRNA containing the $1, 2, ...k$ segments, and $C_i(t),\ R_i(t)$ carry the ith siRNA primer.

Another RNAi model was developed by Groenenboom *et al.* [**Gro05**], who analysed primed and unprimed amplification pathways to account for the dsRNA dosage-dependence of RNAi and to correctly describe the nature of

transient and sustained silencing. Groenenboom and Hogeweg [**Gro08b**] and Rodrigo *et al.* [**Rod11**] have analysed how viral replication is affected by its interactions with RNAi for plus-stranded RNA viruses, with particular account for different viral strategies for evading host immune response. Due to the non-instantaneous nature of the complex processes involved in RNA interference, it is biologically feasible to explicitly include time delays associated with the times required for transport of RNAi components, and assembly of different complexes. Nikolov and Petrov [**Nik07**] and Nikolov *et al.* [**Nik09**] have considered the effects of such time delays within a single amplification pathway as modelled by Bergstrom *et al.* [**Ber03**].

In the context of siRNA-based treatment, Bartlett and Davis [**Bar06**] have performed a detailed analysis of the process of siRNA delivery and its interaction with the RNAi machinery in mammalian cells, and compared it to experimental results in mural cell cultures. This model and associated experiments have provided significant insights into optimising the dosage and scheduling of the therapeutic siRNA-mediated gene silencing. Raab and Stephanopoulos [**Raa04**] also considered siRNA dynamics in mammalian cells with an emphasis on two-gene systems with different kinetics for the two genes. Arciero *et al.* [**Arc04**] studied a model of siRNA-based tumour treatment which targets the expression of TGF-β, thus reducing tumour growth and enhancing immune response against tumour cells.

Since originally RNA interference was discovered in plants [**Nap90**], which present a very convenient framework for experimental studies of RNAi, a number of mathematical models have considered specific aspects of the dynamics of viral growth and its interactions with RNAi in plants. Groenenboom and

Hogeweg [**Gro08a**] have analysed a detailed model for the dynamics of intra- and inter-cellular RNA silencing and viral growth in plants. This spatial model has demonstrated different kinds of infection patterns that can occur on plant leaves during viral infections.

1.1.1 Epidemic models

The earliest example of applying mathematical modelling to describe the dynamics of communicable diseases can be traced back to the 18th century and a member of the famous Bernoulli family [**Het00**]. As a prominent mathematician, who had also trained in medicine, Daniel Bernoulli, was able to develop a mathematical model to describe the transmission dynamics of the smallpox disease under the practise of inoculation. This historical method relied on the introduction of smallpox pustules into the skin of healthy people to induce artificial immunity, and would generally produce less severe symptoms than naturally-acquired smallpox. By using this model, he was able to show that deliberately inoculating a sufficient majority of the population, the universal life expectancy at the time could be increased by approximately 12%. Thus, despite the lack of a sufficient and accurate knowledge of germ theory, the results could still offer a very practical manner in which the smallpox disease could be controlled. According to the predominant theory of disease transmission at the time, it was believed that diseases were spread through a miasma, a form of poisonous air. This was only replaced by the modern understanding of germ theory in the last decade of the 19th century, followed by the discovery of the vector-transmission nature of the malarial parasite which eventually paved the way for modern theoretical epidemiology.

One of the earliest and most significant achievements of mathematical epidemiology was the formulation of the SIR model by Kermack and McKendrick in 1927 [**Ker27**]. The model, despite its simplicity, could be applied to numerous types of epidemics and could successfully predict the temporal dynamics of infectious diseases that typically invade the population suddenly, intensify and finally disappear with a proportion of the population left unaffected by the disease. As such, the SIR model laid the foundation for a whole family of epidemic models that include increasingly more complicated interactions and more realistic assumptions. The classical model compartmentalizes the population into three classes labelled S, I and R, where $S(t)$ denotes the number of susceptible individuals that have never been infected at time t, $I(t)$ is the number of infected who spread the disease to susceptible targets and $R(t)$ is the removed class, which represents the people that carry a zero risk of either transmitting or acquiring the disease (these would normally be recovered or removed/dead individuals). The SIR model can be written as follows

$$\begin{aligned} \frac{dS}{dt} &= -a\frac{S}{N}I, \\ \frac{dI}{dt} &= a\frac{S}{N}I - \alpha I, \\ \frac{dR}{dt} &= \alpha I, \end{aligned} \tag{1.2}$$

where a is the mass-action incidence rate, i.e the average number of individuals receiving the disease from an infected person per unit time, and S/N is the probability of an infected person making contact with someone of the susceptible class. Parameter α is the rate at which infected individuals are naturally cleared

of the disease. One of the key assumptions of this model, is that the population is closed and, no disease-associated deaths or new births are considered. With these assumptions, the total population, $N = S(t) + I(t) + R(t)$, is constant, however, one should note that this assumption is only justifiable when the time scale of the disease is sufficiently smaller than the time scales at which these effects take place. In some cases, this is a rather unrealistic assumption, as endemic diseases are known to cause millions of deaths around the world, and longer time-scales are crucial in understanding the long-term effects of an epidemic. As a first step in addressing this issue, the classical SIR model can be extended to include both birth and death rates [**Bra12**]. Suppose that the average person in the population gives birth to b susceptible individuals per unit time and that the disease is not transmitted vertically. Assume, for simplicity, that no disease-associated deaths are possible but all three classes experience the average death rate μ. By denoting $\beta = \dfrac{a}{N}$ we have the SIR model with vital dynamics

$$\begin{aligned} \frac{dS}{dt} &= bN - \beta SI - \mu S, \\ \frac{dI}{dt} &= \beta SI - (\alpha + \mu)I, \\ \frac{dR}{dt} &= \alpha I - \mu R. \end{aligned} \tag{1.3}$$

Since $dN/dt = (b - \mu)N$, the population size can again be made constant if the mortality rate is chosen to be equal to the birth rate, which itself represents a rather special case. Although this modified model also suffers from some obvi-

ous limitations, it can, nevertheless, provide an example in which slightly more complicated dynamics can be observed. Another efficient way of increasing the accuracy of the model is by including additional categories of individuals for certain epidemics. For example, in specific types of infections, newborns might have immunity to certain diseases offered by antibodies directly acquired from the placenta during pregnancy and the subsequent breast-feeding. However, this protections usually lasts only for the first few months after birth, hence the children of parents who have been previously exposed and recovered from the infection, might not be born into the susceptible compartment but can only acquire the disease after their immunity has expired. To account for this phenomenon, a maternally-derived immunity class can be added to the original model to create what is known as the MSIR model [**Het00**]. Other examples include infectious diseases where complete recovery is not always possible; although an infected individual might not exhibit any visible symptoms, they could be still spreading the disease. As such, it sometimes becomes necessary to complement the model with an additional carrier class $C(t)$, which gives the SIRC model. Similarly, other diseases might require a significant incubation period that is intrinsically large relative to the time-scale of the model. Therefore it often becomes important to not only consider the infectious population but also an exposed class containing the individuals who carry the disease but are not currently infectious [**Kee08**, **Bra12**].

Consequently, numerous different extensions of the SIR model, highlight its flexibility and make this framework a vital approach for deriving mathematical models of epidemics which is important for the research presented in this thesis.

1.1.2 Hopf Bifurcation

The term Hopf bifurcation, also known as a Poincaré–Andronov–Hopf bifurcation, is used to describe the local birth or death of a periodic solution from an equilibrium point as a parameter crosses a critical value. Considering a dynamical system a Hopf bifurcation typically occurs when a complex conjugate pair of eigenvalues of the linearised flow at a fixed point becomes purely imaginary. As such, it is obvious that a Hopf bifurcation can only occur in systems of dimension two or higher. Under reasonably generic assumptions about the dynamical system, it gives birth to a small-amplitude limit cycle that branches from the fixed point. If the real parts of the eigenvalues are negative, the fixed point is a stable focus; when they cross zero and become positive the fixed point becomes an unstable focus, with the solution orbits spiralling out. However, this change of stability is only a local change and the geometric representation of the trajectories of the dynamical system in the phase plane that are sufficiently far from the fixed point will be qualitatively unaffected: if the nonlinearity makes the far flow contracting then orbits will still be coming in and we expect a periodic orbit to appear where a balance between the near and far flow is achieved. The two-dimensional version of the Hopf bifurcation theorem was suggested by Poincaré [**Poi92**] in the early 1890s and was known to Andronov [**And66**] and his associates since the 1930s' whereas a version for arbitrary dimensions was later proved by Hopf [**Hop42**] in 1942.

Theorem 1.1.1 (Hopf bifurcation)**.** *Consider the dynamical system*

$$\begin{aligned} \dot{x} &= f_\mu(x, y), \\ \dot{y} &= g_\mu(x, y), \end{aligned} \tag{1.4}$$

where μ is a parameter. Suppose that the system has a fixed point $(x, y) = (x_0, y_0)$, which may or not depend on μ and let the eigenvalues of the linearised system about this point be described by $\lambda_{1,2} = a(\mu) \pm ib(\mu)$. Further suppose that given a critical value of $\mu = \mu_0$, the following conditions are satisfied:

- *Non-hyperbolicity condition*
  $a(\mu_0) = 0$, $b(\mu_0) = w \neq 0$, *where* $sgn(w) = sgn\left[\left(\dfrac{\partial g_\mu}{\partial x}\right)\Big|_{\mu=\mu_0}(x_0, y_0)\right]$.
- *Transversality condition*
  $\dfrac{da(\mu)}{d\mu}\Big|_{\mu=\mu_0} = d \neq 0.$
- *Genericity condition*
  $p = \dfrac{1}{16}(f_{xxx} + f_{xyy} + g_{xxy} + g_{yyy}) + \dfrac{1}{16w}[f_{xy}(f_{xx} + f_{yy}) - g_{xy}(g_{xx} + g_{yy}) - f_{xx}g_{xx} + f_{yy}g_{yy}]$, *where for example,* $f_{xy} = (\partial^2 f_\mu / \partial x \partial y)|_{\mu=\mu_0}(x_0, y_0)$.

Then, a unique curve of periodic solutions bifurcates from the fixed point (x_0, y_0) into the region $\mu > \mu_0$ and $\mu < \mu_0$ when $pd < 0$ and $pd > 0$ respectively. The fixed point is stable for $\mu > \mu_0$ ($\mu < \mu_0$) and unstable for $\mu < \mu_0$ ($\mu > \mu_0$) if $d < 0$ ($d > 0$) whereas the periodic solutions are stable (unstable) if the fixed point is unstable (stable) on the split side of $\mu = \mu_0$ where the periodic solutions exist.

The amplitude of the periodic orbit grows like $\sqrt{|\mu - \mu_0|}$ whilst their periods will approach $2\pi/|w|$ for $\mu \to \mu_0$. If the bifurcating periodic solutions are stable

(unstable) the bifurcation is called supercritical (subcritical).

1.1.3 Delay differential equations

Similarly to natural or artificial control systems, biological systems, have intrinsic delays that arise from delays in the sensory process of response-initiating variables, the transportation of components that regulate biological interactions, after-effect phenomena in inner dynamics and metabolic functions including the times necessary for synthesis, maturation and reproduction [**Ric03**, **Jus10**]. These delays can often lead to changes in stability and are fundamental in modelling control systems which typically involve a feedback loop. On the other hand, mathematical models without time-delays are based on the assumption that the transmission of signals and biological processes occur instantaneously. Although the time-scale of these delays can sometimes be ignored, e.g when the time-scale of the model is very large compared to the observed delays, there are clear cases where the present and future state of a system depend on its past history. These systems can therefore, only be accurately described with Delay Differential Equations (DDE) rather than the traditional Ordinary Differential Equations (ODE).

The significance of time delays in dynamical systems is a relatively new discovery and was first observed in 1942 by Minorsky in his theoretical analysis of a newly-proposed PID controller used in the automatic steering systems of U.S Navy ships [**Min42**]. Although the U.S Navy did not ultimately adopt the new system, his results had profound implications for the theory of differential equation and generated a significant interest in this research field.

Unlike ODEs with a finite dimensional state vector, i.e where the system

state can be specified by listing a finite set of values, delay differential equations are infinite-dimensional. It is therefore, no surprise that the mathematical analysis of such models is more challenging. This is further complicated by the many different types of delay-differential equations like state-dependent delays or distributed delays, which often require a different type of methodology. However, for the purposes of this thesis, the focus will be on systems with discrete delays. Given a set of constant delays $\tau_i \geq 0$ for all $i = 1, 2, ..., n$, one can write the following DDE

$$\dot{x} = f(x(t), x(t-\tau_1), x(t-\tau_2), ..., x(t-\tau_n)). \tag{1.5}$$

For finite-dimensional systems like ODEs, the initial conditions are simply the initial values of the state variables at a prescribed time. Assuming that the system begins its dynamics at $t = t_0$, and since delay-differential equations depend on past history, it is imperative to specify an initial function x_{t_0} containing the system values prior to the initiating time point, i.e the function $x(t)$ needs to be defined on the interval $[t_0 - \tau_{max}, t_0]$, where t_{max} is the largest delay.

Similarly to ODE systems, linear stability analysis is an essential tool for understanding the dynamics. As a first step we find the different equilibrium points of the system and then study their stability by looking at the behaviour of small perturbations $\delta x(t)$. For convenience of notation, let us denote $x_{\tau_i} = x(t - \tau_i)$. Like for ODEs, an equilibrium point of a DDE is a solution which remains constant for any time. Suppose that equation (1.5) has an equilibrium x^*. Let use perturb the system from this equilibrium by introducing the small perturbation $\delta x(t)$, i.e consider the perturbed point $x(t) = x^* + \delta x(t)$. Note that this perturbation will last from $t = t_0 - \tau_{max}$ to t_0. Thus, equation (1.5)

becomes

$$\dot{x} = \dot{\delta x} = f(x^* + \delta x, x^* + \delta x_{\tau_1}, x^* + \delta x_{\tau_2}, ..., x^* + \delta x_{\tau_n}).$$

Using the Taylor series expansion, one can linearise the differential equation about the equilibrium point to obtain

$$\dot{\delta x} \approx J_0 \delta x + J_{\tau_1} \delta x_{\tau_1} + J_{\tau_2} \delta x_{\tau_2} + ... + J_{\tau_n} \delta x_{\tau_n}, \tag{1.6}$$

where J_0 is the standard Jacobian with respect to $x(t)$, and J_{τ_i} are the Jacobian matrices with respect to each $x(t-\tau_i)$, respectively, evaluated at the equilibrium point x^*. Suppose that similarly to ODEs, linear DDEs also have exponential solutions determined by the eigenvalues of the Jacobian matrix. By substituting the solution $\delta x(t) = Ae^{\mu t}$ into (1.6) and using basic linear algebraic theory, we obtain the characteristic equation of the equilibrium point

$$\left| J_0 + e^{-\mu\tau_1} J_{\tau_1} + e^{-\mu\tau_2} J_{\tau_2} + ... + e^{-\mu\tau_n} J_{\tau_n} - \mu I \right| = 0, \tag{1.7}$$

where I is the identity matrix. Expanding the determinant, one can see that due to the transcendental nature of the exponential terms inside the expression, the characteristic polynomial is not algebraic but in fact a quasi-polynomial. For example, a system with n delays and a degree k, will have its characteristic roots determined by the following equation

$$\begin{aligned} &\mu^k + p_{k-1}(e^{-\mu\tau_1}, ..., e^{-\mu\tau_n})\mu^{k-1} + ... + p_1(e^{-\mu\tau_1}, ..., e^{-\mu\tau_n})\mu + \\ &p_0(e^{-\mu\tau_1}, ..., e^{-\mu\tau_n}) = 0, \end{aligned} \tag{1.8}$$

where $p_0, ..., p_{k-1}$, are polynomials in $e^{-\mu\tau_1}, ..., e^{-\mu\tau_n}$. To give an example with a single time delay present, we show the characteristic equation (2.25) found in Chapter 2:

$$\begin{aligned} &\mu^3 + \left[a_1(\tau_1)e^{-\mu\tau_1} + a_2(\tau_1)\right]\mu^2 + \left[b_1(\tau_1)e^{-\mu\tau_1} + b_2(\tau_1)\right]\mu + \\ &c_1(\tau_1)e^{-\mu\tau_1} + c_2(\tau_1) = 0, \end{aligned} \tag{1.9}$$

Hence, if any of the characteristic roots have a positive real part, it follows that the equilibrium point is unstable, and it is only stable if all the real parts are negative. If one of these roots is zero, then stability cannot be determined normally, as it represents the degenerate case, where, depending on the signs of the remaining roots, the solution may converge to or diverge from a line of equilibria rather than a unique point. For ODEs, the number of complex roots is always equal to the degree of the characteristic polynomial and therefore can be obtained with relative ease. However, for DDEs it becomes apparent that, as there are infinitely many complex values satisfying the transcendental equation in (1.8) [**Nor73**], standard spectral analysis is not feasible. Rather than trying to find an infinite number of characteristic roots one can look at how these roots may be distributed over the complex plane. In fact, one can show that there exists only a finite number of roots that lie to the right of any vertical line $x = c,\ c \in \Re$ in the complex plane. It is therefore, important to introduce the following result given by [**Dri77**].

Theorem 1.1.2 (The number of roots of the transcendental equation (1.8) that lie to the right of any vertical line in the complex plane is finite)**.** *For any $p \in \mathbb{R}$, the characteristic equation (1.8) has at most a finite number of roots μ such that $Re(\mu) \geq p$.*

Proof. Let p be any given real number satisfying $Re(\mu) \geq p$. Thus, for any $j = 1, .., n$ we have that

$$|e^{-\mu\tau_j}| = e^{-Re(\mu)\tau_j} \leq e^{-p\tau_j}. \tag{1.10}$$

This implies that for any particular choice of p, and for any $m = 0, ..., k-1$, there is an appropriate constant A_m that satisfies

$$|p_m(e^{-\mu\tau_1}, ..., e^{-\mu\tau_n})| \leq A_m. \tag{1.11}$$

Let us now consider a positive number B that is sufficiently large to satisfy

$$\frac{A_{k-1}}{B} + ... + \frac{A_1}{B^{k-1}} + \frac{A_0}{B^k} < 1. \tag{1.12}$$

Multiplying both sides with B^k yields

$$A_{k-1}B^{k-1} + ... + A_1B + A_0 < B^k. \tag{1.13}$$

Let us assume that $|\mu| > B$. Then, the above inequality becomes

$$A_{k-1}|\mu|^{k-1} + ... + A_1|\mu| + A_0 < |\mu|^k. \tag{1.14}$$

Since $Re(\mu) \geq p$, it follows from equation 1.8 that

$$\begin{aligned} |\mu|^k =& | - p_{k-1}(e^{-\mu\tau_1}, ..., e^{-\mu\tau_n})\mu^{k-1} - ... - p_1(e^{-\mu\tau_1}, ..., e^{-\mu\tau_n})\mu - p_0(e^{-\mu\tau_1}, ..., e^{-\mu\tau_n})| \\ & \leq A_{k-1}|\mu|^{k-1} + ... + A_1|\mu| + A_0. \end{aligned}$$

However, this violates equation (1.14), which implies that for all roots with $Re(\mu) \geq p$ we must have that $|\mu| < B$.

Lemma 1.1.3 (Isolated zeros of an analytic function)**.** *If D is a domain and $f(z)$ is an analytic function on D that is not identically zero, then the zeros of $f(z)$ are isolated.*

Since μ is bounded, the characteristic polynomial is itself an analytic function with a bounded domain in the complex plane. Using lemma 1.1.3, the zeros of the characteristic polynomial are isolated and since the domain is bounded, it also follows that there is a finite number of zeros. Hence, equation (1.8) has a finite number of roots satisfying $Re(\mu) > p$ for any $p \in \mathbb{R}$. □

Theorem 1.1.4 (Boundedness of solutions of the DDE)**.** *Suppose that for every solution of the characteristic polynomial (1.8) we have that $Re(\mu) < p$. Then, there exists a positive constant M, such that for each $\phi \in C([t_0 - \tau_{max}, t_0], \mathbb{R}^k)$, the solution of (1.5) with initial condition $x_{t_0} = \phi$, satisfies*

$$\|x(t; t_0, \phi)\| \leq M\|\phi\|_{\tau_{max}} e^{p(t-t_0)} \qquad \text{for all } t \geq t_0. \tag{1.15}$$

The proof uses functional analysis and can be found in [**Hal71**, **Sto62**] as Theorem 22.1. This implies that the solutions of linear delay equations have an upper bound that depends on the eigenvalue with the largest real part. Moreover, if all the roots of (1.8) satisfy $Re(\mu) < p$, it follows that $Re(\mu) < p - \epsilon$ for some appropriate $\epsilon > 0$, which gives an even smaller upper bound. This holds true as there can only be a finite number of μ's which satisfy, for example, $Re(\mu) > p - 1$ Thus, the above theorem can be written as follows.

Lemma 1.1.5 (Boundedness of solutions of the DDE)**.** *Suppose that for every solution of the characteristic polynomial (1.8) we have that* $Re(\mu) < p$*. Then, there exists positive constants* M, ϵ*, such that for each* $\phi \in C([t_0 - \tau_{max}, t_0], \mathbb{R}^k)$*, the solution of (1.5) with the initial condition* $x_{t_0} = \phi$*, satisfies*

$$\|x(t; t_0, \phi)\| \leq M\|\phi\|_{\tau_{max}} e^{(p-\epsilon)(t-t_0)} \qquad \text{for all } t \geq t_0. \tag{1.16}$$

This lemma implies that like in the case of ODEs, if all the eigenvalues of the linear delay differential equation have a negative real part, the solutions will exponentially decay to 0, thus converging to a steady state. As such, this result is the foundation of all the stability analyses performed in this thesis.

With the development of appropriate mathematical and computational tools for analysis of delay equations, in recent years there has been an abundance of mathematical models that include time delays to correctly describe dynamical systems in general, and in particular, to model various epidemics. As the task of identifying the stability boundaries and stable regions of such models is adamantly important, many authors have attempted to address this using various methods. Hale and Lunel [**Hal93**], investigated the global geometry of the stability regions for systems with two delays. The authors gave a complete geometrical description of the stable region including the asymptotic behaviour of the stability boundaries. Beretta and Kuang [**Ber02**], obtained general geometric stability switch criteria for delay differential systems with delay-dependent parameters, whereas Gu *et al.* [**Gu05**], performed a detailed study of the stability curves of a general linear time-delay system with two delays and developed an algorithm to obtain such curves.

Examples where temporary immunity and the effects of vaccination in epi-

demic models has been considered by a number of authors. Gao *et al.* [**Gao06**], and Wei *et al.* [**Wei08**] have both considered a delayed SEIRS epidemic model with pulse vaccination and found that either a short period of pulse or a sufficiently high pulse vaccination rate is required for a stable infection-free periodic solution. Arino *et al.* [**Ari04**], considered a delayed epidemic model with a leaky vaccine, whose effectiveness gradually reduces over time determined by a general distribution function. It was shown that given specific parameter values, the model exhibited a backward bifurcation which lead to the existence of sub-threshold endemic equilibria and, therefore, dependence on initial conditions with significant implications for epidemic control. Beretta *et al.* [**Ber95**], investigated the global asymptotic stability of the endemic equilibrium of an SIR model with a single time delay where the force of infection depended on past history rather than the number of infectives at present time. More recently Kyrychko and Blyuss [**Kyr05**, **Bly10**], have used time-delays to represent the temporary immunity in epidemic models and employed a Lyupunov functional approach to show the global stability of the endemic equilibrium. Huang *et al.* [**Hua10**], have used time delays to represent the latency of infection in disease vectors and the latent period of infected hosts, whereas Zhang *et al.* [**Zha10**], have used time-delays to represent the incubation time of disease in SIR epidemics.

Cooke *et al.* [**Coo99**] investigated the effect of maturation delay in epidemic models with a non-linear birth rate. The authors found that increasing the maturation delay acts as a stability switch that makes the unique equilibrium point change its stability. Similarly, Gourley and Kuang [**Gou04**], have shown the importance of maturation delays in models with a stage structure

and demonstrated that, for a specific range of parameters, the model exhibits oscillatory behaviour.

1.2 Motivation

Existing mathematical models of RNAi have primarily focused on the intracellular aspects of this biological mechanism [**Ber03**, **Raa04**, **Gro05**, **Cuc11**]. Most of these models are based on systems of differential equations that describe the dynamics of different RNA populations over time within a single cell, sometimes also including certain amplification pathways depending on the type of cell. Although RNAi has been extensively studied as a gene regulator, its significance as an integral part of the plant immune system, has so far, not been studied mathematically.

Additionally, although there exists a plethora of studies that deal with the dynamics of cross-protection, the majority of this literature involves mathematical models that mainly describe the transmission dynamics between populations of healthy plants and plants that are infected with one or multiple viral strains [**Zha00b**, **Zha01**, **Jeg11**]. By studying the mechanisms of cross-protection on a cellular level, one might achieve a better understanding of the interactions between two viral strains within a single host that would allow one to determine the role played by RNAi in multi-strain infections.

As mentioned earlier, the effects of time delays associated with a single amplification pathway has already been investigated by Nikolov and Petrov [**Nik07**]. These authors were able to show that time delays can induce instability of the model steady state, thus disrupting gene silencing and causing

oscillations. However, this was done under a restrictive and somewhat unrealistic assumption that the natural degradation of RISC-mRNA complex takes place at exactly the same speed as the formation of new dsRNA while also ignoring the possibility of a second amplification pathway. The research in this thesis will thus include the following themes.

- Development and analysis of a model of plant disease dynamics mediated by RNAi within a single host.

- Study of the significance of RNAi under the presence of two viral strains interacting with the same plant host.

- Analysis of the non-instantaneous nature of the two primed amplification pathways associated with dsRNA synthesis from mRNA and garbage RNA, as modelled by time delays.

It will be shown that the respective models can provide an adequate qualitative description of the plant immune response to a viral infection or co-infection and support the main types of observable plant disease dynamics, including resistant and recovery phenotypes. The results also provide a framework in which RNAi can account for both viral synergism and antagonism resulting in cross-protection. A potential application of the first two models lies in better understanding the efficacy of treating plants against viral diseases by means of introducing specific viral strains or genetically modified viruses to trigger an artificial response for gene therapy.

1.3 Thesis outline

In addition to the main introduction, this thesis contains the following chapters:

Chapter 2 is based on the following publication:

- Neofytou, G., Kyrychko, Y.N., Blyuss, K.B., 2016. Time-delayed model of immune response in plants. Journal of Theoretical Biology, Biol. 389, 28-39.

Chapter 3 is based on the publication below

- Neofytou, G., Kyrychko, Y. N., Blyuss, K. B. 2016. Mathematical model of plant-virus interactions mediated by RNA interference. Journal of Theoretical Biology, 403, 129–142.

Chapter 4 is based on the following publication

- G. Neofytou, Y.N. Kyrychko, K.B. Blyuss (2016) Time-delayed model of RNA interference. Ecological Complexity ISSN 1476-945X.

Chapter 2: This chapter revolves around the investigation of the RNA interference mechanism as an integral part of the plant's immune system. We begin with the derivation of a mathematical model of RNA interference as an immune response against a viral infection. The model includes two time delays to account for the maturity time of undifferentiated cells and the intrinsic delay of the propagating RNA silencing signal. In section 2.3 we identify all the steady states of the model together with conditions for their biological feasibility. The following two sections are dedicated to the stability analysis of these steady

states. To better understand the significance of the two time delays, the section also includes specific cases where either the maturation time or the delay of the propagating signal might be considered trivial. Results of the numerical stability calculations and simulations of the model are illustrated in section 2.5. It is shown that the model is capable of exhibiting distinct types of dynamical behaviour, ones that are qualitatively consistent with recovery, resistance and chronic infection phenotypes. The chapter concludes with a detailed summary and conclusions.

Chapter 3: This chapter is concerned with the interactions that occur when two plant viruses are simultaneously infecting the same host, and how RNA interference may lead to either an antagonistic or synergistic relationship between the two viruses. In section 3.2 we describe in detail the main biological assumptions and derive a corresponding mathematical model of plant immune response under co-infection. In Section 3.3 we identify all steady states of the model together with conditions for their biological feasibility and stability as well as introduce the basic reproduction number, which indicates whether the disease-free steady state is stable. Section 3.5 is devoted to an extensive bifurcation analysis of the steady states, as well as numerical simulations of the model for two main purposes. One is to illustrate examples of cross-protection or cross-enhancement between viral strains, and the other is to identify core parameters that dictate the dynamics. The last section includes a summary and discussion of results, in addition to some open problems.

Chapter 4: In this chapter we consider a model of RNAi with primed amplification and focus on the role of two time delays associated with the production of dsRNA directly from mRNA and aberrant RNA. The outline of this

chapter is as follows. In section 4.2 we introduce the model and discuss its basic properties. In Section 4.3 we identify all steady states of the model together with conditions for their biological feasibility. Sections 4.4 and 4.5 are devoted to the stability analysis of these steady states depending on model parameters, including numerical bifurcation analysis and simulations of the model that illustrate different types of dynamical behaviour. The chapter concludes in Section 4.6 with the discussion of results and open problems. An important result obtained in this chapter is the partial destruction of the hysteresis loop: while the original model without time delays is bi-stable, under the influence of time delays, the steady state with either the smallest or the highest concentration of mRNA can lose its stability via a Hopf bifurcation. This leads to the co-existence of a stable steady state and a stable periodic orbit, which has a profound effect on the dynamics of the system.

Chapter 5: The last chapter provides a general summary, conclusions and discussion of further research.

Chapter 2

Time-delayed model of immune response in plants

2.1 Introduction

In this chapter we derive and analyse a new mathematical model of plant immune response with particular account for *post-transcriptional gene silencing* (PTGS), or otherwise known as RNA interference. Besides biologically accurate representation of the RNAi dynamics, the model explicitly includes two time delays to represent the maturation time of the growing plant tissue and the non-instantaneous nature of the PTGS signal. Through analytical and numerical analysis of stability of the steady states of the model we identify parameter regions associated with recovery and resistant phenotypes, as well as possible chronic infections. Dynamics of the system in these regimes is illustrated by numerical simulations of the model.

2.2 Model Derivation

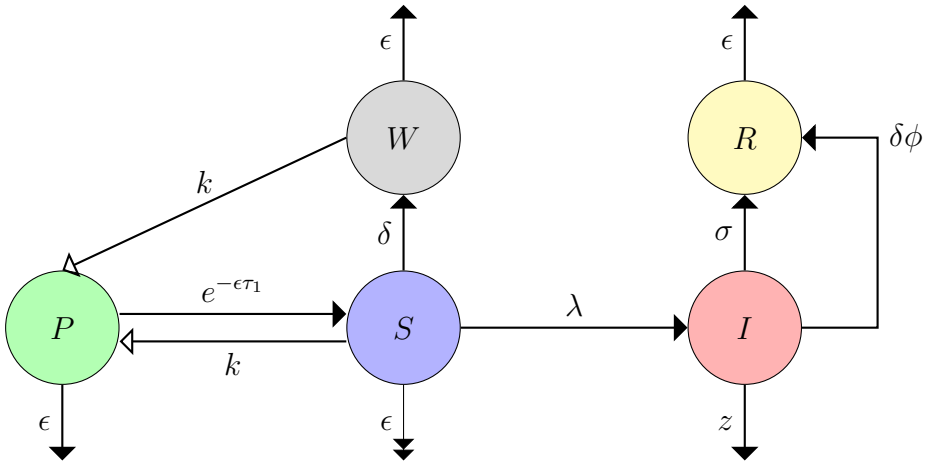

Figure 2.1: A diagram of plant immune response within an extended SIR framework. P, S and W denote the populations of proliferating, susceptible and warned cell whereas I and R stand for infected and recovered cells respectively. Black and white arrowheads represent the direction of recruitment and contribution rates respectively, from one class of cells to another. Note that the population of susceptible cells S dies at a rate $-\epsilon S^2$, driven by cells competing for available resources, where ϵ is the natural death rate of plant cells.

As a first step in the derivation of a mathematical model for interactions between plant cells and a viral infection, we divide the host population of cells $N(t)$ into the classes of susceptible cells $S(t)$ consisting of mature cells that are able to induce RNA interference and are susceptible to infection, infected cells $I(t)$ that spread the infection, recovered cells $R(t)$ that are no longer infectious, warned cells $W(t)$ that emerge from susceptible cells upon them receiving the silencing signal, and proliferating cells $P(t)$ that become susceptible to infection after reaching maturity. All possible transitions between these cell populations are illustrated in Fig. 2.1. We note that the total population of cells is not fixed.

The effective transmission rate between infected cells and the susceptible cells is given by the parameter λ, which is taken to be a cumulative parameter accounting for different aspects of the virus life cycle, as well as the actual process of infection. Infected cells are assumed to recover at a rate σ as a result of RISC-mediated cleavage or RNA-directed DNA methylation (RdDm) of the viral genome, depending on whether it is an RNA or a DNA virus [**Raj08**]. Average mortality rates of non-infected and infected cells are denoted by ϵ and z, respectively, where the infected cells are generally expected to exhibit a reduced lifespan compared to healthy cells, i.e. $z > \epsilon$.

A crucial aspect of the PTGS mechanism is that it cannot be maintained indefinitely in all parts of the plant. Laboratory studies have shown that the silenced state cannot be inherited directly, meaning that a parent cell will most likely be unable to produce daughter cells with the antiviral components needed to deal with the viral infection. It is, therefore, believed that undifferentiated and proliferating cells, e.g meristematic tissue, need to mature or be released from cellular reproduction before they can acquire an antiviral state [**Mit02**]. Hence, we introduce $P(t)$ as the population of proliferating cells that are responsible for promoting new plant growth. The generation of these new cells depends on the availability of mature cells that are responsible for the collection of nutrients, and the generation rate of new cells will be denoted by k. Recovered cells, although mature, are excluded from contributing to the development of new growth since the loss of function experienced during a viral infection can often cause devastating and irreparable damage to the cell. The proliferating cells have the average maturity time τ_1, after which they are recruited to the susceptible class. The property of non-inheritance is also true for many viral

infections, as it is highly unlikely that plant viruses can produce progeny in proliferating cells, in which the silencing state cannot be maintained [**Mat92**, **Fos02**]. One possible explanation for this is the presumed anti-dsRNA activity during cellular mitosis which interferes with the production of dsRNA required for the transmission of the PTGS signal and the replication of a virus and, the existence of a surveillance system that regulates selective entry of RNA into the shoot apex of the plant [**Fos02**]. In fact, tissue culture techniques using meristematic tissue or apical meristem grafting have been shown to produce virus-free plants in potatoes [**AlT11**], garlic [**Tas13**] and sweet peppers [**Kat04**]. Thus, the cell population $P(t)$ will be assumed to have both immunity to viral infection and the inability to express RNA interference.

Evidence suggest that RISC-mediated cleavage of target transcripts only requires the presence of 21-nt siRNAs, whereas a 25-nt siRNA may also induce RNA methylation and the long-distance transmission of the silencing signal [**Mol11**]. From a molecular point of view, it has been suggested that after the initiation of silencing, the primary 2-nt siRNA produced inside the cell can move into surrounding cells regardless of whether they contain any homologous transcripts. In the case where a receiving cell contains homologous transcripts, a second wave of 21-nt siRNA could be synthesized by using these transcripts as templates. Unlike the first wave, the production of a second wave of siRNA does not require the use of a dicer enzyme but relies on the recruitment of RNA-dependent RNA polymerase (RdRp). The importance of this RDR-mediated phase is that it amplifies the silencing signal and, as a result, these secondary RNAs could be the agents responsible for the systemic movement of the RNA silencing signal [**Was00**, **Zha12b**]. In light of these observations, we consider

the class of warned cells $W(t)$ that represent a subgroup of susceptible cells which have successfully acquired immunity to a viral infection by being the recipients of siRNA originating from infected cells. These cells are assumed to express the antiviral components prior to infection, and by doing so, they are capable of degrading the viral genome without any viral interference [**Wat01**].

It is widely understood that pathogens are capable of eliciting, suppressing or delaying the PTGS response of the plant, and that the induction of PTGS is not instantaneous [**Wat99**, **Son00**]. Recent studies have shown that viruses are capable of producing highly specific viral proteins able to interfere with the many different stages of the RNA-degradation mechanism [**Cos13**, **Raj08**, **Rot04**, **Can08**, **Lla00**, **Burg11**]. Taking this into account, in this model we assume that the propagating signal is initiated by the induction of PTGS in infected cells, but it will, however, be treated independently of whether the infected cells can recover or not. This will allow us to investigate specific cases where a virus can avoid silencing within the occupied cell but cannot prevent the propagation of the warning signal to other surrounding cells, and vice versa [**Zve12**]. Hence, the effective warning rate between infected and other target cells will be denoted by δ. We introduce time delay τ_2 to model the average time a cell remains infected before the propagating component of PTGS reaches its target. This is also a cumulative parameter with contributions from viral interference, specific thresholds in dsRNA accumulation necessary for initiation, inherent delay of activation, or the transportation delay of involved components. Other infected cells are also assumed to be the recipients of this signal, and as such, ϕ will denote the effective rate at which silencing of infected cells can be amplified. Hence, for any time t, we assume that $\delta I(t - \tau_2)$ is the signal

that has reached susceptible and infected cells, so multiplying this with $S(t)$ gives the number of susceptible cells that become warned by the PTGS signal, whereas multiplying with $I(t)$ and the amplification factor ϕ gives the total number of infected cells that are silenced by the propagating PTGS. This is consistent with the notion of the dsRNA dosage dependence of PTGS: once the virus infects a cell and starts reproducing, it is believed that enough viral dsRNA has to accumulate before PTGS can take place [**Ten01**]. However, if an infected cell receives additional antiviral components from other neighbouring cells, it is reasonable to assume that degradation of the viral genome could be initiated either sooner or more efficiently, therefore a stronger immune response might be possible.

We assume that in the absence of infection the population of susceptible cells should be bounded. To account for this in the model, the population of susceptible cells is taken to decrease at a rate ϵS^2, where ϵ is the death rate of non-infected cells, as introduced earlier. Effectively, this corresponds to a logistic growth for susceptible cells, which has been successfully used in other models for the spread of viral infections [**Cam61**, **Ber01a**, **Per02**, **Gou05**]. Different forms of growth of susceptible cells are discussed in De Leenheer and Smith [**Smi03**] who also provide arguments for only including susceptible cells into the competition term of the logistic growth, in a manner similar to the 'Campbell model' [**Cam61**, **Ber01a**]. From a biological perspective this can effectively account for an additional defensive strategy employed by the plant. Studies suggest that plants afflicted with disease are often able to demonstrate a flexible resource allocation [**Sch13**, **Ber07**]. This regulatory function is believed to be a highly complicated process operating through various channels and is

currently not fully understood. However, the core idea is that while pathogens try to absorb as many nutrients as possible, the plant can dynamically transfer resources from one location to another to either suppress microbial growth or accommodate a defensive response [**Sch13**, **Roj14**, **Ehn97**]. Hence, it is reasonable to assume that during a viral infection, warned and infected cells will be given priority over resources in order to mount and sustain a proactive and reactive defensive response respectively, whereas susceptible cells will have to compete with each other.

The system describing the dynamics of interactions between plant cells and a viral infection takes the following form

$$\begin{aligned}
\frac{dP}{dt} &= k[S(t) + W(t)] - P_s(t) - \epsilon P(t), \\
\frac{dS}{dt} &= P_s(t) - \lambda S(t)I(t) - \delta S(t)I(t-\tau_2) - \epsilon S(t)^2, \\
\frac{dI}{dt} &= \lambda S(t)I(t) - (z+\sigma)I(t) - \delta\phi I(t)I(t-\tau_2), \\
\frac{dR}{dt} &= \sigma I(t) + \delta\phi I(t)I(t-\tau_2) - \epsilon R(t), \\
\frac{dW}{dt} &= \delta S(t)I(t-\tau_2) - \epsilon W(t),
\end{aligned} \tag{2.1}$$

where $P(t)$, $S(t)$, $I(t)$, $R(t)$ and $W(t)$ denote the populations of proliferating, susceptible, infected, recovered and warned cells, respectively, and

$$P_s(t) = ke^{-\epsilon\tau_1}[S(t-\tau_1) + W(t-\tau_1)]$$

represents the population of undifferentiated cells that were born at time $t-\tau_1$, have survived for the period of time τ_1 in the class of proliferating cells, and upon maturation move into the class of susceptible cells at time t. For biological reasons, system (2.1) is augmented with non-negative initial conditions

$$S(s) = S_0(s) > 0, \quad W(s) = W_0(s) \geq 0 \ \text{ for all } \ s \in [-\tau_1, 0], \quad P(0) \geq 0,$$

$$I(s) = I_0(s) \geq 0 \ \text{ for all } \ s \in [-\tau_2, 0), \quad \text{with } \ I(0) > 0, \quad R(0) \geq 0. \tag{2.2}$$

Table 2.1: Baseline parameters for system (2.1)

Symbol	Definition	Baseline values	Units
λ	Rate of infection	1.5	$cells^{-1}time^{-1}$
k	Growth rate	1	$time^{-1}$
σ	Recovery rate	0.5	$time^{-1}$
δ	Propagation rate of silencing signal	0.5	$cells^{-1}time^{-1}$
ϕ	Amplification factor of recovery	1	n/a
ϵ	Natural death rate of cells	0.3	$time^{-1}$
z	Death rate of infected cells	0.6	$time^{-1}$
τ_1	Maturation time of proliferating tissue	1	time
τ_2	PTGS propagation delay	1	time

The system (2.1) can be reduced to the following closed system of equations

$$\begin{aligned}
\frac{dS}{dt} &= k[S(t-\tau_1) + W(t-\tau_1)]e^{-\epsilon\tau_1} - S(t)[\lambda I(t) + \delta I(t-\tau_2) + \epsilon S(t)], \\
\frac{dI}{dt} &= I(t)[\lambda S(t) - (z+\sigma) - \delta\phi I(t-\tau_2)], \\
\frac{dW}{dt} &= \delta S(t) I(t-\tau_2) - \epsilon W(t).
\end{aligned} \tag{2.3}$$

The remaining two variables $P(t)$ and $R(t)$ are determined by the solutions of this reduced system through

$$\begin{aligned}
P(t) &= P(0)e^{-\epsilon t} + k\int_{t-\tau_1}^{t} [S(x) + W(x)]e^{-\epsilon(t-x)}dx, \\
R(t) &= R(0)e^{-\epsilon t} + \int_{0}^{t} [\sigma I(x) + \delta\phi I(x)I(x-\tau_2)]e^{-\epsilon(t-x)}dx.
\end{aligned} \tag{2.4}$$

The solutions above are simply obtained by integrating the equations $\dot{P}$ and $\dot{R}$ over $[0, t]$. For example, we have that

$$\dot{R} + \epsilon R(t) = \sigma I(t) + \delta\phi I(t) I(t-\tau_2)$$

Using the integrating factor $m = e^{\epsilon t}$ we have that

$$\begin{aligned}
\left[\frac{d(Re^{\epsilon t})}{dt}\right]_0^t &= \int_0^t [\sigma I(x) + \delta\phi I(x)I(x-\tau_2)]e^{\epsilon x}dx \\
R(t)e^{\epsilon t} - R(0) &= \int_0^t [\sigma I(x) + \delta\phi I(x)I(x-\tau_2)]e^{\epsilon x}dx \\
R(t) &= R_0 e^{-\epsilon t}\int_0^t [\sigma I(x) + \delta\phi I(x)I(x-\tau_2)]e^{\epsilon(x-t)}dx
\end{aligned} \tag{2.5}$$

Since the model (2.1) and its reduced version (2.3) describe the dynamics of cell populations over time, it is essential from a biological perspective for all cell populations to remain non-negative and bounded, as given by the following results.

Theorem 2.2.1 (Positivity of solutions)**.** *Solutions $P(t), S(t), I(t), W(t), R(t)$ of the system (2.1) and $S(t), I(t), W(t)$ of the system (2.3) with initial conditions (2.2) are non-negative for all $t \geq 0$.*

This result can be proven using standard techniques, and it also follows from Theorem 5.2.1 in [**Smi95**] (see Theorem A.0.2). The next step is to establish that solutions of system (2.1) remain bounded during time evolution.

Theorem 2.2.2 (Boundedness of solutions)**.** *Suppose there exists $T > 0$, such that the solution $S(t)$ of the system (2.1) satisfies the condition $S(t) \leq M$ for $t \geq T$ with some $M > 0$. Then the solutions $P(t), I(t), W(t), R(t)$ of the system (2.1) with initial conditions (2.2) are bounded for all $t \geq T$.*

Proof. Starting with an equation for $I(t)$ in (2.1) and using the bound on $S(t)$,

we have for $t \geq T$

$$\frac{dI}{dt} \leq I(t)[\lambda M - \delta\phi I(t-\tau_2)].$$

Introducing rescaled variables

$$t = \frac{1}{\lambda M}\tilde{t}, \quad I(t) = \frac{\lambda M}{\delta\phi}\tilde{I}(\tilde{t}), \quad \tau_2 = \frac{1}{\lambda M}\tilde{\tau}_2,$$

the above inequality can be rewritten as

$$\frac{d\tilde{I}}{d\tilde{t}} \leq \tilde{I}(\tilde{t})[1 - \tilde{I}(\tilde{t}-\tilde{\tau}_2)]. \tag{2.6}$$

Proposition 5.13 in [**Smi11**] (see Proposition A.0.3) together with a comparison theorem (see Theorem (A.0.1)) implies that the solution of this inequality satisfies

$$\limsup_{t\tilde{\to}\infty} \tilde{I}(\tilde{t}) \leq e^{\tilde{\tau}_2},$$

or, in terms of the original variables,

$$I(t) \leq \frac{\lambda}{\delta\phi} M e^{\lambda\tau_2 M},$$

which shows that $I(t)$ is bounded for $t \geq T$. Alternatively, we have that $\frac{d\tilde{I}(\tilde{t})}{\tilde{d}(\tilde{t})} \leq \tilde{I}(\tilde{t})$. Integrating this inequality over $[\tilde{t}-\tilde{\tau}_2]$ yields $\tilde{I}(\tilde{t}) \geq \tilde{I}(\tilde{t})e^{-\tilde{\tau}_2}$. Using this in (2.6), we have that $\frac{d\tilde{I}(\tilde{t})}{d\tilde{t}} \leq \tilde{I}(\tilde{t})[1-\tilde{I}(\tilde{t})e^{-\tilde{\tau}_2}]$. which implies that $\limsup_{t\to\infty} \tilde{I}(\tilde{t}) \leq e^{\tilde{\tau}_2}$. Applying the bounds on $S(t)$ and $I(t)$ in equations for P, W and R, and

using the comparison theorem gives the following results for $t \geq T$

$$P(t) \leq \frac{kM}{\epsilon}\left(1 + \frac{\lambda M}{\phi\epsilon}e^{\lambda\tau_2 M}\right) + \left[P(0) - \frac{kM}{\epsilon}\left(1 + \frac{\lambda M}{\phi\epsilon}e^{\lambda\tau_2 M}\right)\right]e^{-\epsilon t},$$

$$W(t) \leq \frac{\lambda M^2}{\phi\epsilon}e^{\lambda\tau_2 M} + \left[W(0) - \frac{\lambda M^2}{\phi\epsilon}e^{\lambda\tau_2 M}\right]e^{-\epsilon t},$$

$$R(t) \leq \frac{\lambda M}{\delta\phi\epsilon}e^{\lambda\tau_2 M}\left(\sigma + \lambda M e^{\lambda\tau_2 M}\right) + \left[R(0) - \frac{\lambda M}{\delta\phi\epsilon}e^{\lambda\tau_2 M}\left(\sigma + \lambda M e^{\lambda\tau_2 M}\right)\right]e^{-\epsilon t}.$$

These inequalities prove that the solutions $P(t)$, $W(t)$ and $R(t)$ also remain bounded for $t \geq T$.

□

Remark (Boundedness of variables)**.** *In all numerical simulations, some of which will be presented in Section 2.4.3, the solutions of the system (2.1) always satisfy the condition that $S(t)$ remains bounded, which, in light of* **Theorem 2.2***, implies boundedness of all other variables.*

Since the variables $P(t)$ and $R(t)$ are fully determined by solutions of the system (2.3) through expressions given by (2.4), from now on we will focus on the dynamics of reduced system (2.3).

2.3 Steady states and feasibility conditions

The system (2.3) has up to three possible steady states. For any parameter values it admits a trivial steady state $E_0 = (0, 0, 0)$ that corresponds to all cell populations going extinct.

The second steady state of the system (2.3) that also exists for any parameter values is a disease-free steady state given by

$$E_1 = \left(\epsilon^{-1}K(\tau_1), 0, 0\right), \tag{2.7}$$

where

$$K(\tau_1) = ke^{-\epsilon\tau_1}.$$

It is easy to see that $K(\tau_1) \leq k$ for all $\tau_1 \geq 0$, thus k is un upper bound for the number of cells in the disease-free steady state.

The third, endemic steady state $E_2 = (S^*, I^*, W^*)$ is characterised by all cell populations being non-zero, and it can be found as

$$S^* = S(\tau_1) = \frac{K(\tau_1)}{\epsilon} - \frac{[\delta K(\tau_1) - \epsilon(\lambda+\delta)][\lambda K(\tau_1) - \epsilon(z+\sigma)]}{\epsilon[\epsilon\lambda^2 - \delta\lambda(K(\tau_1)-\epsilon) + \delta\phi\epsilon^2]},$$

$$I^* = I(\tau_1) = \frac{\epsilon[\lambda K(\tau_1) - \epsilon(z+\sigma)]}{\epsilon\lambda^2 - \delta\lambda[K(\tau_1)-\epsilon] + \delta\phi\epsilon^2},$$

$$W^* = W(\tau_1) = \frac{\delta\left[\epsilon\delta\phi K(\tau_1) - (z+\sigma)(\delta K(\tau_1) - \epsilon(\lambda+\delta))\right]\left[\lambda K(\tau_1) - \epsilon(z+\sigma)\right]}{[\epsilon\lambda^2 - \delta\lambda(K(\tau_1)-\epsilon) + \delta\phi\epsilon^2]^2}. \tag{2.8}$$

For the endemic steady state E_2 to be biologically feasible, all components S^*, I^* and W^* must be positive. It is easy to show that $I^* > 0$ implies $S^*, W^* > 0$, hence for this steady state to be plausible, it is sufficient to require $I^* > 0$.

Let $C = \left\{\frac{\epsilon(z+\sigma)}{\lambda}, \frac{\epsilon(\lambda^2+\delta\lambda+\delta\phi\epsilon)}{\delta\lambda}\right\}$ and choose $C_{\min} = \min(C)$ and $C_{\max} = \max(C)$. Hence, the feasibility condition of the endemic steady state is

given by $C_{\min} < K(\tau_1) < C_{\max}$ or equivalently

$$\frac{\ln(k) - \ln(C_{\max})}{\epsilon} < \tau_1 < \frac{\ln(k) - \ln(C_{\min})}{\epsilon}. \tag{2.9}$$

Recalling that $K(\tau_1) = ke^{-\epsilon\tau_1}$, we have $K(\tau_1) \leq k$ for all $\tau_1 \geq 0$. Hence, we have proved the following result.

Theorem 2.3.1 (Feasibility of endemic steady state)**.** *Let the endemic steady state be given by $E_2 = (S^*, I^*, W^*)$. Then the following statements hold.*

(i) For $k \leq C_{\min}$, the steady state E_2 is not feasible.

(ii) For $C_{\min} < k \leq C_{\max}$, the endemic steady state exists if and only if $0 < \tau_1 < [\ln(k) - \ln(C_{\min})]/\epsilon$.

(iii) For $k > C_{\max}$, E_2 is feasible if and only if the condition (2.9) is satisfied.

The conditions of this theorem imply that whilst the trivial and the disease-free steady states exist for any parameter values, the endemic steady state can only exist, provided the growth rate of new plant cells is sufficiently large. This is needed to ensure that a sufficient number of new infections occur before the infection is cleared by the immune response.

2.4 Stability analysis of the steady states

2.4.1 Trivial steady state

Linearisation of the system (2.3) near the steady state $E_0 = (0, 0, 0)$ yields a characteristic equation

$$(\mu + \epsilon)(\mu + \sigma + z)(ke^{-\epsilon\tau_1}e^{-\mu\tau_1} - \mu) = 0. \tag{2.10}$$

Since all parameters are positive, this equation admits two negative roots $\mu_1 = -\epsilon$ and $\mu_2 = -(\sigma + z)$, and all remaining roots are determined by the solutions of the transcendental equation

$$\mu = ke^{-\epsilon\tau_1}e^{-\mu\tau_1}. \tag{2.11}$$

This equation has a real root $\mu > 0$ for any values of $k > 0$ and $\tau_1 \geq 0$, implying that the trivial steady state E_0 is unstable for any values of system parameters, and hence, it is impossible for all cell populations to become extinct. One can show that such a real root $\mu > 0$ exists by plotting both the LHS and RHS of (2.11) together and noting that the line $y = \mu$ will inevitably cross the curve defined by $y = ke^{-\epsilon\tau_1}e^{-\mu\tau_1}$ at least one time. This is illustrated with the following figure.

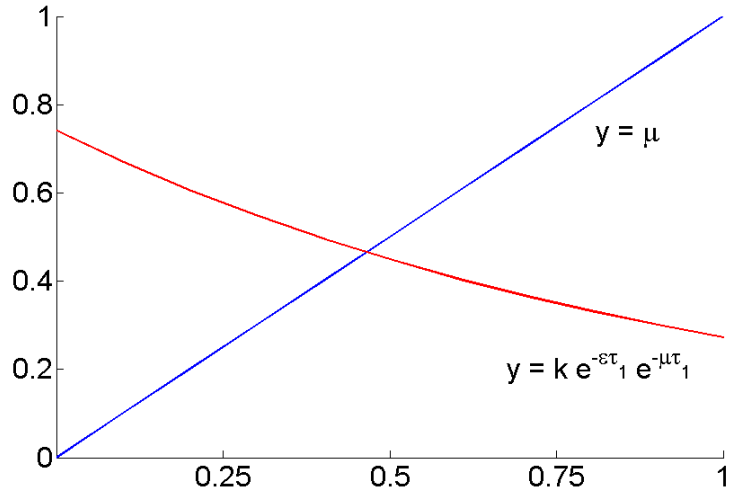

Figure 2.2: Blue and Red denote the LHS and RHS of equation (2.11) respectively. Parameter values are taken from table (2.1).

2.4.2 Disease-free steady state

The characteristic equation of linearisation near the disease-free steady state E_1 is given by

$$(\mu+\epsilon)\left[\mu+\sigma+z-\frac{\lambda K(\tau_1)}{\epsilon}\right]\left[-2K(\tau_1)-\mu+K(\tau_1)e^{-\mu\tau_1}\right]=0. \qquad (2.12)$$

One eigenvalue $\mu_1=-\epsilon$ is always negative. The second eigenvalue

$$\mu_2=\frac{\lambda K(\tau_1)}{\epsilon}-(z+\sigma),$$

is negative for $\tau_1=0$ if

$$k<k_{\min}, \quad k_{\min}=\frac{\epsilon(\sigma+z)}{\lambda},$$

and for $\tau_1 > 0$, if

$$k > k_{\min}, \quad \tau_1 > \frac{\ln(k) - \ln(k_{\min})}{\epsilon}.$$

The last eigenvalue of the characteristic equation (2.12) satisfies the transcendental equation

$$\mu_3 = K(\tau_1)(e^{-\mu_3 \tau_1} - 2). \tag{2.13}$$

For $\tau_1 = 0$, we have $\mu_3 = -k < 0$. For $\tau_1 > 0$, it immediately follows that $\mu_3 = 0$ is not a root of (2.13), so we look for the roots of this equation in the form $\mu_3 = iw$, $w > 0$. Substituting this into (2.13) yields

$$K(\tau_1)[\cos(w\tau_1) - 2] - iK(\tau_1)\sin(w\tau_1) = 0. \tag{2.14}$$

Since $[\cos(w\tau_1) - 2] < 0$ for any $\tau_1 > 0$, this implies that the equation (2.12) does not admit purely imaginary roots. Hence, we have proven the following result.

Theorem 2.4.1 (Stability of the disease-free steady state)**.** *Let the disease-free steady state be given by* $E_1 = \left(\frac{K(\tau_1)}{\epsilon}, 0, 0\right)$*, and denote* $k_{\min} = \frac{\epsilon(\sigma + z)}{\lambda}$*. Then, the following statements hold.*

(a) Given $k < k_{\min}$*,* E_1 *is linearly asymptotically stable for all* $\tau_1 \geq 0$*.*

(b) Given $k \geq k_{\min}$ *and* $\tau_{min} = \frac{\ln(k) - \ln(k_{\min})}{\epsilon}$*,* E_1 *is linearly asymptotically stable for* $\tau_1 > \tau_{min}$*, unstable for* $\tau_1 < \tau_{min}$*, and undergoes a steady-state bifurcation at* $\tau_1 = \tau_{min}$*.*

This theorem indicates that the disease-free steady is stable, as long as new infections appear slower than they are cleared by recovery or death of the in-

fected cells. Additionally, the theorem suggests that stability of the disease-free steady state depends only on the maturation time of undifferentiated proliferating cells, natural and infection-induced mortality rates, and the rates at which infected cells spread the infection and recover. This immediately implies that the propagation of the warning signal and the acquired immunity of uninfected cells is not enough for a complete recovery of the host. Moreover, this suggests that the propagating component of PTGS acts only as an amplifier of immune response rather than playing an essential role in recovery. Hence, in plants with a strong localized immune response, suppression of the warning signal would most likely only delay recovery rather than completely inhibit it. Equivalently, a localized immune response that is too weak will most likely never lead to a complete recovery despite a potentially strong propagating warning signal.

2.4.3 Stability analysis of the endemic steady state

Linearisation near the endemic steady state $E_2 = (S^*, I^*, W^*)$ yields the following characteristic equation

$$\mu^3 + p_2(\mu, \tau_1, \tau_2)\mu^2 + p_1(\mu, \tau_1, \tau_2)\mu + p_0(\mu, \tau_1, \tau_2) = 0, \tag{2.15}$$

where

$$\begin{aligned}
p_2 &= -K(\tau_1)e^{-\mu\tau_1} + \delta\phi I^* e^{-\mu\tau_2} + I^*(\lambda + \delta) + \epsilon(1 + 2S^*),\\
p_1 &= e^{-\mu\tau_1}p_{11} + e^{-\mu\tau_2}p_{12} + e^{-\mu(\tau_1+\tau_2)}p_{13} + p_{14},\\
p_0 &= e^{-\mu\tau_2}p_{01} + e^{-\mu(\tau_1+\tau_2)}p_{02} + p_{03},
\end{aligned}$$

and

$$
\begin{aligned}
p_{11} &= -K\left(\tau_1\right)\left(\epsilon+\delta\, I^*\right), \\
p_{12} &= \delta\phi\,\left(\lambda+\delta\right) I^{*2} + \left[\left(\lambda+2\,\phi\,\epsilon\right)\delta\, S^* + \delta\,\phi\,\epsilon\right] I^*, \\
p_{13} &= -K(\tau_1)\delta\phi I^*, \quad p_{14} = \left(\lambda\,\epsilon+\delta\,\epsilon+\lambda^2 S^*\right) I^* + 2\,\epsilon^2 S^*, \\
p_{01} &= \delta\phi\left(\delta\,\epsilon+\lambda\,\epsilon\right) I^{*2} + \epsilon\left(2\,\epsilon\phi+\lambda\,\right)\delta\, S^* I^*, \\
p_{02} &= -K\left(\tau_1\right)\delta\, I^*\,\left(I^*\,\delta\,\phi+\phi\,\epsilon+\lambda\, S^*\right), \quad p_{03} = \lambda^2\epsilon\, S^* I^*.
\end{aligned}
$$

Instantaneous maturity

As a first step in the analysis, we consider the case when the proliferating cells immediately achieve maturity, i.e. $\tau_1 = 0$. In this case, the equation (2.15) reduces to

$$\mu^3 + (a_1 e^{-\mu\tau_2} + a_2)\mu^2 + (b_1 e^{-\mu\tau_2} + b_2)\mu + (c_1 e^{-\mu\tau_2} + c_2) = 0, \tag{2.16}$$

where

$$
\begin{aligned}
a_1 &= \delta\,\phi I^*, \quad a_2 = \left(\lambda+\delta\right) I^* + \left(2\,S^*+1\right)\epsilon - k, \\
b_1 &= \delta\phi\left(\delta+\lambda\right) I^{*2} + \left[\left(\epsilon-k+2\,\epsilon\, S^*\right)\phi + \lambda\, S^*\right]\delta\, I^*, \\
b_2 &= \left[\left(\lambda+\delta\right)\epsilon - \delta\, k + \lambda^2 S^*\right] I^* - k\epsilon + 2\,\epsilon^2 S^*, \\
c_1 &= -\delta I^*\left[\left[k\delta-\epsilon\left(\delta+\lambda\right)\right]\phi\, I^* + \left(k\lambda-\,\epsilon(2\epsilon\phi+\lambda)\right) S^* + k\phi\,\epsilon\right], \\
c_2 &= \lambda^2\epsilon\, S^* I^*.
\end{aligned}
$$

When $\tau_2 = 0$, the characteristic equation (2.16) reduces to

$$\mu^3 + (a_1+a_2)\mu^2 + (b_1+b_2)\mu + (c_1+c_2) = 0.$$

By the Routh-Hurwitz criterion, the roots of this equation have negative real part if and only if

$$a_1 + a_2 > 0,\ c_1 + c_2 > 0,\ (a_1 + a_2)(b_1 + b_2) > c_1 + c_2. \tag{2.17}$$

To investigate for any potential Hopf bifurcations given $\tau_2 > 0$, we follow the methodology of Ruan and Wei [**Rua01**] and look for the roots of the characteristic equation (2.16) in the form $\mu = i\omega$, $\omega > 0$, which gives

$$(ib_1\omega + c_1 - a_1\omega^2)(\cos\omega\tau_2 - i\sin\omega\tau_2) - i\omega^3 - a_2\omega^2 + c_2 + ib_2\omega = 0.$$

Separating this equation into real and imaginary parts yields

$$\begin{aligned} b_1\omega\sin\omega\tau_2 - (a_1\omega^2 - c_1)\cos\omega\tau_2 &= a_2\omega^2 - c_2, \\ b_1\omega\cos\omega\tau_2 + (a_1\omega^2 - c_1)\sin\omega\tau_2 &= \omega^3 - b_2\omega. \end{aligned} \tag{2.18}$$

Squaring and adding these two equations gives the following equation for the Hopf frequency ω:

$$\omega^6 + ({a_2}^2 - {a_1}^2 - 2b_2)\omega^4 + (2c_1a_1 - 2c_2a_2 + {b_2}^2 - {b_1}^2)\omega^2 + {c_2}^2 - {c_1}^2 = 0. \tag{2.19}$$

Introducing an auxiliary variable $v = \omega^2$, the last equation can be rewritten as

$$h(v) = v^3 + pv^2 + qv + r = 0, \tag{2.20}$$

where

$$p = ({a_2}^2 - {a_1}^2 - 2b_2),$$
$$q = (2c_1a_1 - 2c_2a_2 + {b_2}^2 - {b_1}^2),$$
$$r = {c_2}^2 - {c_1}^2.$$

It is straightforward to see that $h(0) = r$ and $\lim_{v\to\infty} h(v) = \infty$, hence given $r < 0$, by the intermediate value theorem $h(v)$ has a zero $v_0 \in (0, \infty)$. To investigate what happens when r is positive, we look at the critical points of the function $h(v)$ as given by:

$$v_{1,2} = \frac{-p \pm \sqrt{p^2 - 3q}}{3}. \tag{2.21}$$

One can see that for $\Delta = p^2 - 3q < 0$, the quadratic $h'(v)$ has no real roots, and so the function $h(v)$ must be monotonic. With $\lim_{v\to\infty} h(v) = \infty$, the function $h(v)$ must also be an increasing function, and since $h(0) = r \geq 0$, we must have that equation (2.20) has no positive real roots.

Suppose that $\Delta \geq 0$. Then, for $v_{1,2} = \frac{-p \pm \sqrt{\Delta}}{3}$, we have $h''(v_{1,2}) = \pm\sqrt{\Delta}$, and, therefore, v_1 is a local minimum, whereas v_2 is a local maximum of $h(v)$. Note that $v_2 < v_1$, and hence, $v_1 < 0$ implies $v_2 < 0$. If $v_1 < 0$ is the local minimum and $h(0) = r > 0$, $h(v)$ is an increasing function on the domain $[v_1, \infty)$, and therefore, there are no positive real roots of $h(v) = 0$. Equivalently, if $v_1 > 0$, the function $h(v)$ is increasing in the interval $[v_1, \infty)$, hence a positive root can only exist if $h(v_1) \leq 0$. We have, therefore, proved the following lemma.

Lemma 2.4.2 (Conditions for positive roots of (2.20))**.** *Let $v_{1,2}$ be given by (2.21).*

(i) If $r < 0$, the equation (2.20) has at least one positive root.

(ii) If $r \geq 0$ and $\Delta < 0$, or $\Delta > 0$ and $v_1 < 0$, or $\Delta > 0$, $v_1 > 0$ and $h(v_1) > 0$, the equation (2.20) has no positive roots.

(iii) If $r \geq 0$, $v_1 > 0$ and $h(v_1) \leq 0$, the equation (2.20) has at least one positive root.

Without loss of generality, let us assume that equation (2.20) has three distinct positive roots denoted by v_1, v_2 and v_3. This implies that the equation (2.19) also has at least three positive roots

$$w_1 = \sqrt{v_1},\ w_2 = \sqrt{v_2},\ w_3 = \sqrt{v_3}.$$

Solving the system (2.18) for τ_2 yields

$$\tau_2{}^{(j)}(n) = \frac{1}{w_n}\left[\arctan\left(\frac{a_1 {w_n}^5 + (b_1a_2 - c_1 - a_1b_2)\,{w_n}^3 + (c_1b_2 - b_1c_2)\,w_n}{(b_1 - a_1a_2)\,{w_n}^4 + (c_1a_2 + a_1c_2 - b_1b_2)\,{w_n}^2 - c_1c_2}\right) + (j-1)\pi\right],$$

$$n = 1, 2, 3;\quad j \in \mathbb{N}. \tag{2.22}$$

This allows us to define the following:

$$\tau_2{}^* = \tau_2{}^{(j_0)}(n_0) = \min_{1 \leq n \leq 3,\, j \geq 1}\{\tau_2{}^{(j)}(n)\}, w_0 = w_{n_0}. \tag{2.23}$$

In order to establish whether the steady state E_2 actually undergoes a Hopf bifurcation at $\tau_2 = \tau_2{}^*$, we compute the sign of $\dfrac{d[\mathrm{Re}\,\mu(\tau_2{}^*)]}{d\tau_2}$. Differentiating

both sides of equation (2.16) with respect to τ_2 yields

$$\left(\frac{d\mu}{d\tau_2}\right)^{-1} = \frac{(3\,\mu^2 + 2\,a_2\mu + b_2)\,e^{\mu\,\tau_2} + 2\,a_1\mu + b_1}{\mu\,(a_1\mu^2 + b_1\mu + c_1)} - \frac{\tau_2}{\mu}.$$

Introducing the notation $V = {w_0}^2\left[\left(c_1 - {w_0}^2 a_1\right)^2 + {w_0}^2 {b_1}^2\right]$, it follows that $V > 0$ for all $w_0 > 0$, and

$$\left(\frac{d\,\mathrm{Re}\,\mu(\tau_2{}^*)}{d\tau_2}\right)^{-1} = \frac{w_0}{V}\left[\underbrace{A\cos(w_0\tau_2) + wB\sin(w_0\tau_2)}_{:=\Gamma} - {b_1}^2 w_0 + 2\,a_1 w_0\left(c_1 - {w_0}^2 a_1\right)\right],$$

where

$$\begin{aligned} A &= \left(3\,{w_0}^2 - b_2\right) b_1 w_0 - 2\,w_0 a_2\left({w_0}^2 a_1 - c_1\right), \\ B &= 2\,{w_0}^2 a_2 b_1 + \left(3\,{w_0}^2 - b_2\right)\left({w_0}^2 a_1 - c_1\right), \end{aligned}$$

and

$$\Gamma = 3\,{w_0}^5 + \left(2\,{a_2}^2 - 4\,b_2\right){w_0}^3 + \left({b_2}^2 - 2\,a_2 c_2\right) w_0$$

Consequently, with $v_0 = {w_0}^2$ we have

$$\left(\frac{d\,\mathrm{Re}\,\mu(\tau_2{}^*)}{d\tau_2}\right)^{-1} = \frac{1}{V}\left[3{w_0}^6 + 2\left({a_2}^2 - {a_1}^2 - 2b_2\right){w_0}^4 + \left(2a_1c_1 - 2a_2c_2 + {b_2}^2 - {b_1}^2\right){w_0}^2\right]$$

$$= \frac{1}{V}\left[3{w_0}^6 + 2p{w_0}^4 + q{w_0}^2\right] = \frac{1}{V}\left[3v_0^3 + 2pv_0^2 + qv_0\right] = \frac{v_0}{V}h'(v_0), \tag{2.24}$$

where $h(v)$ is defined in (2.20). Since $v_0 = {w_0}^2 > 0$, this implies

$$\mathrm{sign}\left(\frac{d\,\mathrm{Re}\,\mu(\tau_2{}^*)}{d\tau_2}\right) = \mathrm{sign}\left(\frac{d\,\mathrm{Re}\,\mu(\tau_2{}^*)}{d\tau_2}\right)^{-1} = \mathrm{sign}\left[v_0 h'(v_0)\right] = \mathrm{sign}\left[h'(v_0)\right].$$

These calculations can now be summarised in the following theorem.

Theorem 2.4.3 (Stability of the endemic steady state)**.** *Let the coefficients of the characteristic equation (2.16) satisfy* $a_1 + a_2 > 0, c_1 + c_2 > 0$ *and* $(a_1 + a_2)(b_1 + b_2) > c_1 + c_2$*. Additionally, let* $w_0, {\tau_2}^*$ *be defined as in (2.23) with* $v_0 = {w_0}^2$*, and let* $h'(v_0) > 0$*. Then, the following holds.*

(i) If $r \geq 0$ *and* $p^2 < 3q$*, or* $p^2 > 3q$ *and* $v_1 < 0$*, or* $p^2 > 3q$ *and* $v_1 < 0$ *and* $h(v_1) > 0$*, the endemic steady state* E_2 *of the system (2.3) is linearly asymptotically stable for all* $\tau_2 \geq 0$*.*

(ii) If $r < 0$*, or if* $r \geq 0$ *and* $h(v_1) < 0$*, the endemic steady state* E_2 *of system (2.3) is linearly asymptotically stable when* $\tau_2 \in [0, {\tau_2}^*)$*, unstable for* $\tau_2 > \tau_2^*$*, and undergoes Hopf bifurcation at* $\tau_2 = \tau_2^*$*.*

Fast-spreading PTGS signal

In the case when the PTGS signal is spreading very quickly, the time delay τ_2 associated with the spread of this signal is negligibly small compared to other timescales in the system. In this case, setting $\tau_2 = 0$ in the characteristic equation (2.15) reduces it to

$$\begin{aligned} &\mu^3 + \left[a_1(\tau_1)e^{-\mu\tau_1} + a_2(\tau_1)\right]\mu^2 + \left[b_1(\tau_1)e^{-\mu\tau_1} + b_2(\tau_1)\right]\mu + \\ &c_1(\tau_1)e^{-\mu\tau_1} + c_2(\tau_1) = 0, \end{aligned} \tag{2.25}$$

where

$$
\begin{aligned}
&a_1(\tau_1) = -K(\tau_1), \quad a_2(\tau_1) = (\delta + \lambda + \delta\,\phi)\,I^* + 2\,\epsilon\,S^* + \epsilon,\\
&b_1(\tau_1) = -\left[\epsilon + \delta\,(\phi + 1)\,I^*\right] K\,(\tau_1)\,,\\
&b_2(\tau_1) = \delta\,\phi\,(\lambda\, + \delta)\,I^{*2} + \left[S^*\left[(\lambda + 2\,\phi\,\epsilon)\,\delta + \lambda^2\right] + (\epsilon + \phi\,\epsilon)\,\delta + \lambda\,\epsilon\right] I^* + 2\,\epsilon^2 S^*,\\
&c_1(\tau_1) = -K\,(\tau_1)\;(I^*\,\delta\,\phi + \phi\,\epsilon + \lambda\,S^*)\,\delta\,I^*,\\
&c_2(\tau_1) = \delta\phi\epsilon\,(\delta + \lambda\,)\,I^{*2} + \left[\left(2\,\epsilon^2\phi + \lambda\,\epsilon\right)\delta + \lambda^2\epsilon\right] S^* I^*.
\end{aligned}
$$

Looking for purely imaginary solutions of equation (2.25) in the form $\mu = iw$ $(w > 0)$, and separating the real and imaginary parts gives

$$
\begin{aligned}
&b_1(\tau_1)w\sin(w\tau_1) - [a_1(\tau_1)w^2 - c_1]\cos(w\tau_1) = [a_2(\tau_1)w^2 - c_2(\tau_1)],\\
&b_1(\tau_1)w\cos(w\tau_1) + [a_1(\tau_1)w^2 - c_1]\cos(w\tau_1) = [w^3 - b_2(\tau_1)w].
\end{aligned}
\tag{2.26}
$$

With the help of auxiliary functions

$$
g_1(\tau_1) = b_1(\tau_1)w, \quad g_2(\tau_1) = a_1(\tau_1)w^2 - c_1(\tau_1),
$$

$$
L_1(\tau_1) = a_2(\tau_1)w^2 - c_2(\tau_1), \quad L_2(\tau_1) = w^3 - b_2(\tau_1)w,
$$

the system of equations (2.26) can be re-written as follows

$$
\begin{aligned}
&g_1(\tau_1)\sin(w\tau_1) - g_2(\tau_1)\cos(w\tau_1) = L_1(\tau_1),\\
&g_1(\tau_1)\cos(w\tau_1) + g_2(\tau_1)\sin(w\tau_1) = L_2(\tau_1).
\end{aligned}
\tag{2.27}
$$

Solving this system yields

$$\begin{aligned} &{\tau_1}^{(j)}(n) = \frac{1}{w_n}\left[\tan^{-1}U(\tau_1) + (j-1)\pi\right], \qquad n = 1,2,3; \;\; j \in \mathbb{N}, \\ &U(\tau_1) = \frac{g_1(\tau_1)L_1(\tau_1) + L_2(\tau_1)g_2(\tau_1)}{L_2(\tau_1)g_1(\tau_1) - L_1(\tau_1)g_2(\tau_1)}, \end{aligned} \tag{2.28}$$

though, unlike the case of instantaneous maturity, w_n is now itself the function of τ_1, and hence, it does not prove possible to find the closed form expression for the critical time delay τ_1^*.

Equal PTGS delay and maturity time

Let us consider the third degree transcendental polynomial that is obtained by setting $\tau_1 = \tau_2 = \tau \neq 0$ in (2.15)

$$\mu^3 + \left[a_1(\tau)e^{-\mu\tau} + a_2(\tau)\right]\mu^2 + \left[b_1(\tau)e^{-\mu\tau} + b_2(\tau)e^{-2\mu\tau} + b_3(\tau)\right]\mu + c_1(\tau)e^{-\mu\tau} + c_2(\tau)e^{-2\mu\tau} + c_3(\tau) = 0,$$

where

$$
\begin{aligned}
a_1(\tau) &= \delta\,\phi\,I^* - K\,(\tau)\,,\\
a_2(\tau) &= (\lambda+\delta)\,I^* + 2\,\epsilon\,S^* + \epsilon,\\
b_1(\tau) &= \delta\phi\,(\delta+\lambda\,)\,{I^*}^2 + (\phi\,\epsilon - K\,(\tau) + 2\,\epsilon\,\phi S^* + \lambda\,S^*)\,\delta\,I^* - K\,(\tau)\,\epsilon,\\
b_2(\tau) &= -K\,(\tau)\;\delta\,\phi\,I^*,\\
c_1(\tau) &= \delta\phi\epsilon\,(\delta+\lambda)\,{I^*}^2 + \epsilon\,(\lambda\;+2\,\epsilon\phi)\,\delta\,S^*I^*,\\
c_2(\tau) &= -K\,(\tau)\,\delta\;\;(\,\delta\,\phi I^* + \phi\,\epsilon + \lambda\,S^*)\,I^*.\\
c_3(\tau) &= \lambda^2\,\epsilon S I^*
\end{aligned}
$$

Substituting $\mu = iw(w>0)$ in the equation above and separating the real and imaginary parts yields

$$
\begin{aligned}
f(\tau)\cos(w\tau) + wb_1(\tau)\sin(w\tau) &=\\
G_1(\tau) - [b_2(\tau)w\sin(2w\tau) + c_2(\tau)\cos(2w\tau)],&\\
-\,f(\tau)\sin(w\tau) + wb_1(\tau)\cos(w\tau) &=\\
G_2(\tau) - b_2(\tau)w\cos(2w\tau) + c_2(\tau)\sin(2w\tau),&
\end{aligned}
\tag{2.29}
$$

where we have introduced the following notation

$$
\begin{gathered}
f(\tau) = c_1\,(\tau) - a_1\,(\tau)\,w^2,\\
G_1(\tau) = a_2\,(\tau)\,w^2 - c_3\,(\tau)\,,\quad G_2(\tau) = w^3 - b_3\,(\tau)\,w.
\end{gathered}
$$

Introducing auxiliary parameters

$$\begin{aligned} u &= 2w\tau, \\ \alpha(\tau) &= 2\left[wb_2(\tau)G_1(\tau) - c_2(\tau)G_1(\tau)\right], \\ \beta(\tau) &= 2\left[c_2(\tau)G_1(\tau) + wb_2(\tau)G_2(\tau)\right], \\ \gamma(\tau) &= {G_1}^2(\tau) + {G_2}^2(\tau) + w^2\left[{b_2}^2(\tau) - {b_1}^2(\tau)\right] + {c_2}^2(\tau) - f^2(\tau), \end{aligned}$$

squaring both sides of the two equations in (2.29) and adding them together yields

$$\alpha(\tau)\sin(u) + \beta(\tau)\cos(u) = \gamma. \tag{2.30}$$

Dividing by $\sqrt{\alpha^2(\tau) + \beta^2(\tau)}$ gives

$$\frac{\alpha(\tau)\sin(u)}{\sqrt{\alpha^2(\tau) + \beta^2(\tau)}} + \frac{\beta(\tau)\cos(u)}{\sqrt{\alpha^2(\tau) + \beta^2(\tau)}} = \frac{\gamma(\tau)}{\sqrt{\alpha(\tau)^2 + \beta(\tau)^2}}. \tag{2.31}$$

Note that $\left(\frac{\alpha(\tau)}{\sqrt{\alpha^2(\tau) + \beta^2(\tau)}}\right)^2 + \left(\frac{\beta(\tau)}{\sqrt{\alpha^2(\tau) + \beta^2(\tau)}}\right)^2 = 1$, which implies that there exists θ such that

$$\sin(\theta) = \frac{\alpha(\tau)}{\sqrt{\alpha^2(\tau) + \beta^2(\tau)}},\ \cos(\theta) = \frac{\beta(\tau)}{\sqrt{\alpha^2(\tau) + \beta^2(\tau)}}, \tag{2.32}$$

and $\theta = \arctan\left(\frac{\alpha(\tau)}{\beta(\tau)}\right)$. Thus, equation (2.31) can be re-written as

$$\sin(u + \theta) = \frac{\gamma(\tau)}{\sqrt{\alpha^2(\tau) + \beta^2(\tau)}}. \tag{2.33}$$

Hence we have

$$\tau = \frac{1}{w}\left[-\arctan\left(\frac{\alpha(\tau)}{\beta(\tau)}\right) + \arcsin\left(\frac{\gamma(\tau)}{\sqrt{\alpha^2(\tau)+\beta^2(\tau)}}\right) + j\pi\right], \quad j \in \mathbb{N}, \tag{2.34}$$

where

$$\begin{aligned}
\alpha(\tau) &= 2\left(w^3 - b_4 w\right)\left(c_2 - \left(a_1 \mathrm{e}^{-\epsilon\tau} + a_2\right) w^2\right) - 2\left(a_3 w^2 - c_4\right)\left(b_1 \mathrm{e}^{-\epsilon\tau} + b_2\right) w, \\
\beta(\tau) &= -2\left(a_3 w^2 - c_4\right)\left(c_2 - \left(a_1 \mathrm{e}^{-\epsilon\tau} + a_2\right) w^2\right) - 2\left(w^3 - b_4 w\right)\left(b_1 \mathrm{e}^{-\epsilon\tau} + b_2\right) w, \\
\gamma(\tau) &= \left(a_3 w^2 - c_4\right)^2 + \left(w^3 - b_4 w\right)^2 + \left(c_2 - \left(a_1 \mathrm{e}^{-\epsilon\tau} + a_2\right) w^2\right)^2 + \left(b_1 \mathrm{e}^{-\epsilon\tau} + b_2\right)^2 w^2.
\end{aligned} \tag{2.35}$$

It is easy to see that since α, β, and γ depend on τ , one cannot obtain a closed form expression of the critical time-delay. We conclude with the following remark.

Remark (Case with equal time delays)**.** *In the case when maturation delay and the PTGS propagation delay coincide, i.e.* $\tau_1 = \tau_2 = \tau \neq 0$*, the characteristic equation (2.15) once again becomes an equation with a single time delay. However, similarly to the case just considered, the critical value of the time delay can only be found implicitly, as the coefficients of the characteristic equation themselves depend on the time delay. In the case where both* $\tau_1 > 0$ *and* $\tau_2 > 0$*, application of a methodology discussed in Gu et al. [***Gu05***] and Blyuss et al. [***Bly08***], would provide a parametrisation of critical time delays, but such parametrisation would also be implicit.*

2.5 Numerical stability analysis and simulations

In order to gain a better insight into how different parameters affect biological feasibility and stability of different steady states, as well as to understand the dynamics inside stability regions, especially when $\tau_{1,2} > 0$, we use a Matlab suite traceDDE [**Bre06**] to numerically compute eigenvalues of the characteristic equation (2.15). Since RNAi is known to be a complex multi-component process, obtaining accurate values for parameters to be used in the model is very problematic, especially since there is a significant variation in reported values for many of the parameters, and some cannot even be currently measured [**Mel11**, **Lia12**, **Him15**]. In light of this, we complement theoretical analysis from the previous sections by an extensive numerical bifurcation analysis of the model. This provides qualitative insights into possible dynamics, which can be further improved once more advanced measurement techniques are developed, and the precise mechanisms of PTGS are elucidated.

Fig. 2.3 shows the regions of stability of the disease-free steady state, as well as feasibility and stability of the endemic steady state. For parameter values specified in Table 2.1 and $k = 1$, it follows from Theorems 2.4.1 and 2.4.3 that the endemic steady state is only feasible for $\tau_1 \in [0, 5.05)$, whereas for $\tau_1 \geq 5.05$, the endemic steady state disappears, and the disease-free steady state becomes asymptotically stable, as shown in Figs. 2.3 (a) and (c). When the growth rate k is increased, a qualitatively similar picture is observed, however, there is some minimum value of τ_1, below which the endemic steady state is not biologically feasible. Figs. 2.3 (b) and (d) illustrate that in this case, the endemic steady state is only feasible for $\tau_1 \in [1.54, 7.36)$, and for $\tau_1 \geq 7.36$ the disease-free

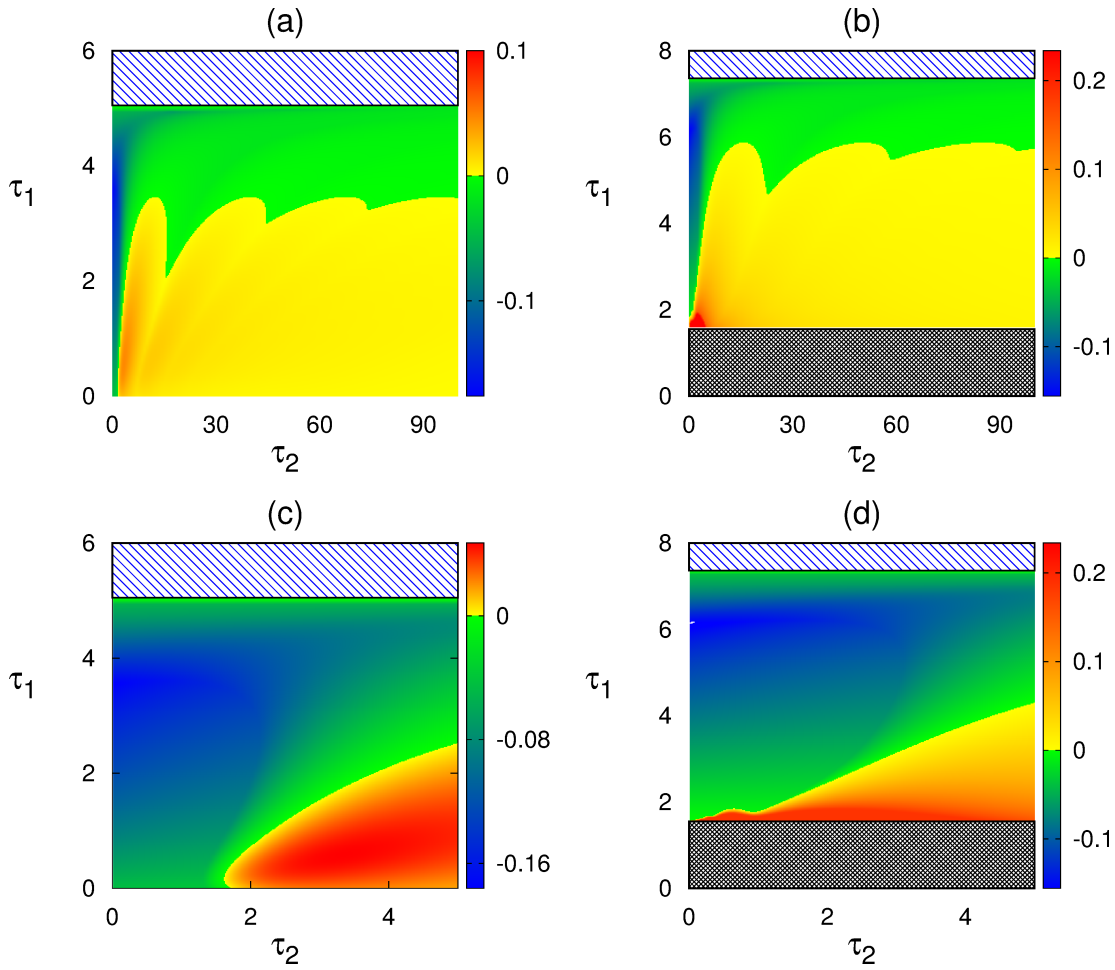

Figure 2.3: Stability of the endemic and disease-free steady states with parameter values from Table 2.1. (a) and (c) $k = 1$. (b) and (d) $k = 2$. Diagonal blue indicates the region where the disease-free steady state is asymptotically stable, and the endemic steady state is not feasible. The black grid shows the region where the endemic steady state is not feasible, and none of the steady states is stable. Colour code denotes max[Re(μ)] for the endemic steady state when it is feasible.

steady state is asymptotically stable. This figure suggests that by adequately increasing the time delay τ_2 after which susceptible cells acquire immunity, the endemic steady state can generally become unstable, whereas there are regions in which the solution of the system alternates between the stable endemic steady state and solutions of a periodic or possibly chaotic nature. From a biological perspective, this is an interesting and rather surprising result since intuitively one would expect that increasing the time delay associated with the spread of PTGS signal (i.e. time necessary to acquire immunity) would promote stabilization of the endemic steady state. We also note that the figure shows a region (black grid) in which there are no stable steady states and the endemic steady state is also not feasible. This would suggest a type of solution in which the population of susceptible cells $S(t)$ oscillates about $K(\tau_1)/\epsilon$ but the remaining state variables, namely $W(t)$ and $I(t)$ remain zero.

As a next step, we investigate how the relative values of the time delays and the amplification factor ϕ, affect stability of the steady states. Fig. 2.4(a) shows that the endemic steady state, when feasible, is asymptotically stable for sufficiently high values of the maturation delay τ_1, but can lose stability once τ_1 becomes lower than some critical value that is itself increasing with ϕ. This implies that both the higher amplification factor and the faster maturation of the new plant tissue are prone to make the endemic steady state, characterised by some permanent level of infection, unstable. Fig. 2.4(b) demonstrates the above-mentioned counter-intuitive result, which suggests that the endemic steady state is stable only for sufficiently fast-spreading PTGS signal, i.e. sufficiently small τ_2. Due to the functional form of the term representing recovery of infected cells associated with the spreading PTGS signal, it is natural to expect that the

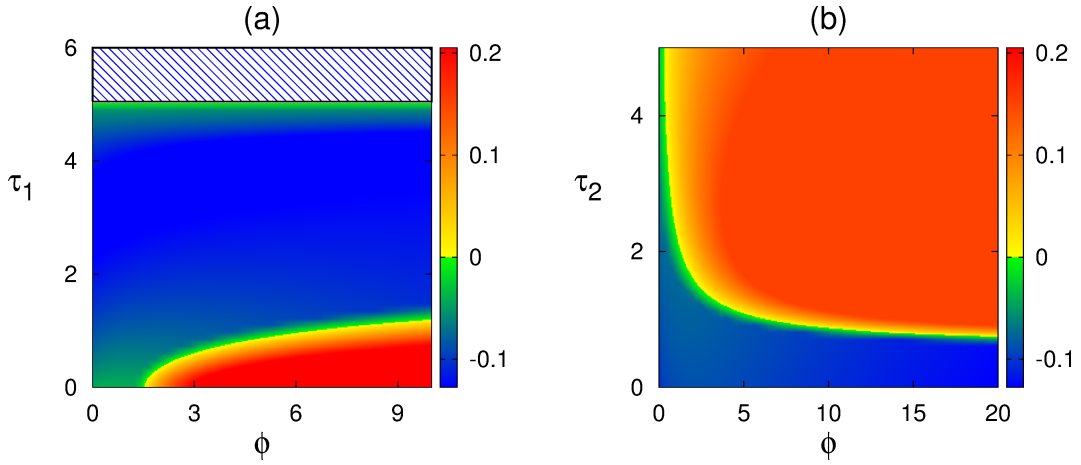

Figure 2.4: Stability of the endemic and disease-free steady states with parameter values from Table 2.1. Diagonal blue indicates the region where the disease-free steady state is asymptotically stable, and the endemic steady state is not feasible. Colour code denotes max[Re(μ)] for the endemic steady state when it is feasible.

critical time delay τ_2 would be inversely proportional to ϕ, and this is indeed what is observed in Fig. 2.4(b). It is noteworthy that in the parameter region where the endemic steady state is unstable, the disease-free steady state is also unstable. This highlights one of our earlier conclusions, namely that the amplification of recovery by the propagation of the warning signal, which in this case is transmitted from infected cells to other infected cells, has a limited impact on the outcome of the infection. Moreover, it is not by itself sufficient to achieve complete annihilation of the virus from its plant host.

Fig. 2.5 shows that if the infection rate λ is sufficiently small, or if the maturation of the growing tissue is sufficiently slow (i.e. τ_1 is large), the disease-free steady state is asymptotically stable. On the other hand, if the infection rate is high, the endemic steady state is asymptotically stable, and the PTGS propaga-

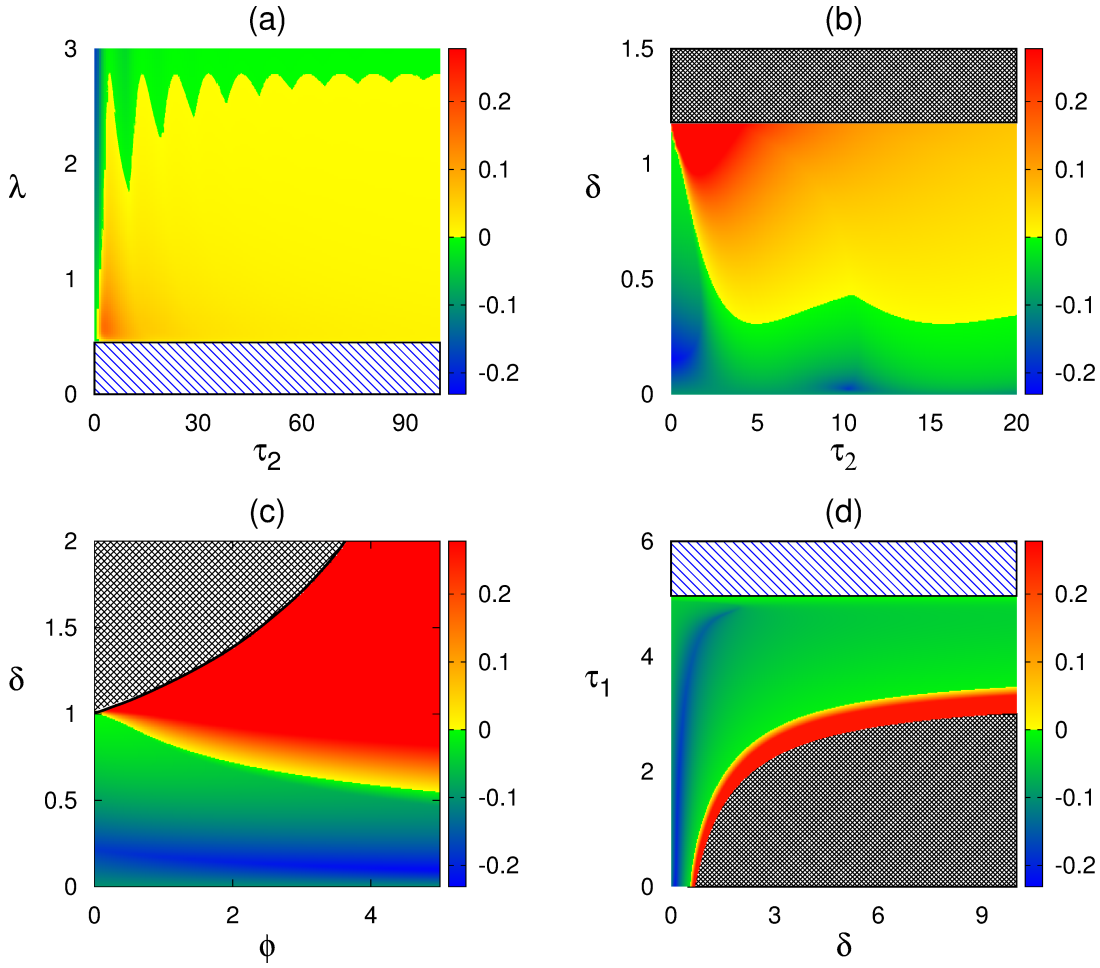

Figure 2.5: Stability of the endemic and disease-free steady states with parameter values from Table 2.1. Diagonal blue indicates the region where the disease-free steady state is asymptotically stable, and the endemic steady state is not feasible. The black grid shows the region where the endemic steady state is not feasible, and none of the steady states is stable. Colour code denotes max[Re(μ)] for the endemic steady state when it is feasible.

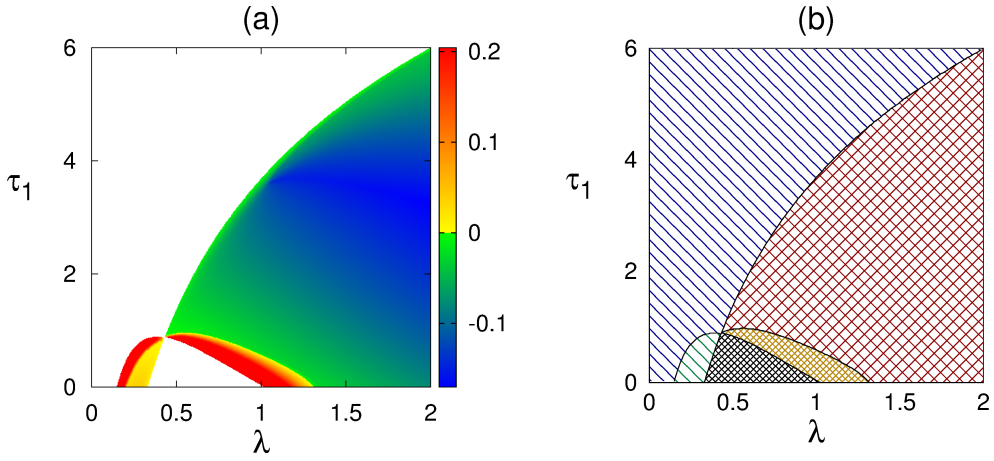

Figure 2.6: (a) Colour code denotes max[Re(μ)] for the endemic steady state when it is feasible. (b) Stability regions of all steady states with parameter values from Table 2.1. The black grid shows the region where the endemic steady state is not feasible, and none of the steady states is stable. The area covered with diagonal lines signifies the region where the disease-free steady state is asymptotically stable; in the region with green diagonal lines all steady states are feasible, whereas for blue lines the endemic steady state is not feasible. The red grid represents the area for which the endemic steady state is asymptotically stable. The brown grid shows the region where both the endemic and disease free steady state are feasible but none are stable.

tion delay τ_2 becomes irrelevant to the long-term behaviour of the system. One can observe that for a sufficiently small warning rate δ, the endemic steady state can be asymptotically stable for any value of τ_2, whereas if δ is large enough, neither endemic, nor disease-free steady states are stable. The same happens in the case when the new plant tissue is maturing fast, i.e. τ_1 is sufficiently small.

In Fig. 2.6 we have used the results from Theorems 2.4.1 and 2.4.3 to identify regions in which the system transitions from a stable disease-free to the endemic steady state. When all other parameters remain fixed, this figure suggests that there is a minimum value of λ for which the endemic steady state E_2 is

asymptotically stable provided that the time delay τ_1 is small enough. However, for any value of λ below that threshold, either the system reverts back to the stable disease-free steady state, or the time-delay τ_1 has to be within a specific range for the endemic steady state to be feasible and asymptotically stable. Our results up to this point suggest that τ_1 is perhaps the most important bifurcation parameter in the model. From a biological perspective, this can be explained by interpreting the time delay τ_1 as a temporary immunity inherent to the nature of proliferating and undifferentiated cells responsible for new growth. Equivalently, these results imply that whether or not the disease can successfully take over the plant depends on how fast the virus can gain access to the newly formed parts of the plant. If the infection rate is not sufficiently high, the infected parts of the plant will eventually die out before the newer generation of cells becomes vulnerable to infection.

Fig. 2.7 illustrates the regions of feasibility and stability of the disease-free and endemic steady states when the time delays are fixed, and other parameters are allowed to vary. Naturally, the disease-free steady state is stable for lower values of the disease transmission rate λ, while for higher λ there is a propensity for the endemic steady state to be stable. Higher speed of propagation of the PTGS signal δ and higher amplification factor ϕ lead to a de-stabilisation of the endemic steady state. It is worth noting the behaviour shown in Figs. 2.7(c) and (d), where for sufficiently high amplification rate, increase in the disease transmission rate λ also destabilises the endemic steady state.

To illustrate different types of dynamical behaviour that can be exhibited by the model (2.3), we solve this system numerically with parameter values given in Table 2.1 and different values of the time delays τ_1 and τ_2. Figs 2.8(a), (c)

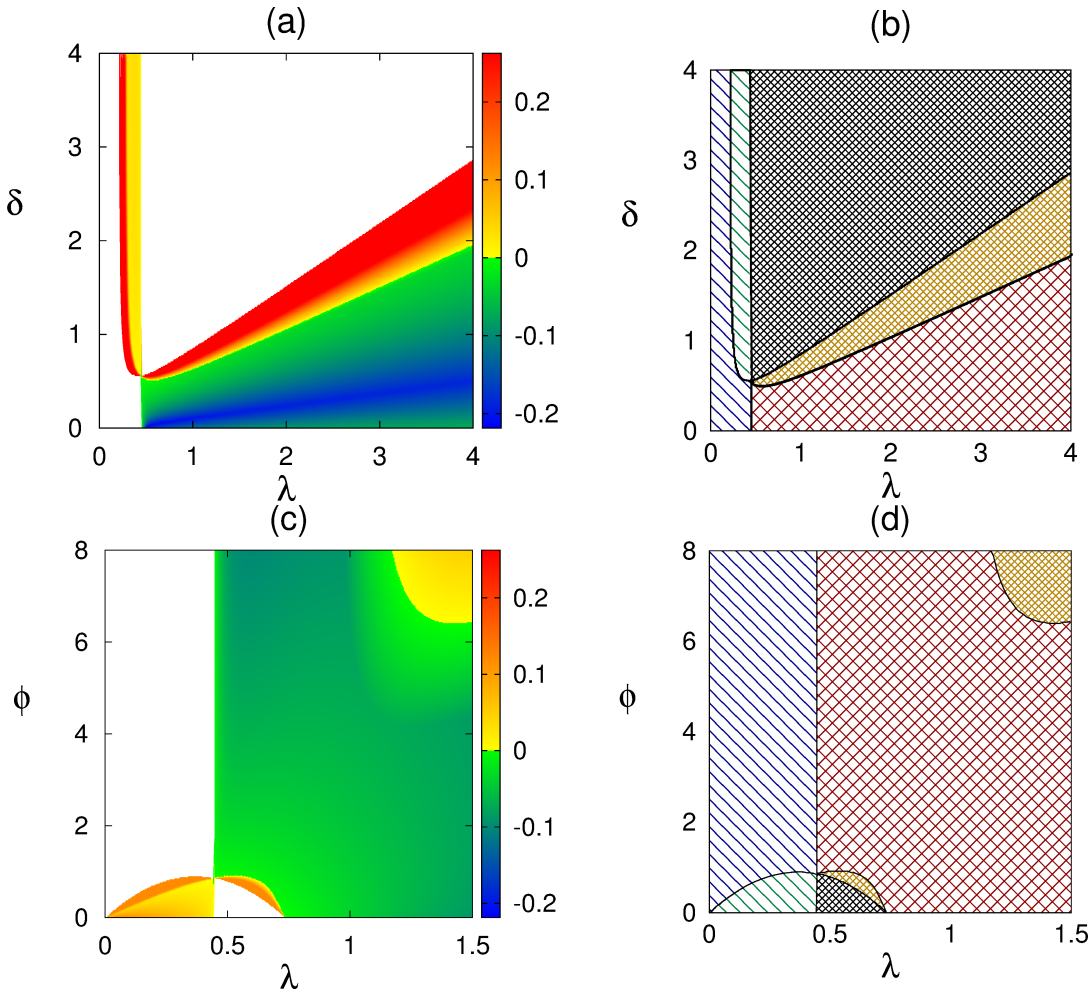

Figure 2.7: (a), (c) Colour code denotes max[Re(μ)] for the endemic steady state when it is feasible. (b), (d) Stability regions of all steady states with parameter values from Table 2.1. The black grid shows the region where the endemic steady state is not feasible, and none of the steady states is stable. The area covered with diagonal lines signifies the region where the disease-free steady state is asymptotically stable; in the region with green diagonal lines all steady states are feasible, whereas for blue lines the endemic steady state is not feasible. The red grid represents the area for which the endemic steady state is asymptotically stable. The brown grid shows the region where both the endemic and disease free steady state are feasible but none are stable.

and (d) demonstrate partial immune response that is not sufficient to eradicate the virus in the host. This is the type of behaviour one might expect from susceptible plants with a weak response against a viral disease, and it results in a chronic condition. Another possibility for a chronic infection is represented by periodic solutions shown in Fig. 2.8(b) and (e), where the severity of infection varies over time, with periods of high viral production being interspersed with periods of quiescence. From a biological perspective, these scenarios could be interpreted as situations where the evolutionary race between viral pathogen and the host immune system has not yet concluded and, as a result, neither the plants immune system, nor the ability of the virus to suppress immune responses can prevail. Fig. 2.8(f) demonstrates a type of immune response consistent with a recovery phenotype, where initially the disease appears to overwhelm the plant by infecting a dominating or significant part of its body. However, as the warning signal propagates to surrounding cells, newly grown tissue and uninfected cells are able to acquire immunity and thus prevent the spread of the disease. This localizes the infection and eventually leads to the eradication of the invading virus, and consequently the system approaches a disease-free steady state. Similar type of behaviour is observed in the system with a very strong immune response that would be consistent with highly resistant plants; in this case the infection is almost immediately localized due to the high efficacy of the propagating warning signal and the antiviral activity in the cells that are already infected.

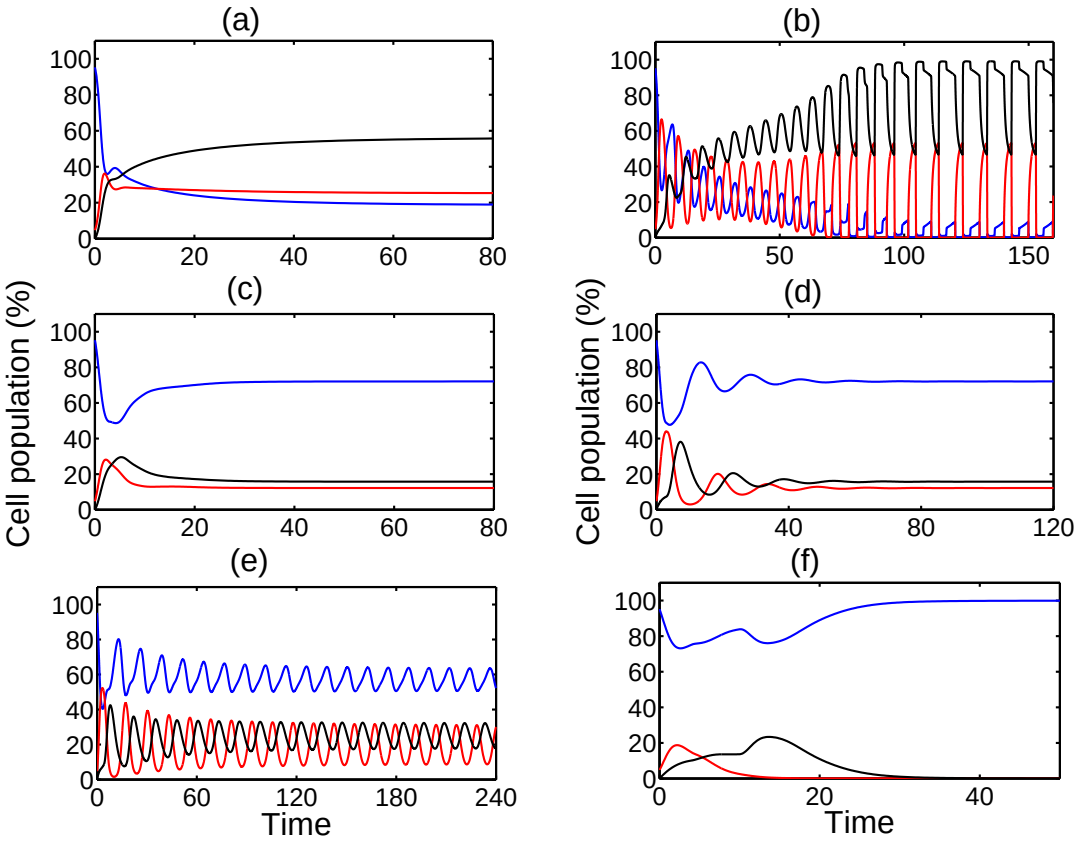

Figure 2.8: Numerical solution of the system (2.3) with parameter values from Table 2.1. (a) $\tau_1 = \tau_2 = 0$. (b) $\tau_1 = 0$, $\tau_2 = 3$. (c) $\tau_1 = 3$, $\tau_2 = 0$. (d) $\tau_1 = \tau_2 = 3$. (e) $\tau_1 = 2$, $\tau_2 = 4$. (f) $\tau_1 = 4$, $\tau_2 = 10$, $\sigma = 1$, $\phi = 0.1$. Colours represent scaled populations of susceptible S (blue), infected I (red) and warned W cells (black).

2.6 Chapter conclusions

In this chapter we have developed and analysed a new mathematical model of the plant immune response to a viral infection, with particular emphasis on the role of RNA interference. To achieve better biological realism, this model explicitly includes two different time delays, one to represent maturation period of undifferentiated cells which effectively acts as a form of inherent immunity against infection, and another to account for the time required for the PTGS signal to reach other parts of the plant resulting in either recovery or warning of susceptible cells.

Stability analysis of the model has demonstrated the role played by system parameters in the dynamics. In the present model, it is impossible for all plant cells to die due to the constant emergence of new susceptible cells. Even if a plant were to experience a severe case of stunting due to the infection, it would be highly unlikely that every healthy cell would become infected and therefore, lead to the death of the plant. Although our model cannot capture this scenario, realistically, such events do occur quite rarely in nature depending also on the environmental and host conditions at the time of infection [**Sut99**, **Ger06**]. Stability of the disease-free steady state appears to depend only on the maturation period but not on the speed of propagation or the strength of the PTGS signal, suggesting that a faster PTGS signal can at most help the plant to recover faster, but by itself it is not sufficient for a recovery. Endemic steady state, where the plant supports some constant level of infection, is only biologically feasible when the growth rate of the new tissue is higher than some minimum value. An interesting and counter-intuitive result is that slower PTGS signal (i.e. larger value of τ_2) can actually lead to a destabilisation of this

steady state, resulting in sustained periodic oscillations. Another possibility for the endemic steady state to lose stability is when the amplification factor ϕ increases, or the new uninfected tissue is produced faster, i.e. for a lower maturation time delay τ_1.

Numerical simulations have shown that the model can support resistant- and recovery-type behaviours, whereby the plant immune system is able to mount sufficient response to eradicate the infection. Both of these situations are characterised by a strong localised immune response, but if additionally the warning signal is sufficiently strong, the plant exhibits the resistant phenotype, where the spread of infection is almost fully prevented, and the amount of the virus is diminished significantly faster than in the recovery case. On the other hand, if both the localised immune response and the propagating signal are sufficiently weak, the plant will be very susceptible to infection, however, the infection cannot result in the death of the host in our model. Periodic solutions of the model signify specific cases where the plant immune system cannot mount a sufficient response to eradicate the virus, and at the same time the virus also cannot adequately suppress the immune response of the plant. As a result, the plant undergoes periods of time in which the symptoms of the disease are manifested more prominently, with other periods where the infection is at a very low level.

Simulations suggest that the propagating component of the PTGS has a very limited impact on the long-term recovery of the plant. At the same time, the duration of the maturation period of undifferentiated cells does play a very important role in controlling the spread of the infection, as it represents how fast the newly developed part of the plant becomes accessible to the virus.

Chapter 3

Model of plant-virus interactions mediated by RNA interference

3.1 Introduction

In this chapter we derive and analyse a new mathematical model of the interactions between two competing viruses with particular account for RNA interference. Our results will show that co-infection of the host can either increase or decrease the potency of individual infections depending on the levels of cross-protection or cross-enhancement between different viruses. Analytical and numerical bifurcation analyses are employed to investigate the stability of all steady states of the model in order to identify parameter regions where the system exhibits synergistic or antagonistic behaviour between viral strains, as well as different types of host recovery. We show that not only viral attributes but also the propagating component of RNA-interference in plants can play an important role in determining the dynamics.

3.2 Model derivation

To investigate the dynamics of biological interactions taking place during a co-infection of a plant with two viruses, we divide the total population of plant cells into the following compartments: susceptible cells $S(t)$, populations $I_1(t)$ and $I_2(t)$ of cells infectious with virus 1 or virus 2 and warned cells $W_1(t)$ and $W_2(t)$ that are immune to viruses 1 and 2 respectively. We also include the cells $H_i(t)$, $i = 1, 2$ that have recovered from a primary infection from virus $j \neq i$, and are currently infectious with the virus i. That is to say, for example, that $H_1(t)$ denotes the cells which have been previously infected by virus 2, have recovered from virus 2 and are now infected by virus 1. Finally, we have the population of super-protected cells $W_{12}(t)$ that are immune to both viruses. Transitions between these different cell populations are illustrated in Fig. 3.1.

For the sake of model simplicity, spatial components associated with host-specific anatomy will not be considered, and the cell populations are assumed to be uniformly distributed within the plant. Despite potentially overlooking some aspects of the dynamics, the assumption of spatial uniformity has been effective in understanding viral dynamics [**Per02**, **Wod02**]. Non-spatial models can provide significant insights into the dynamics and become the basis upon which more detailed models can be built. Additionally, in the case of field plants, it is biologically reasonable to assume that multiple infection sites could be distributed all over the host. Targeted plants could be exposed multiple times during vector movement or feeding, as vector-borne pathogens have been found capable of even altering the phenotypes of their hosts and vectors in such a way that the frequency and the nature of interactions between them promotes the transmission of the disease [**Mau10**, **Mor13**]. Furthermore, all

plant cells are connected through plasmodesmata, the phloem and the xylem vessels responsible for resource translocation [**Lal04**], and these pathways can also be used by viruses for systemic infections of their host [**Opa98**, **Wan15**].

Plant growth models can generally be divided into two classes: the ones where cell populations are allowed to exhibit unbounded growth, and the ones that assume a certain asymptotic final size due to finite resources or ontogenetic changes, like flowering of the plant. Asymptotic growth models are more favourable in the studies which consider the entire lifespan of the plant [**Pai12**, **Hei99**]. Hence, we will describe plant growth by the logistic growth function with a linear growth factor r and a carrying capacity K, with all cell populations contributing to the competition term, as has been effectively done in other models of immune response to infections, such as influenza [**Tri10**], HIV [**Per99**] and HBV [**Ciu07**].

Once a plant becomes infected, infected cell populations $I_1(t)$ and $I_2(t)$ produce new infections by infecting susceptible (healthy) cells at rates λ_1 and λ_2, respectively. Due to various metabolic changes and the loss of functions that occur after a viral takeover, the lifespan of infected cells is normally shorter than that of healthy cells, as characterised by higher death rates ϵ_1 and ϵ_2. Another possible explanation of a premature death of infected cells is given by the hypersensitive response of the plant, where infected cells would be programmed to a premature death in order to avoid the spread of the infection and to isolate the infectious site [**Zve12**, **Hir98**, **Fri07**].

For this study it will be assumed that a viral infection does not always have a devastating effect on the cell, and hence it is possible for infected cells to recover before experiencing critical damage. Such recovered cells, denoted by $W_1(t)$ and

$W_2(t)$, will be considered immune to the corresponding viruses in a sense that they are no longer infectious. The recovery rates σ_1 and σ_2 represent cumulative effects of the two events mentioned above and represent the rates of transition from infected to warned compartments for each of the two viruses. As described in the Introduction, one of the core mechanisms of the plant immune system is the ability to spread a warning signal that is initiated at infectious sites to other parts of the plant, and to protect neighbouring cells against the imminent virus infection. For the sake of simplicity, the cells that have acquired immunity via this warning signal are also included in $W_1(t)$ and $W_2(t)$ populations. We assume that infected cells initiate and spread the warning signal to healthy cells at the rates δ_1 and δ_2, respectively. Cells that have been the recipients of the propagating signal for both viruses or have recovered from both a primary and a subsequent secondary infection will be represented by the super-protected population of cells $W_{12}(t)$ taken to be immune to both viruses. Thus, warned cells $W_1(t)$ and $W_2(t)$ will be recruited to the super-protected population $W_{12}(t)$ at modified warning rates $\gamma_2\delta_2$ and $\gamma_1\delta_1$, respectively. It is important to note that the resistance to the disease is almost always accompanied by a reduction of fitness normally represented by a reduced reproduction capability of cells [**Bur03**, **Tia03**]. In this model we assume no fitness cost in the traditional way, however, immune cells might also experience a shorter lifespan compared to susceptible cells and, therefore, some fitness cost can be implemented by choosing the appropriate death rate ϵ_0 for super-protected cells $W_{12}(t)$.

The warned cells that have acquired immunity to a primary infection but have successfully been infected by a secondary infection will be denoted by $H_i(t)$, where the index $i = 1, 2$ signifies the current infectious state of the cell.

Because of their acquired immunity to one of the viruses, these cells may be less or more resistant to the other virus. If the degree of homology between the two viruses is high, i.e the two viruses are closely immunologically related, it would imply that a cell which is immune or highly resistant to one of the viruses would express the same amount of resistance to both of viruses. On the other hand, if the two viruses are not related, it is reasonable to assume that expressing an antiviral resistance to one of the viruses could induce a susceptibility to a secondary non-related infection by reducing the efficacy of the immune response.

From a biological perspective there could be a limited number of components in the cell that can be used to mount an immune response against a viral infection. For example, unless a cell is warned by both propagating signals, it might be the case that all components able to form antiviral complexes within the cell are being used to prepare only for a single infection, or that there might not be enough components in general to mount a sufficient immune response to both infections simultaneously. Moreover, chemical changes within the cell introduced during the primary infection and the corresponding immune response could potentially provide more favourable conditions in which the secondary infection is established more easily. In light of these observations, the infectious cells $H_1(t)$ and $H_2(t)$ will infect other cells at the modified infection rates $a_1\lambda_1$ and $a_2\lambda_2$ to account for either enhanced ($a_{1,2} > 1$) or reduced ($a_{1,2} < 1$) viral transmissibility. Similarly, we introduce the susceptibility modifiers β_1 and β_2 for the warned cells $W_2(t)$ and $W_1(t)$, respectively, which will be assumed to be either susceptible ($\beta_{1,2} > 1$) or resistant ($\beta_{1,2} < 1$) to the virus against which they have not yet acquired immunity. To account for a prior infection, the recovery rates of cells H_i are modified by the factors p_i, so these cells are re-

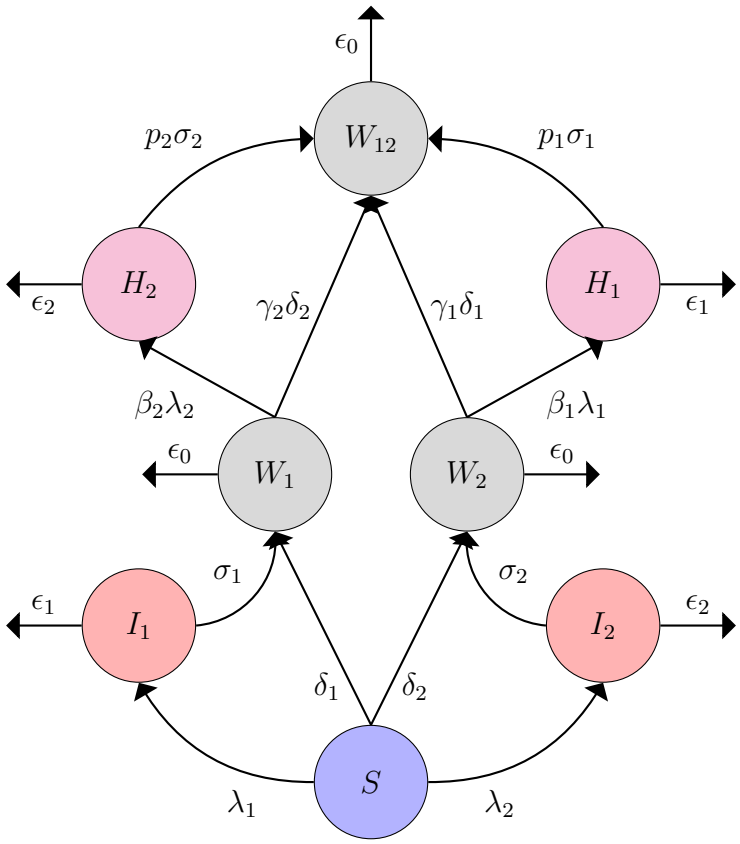

Figure 3.1: A diagram of interactions between two competing viruses and the corresponding plant immune response. Here S denotes the susceptible cells, $I_{1,2}$ and $W_{1,2}$ are the infected and the warned cells for each virus, respectively. Warned cells subsequently infected by a primary or secondary virus are denoted by H_1 and H_2. Finally, W_{12} denotes the super-protected cells immune to both viruses. The arrows indicate the rates of transitions from one category of cells to another.

cruited into the super-protected population at rates $p_1\sigma_1$ and $p_2\sigma_2$, respectively. Therefore, in this model the parameters that define viral cooperation will be the modifiers $a_i,\ \beta_i$ and p_i, which can be interpreted as either functions of the antigenic distance or other specific relation between two viruses. For simplicity, we will ignore the possibility of random mutations, so that these modifiers will remain constant.

Under the above assumptions, the model describing the dynamics of plant immune response to two viral infections can be written as follows,

$$\begin{aligned}
\frac{dS}{dt} &= r\widehat{S}\left(1-\frac{N}{K}\right) - S\left[(\lambda_1+\delta_1)I_1 + (\lambda_2+\delta_2)I_2 + a_2\lambda_2 H_2 + a_1\lambda_1 H_1\right], \\
\frac{dI_1}{dt} &= I_1(\lambda_1 S - \sigma_1 - \epsilon_1) + a_1\lambda_1 H_1 S, \\
\frac{dI_2}{dt} &= I_2(\lambda_2 S - \sigma_2 - \epsilon_2) + a_2\lambda_2 H_2 S, \\
\frac{dW_1}{dt} &= I_1(\sigma_1 + \delta_1 S) - W_1\left[\epsilon_0 + (\beta_2\lambda_2 + \gamma_2\delta_2)I_2 + \beta_2 a_2\lambda_2 H_2\right], \\
\frac{dW_2}{dt} &= I_2(\sigma_2 + \delta_2 S) - W_2\left[\epsilon_0 + (\beta_1\lambda_1 + \gamma_1\delta_1)I_1 + \beta_1 a_1\lambda_1 H_1\right], \\
\frac{dH_1}{dt} &= W_2(\beta_1\lambda_1 I_1 + \beta_1 a_1\lambda_1 H_1) - H_1(\epsilon_1 + p_1\sigma_1), \\
\frac{dH_2}{dt} &= W_1(\beta_2\lambda_2 I_2 + \beta_2 a_2\lambda_2 H_2) - H_2(\epsilon_2 + p_2\sigma_2),
\end{aligned} \tag{3.1}$$

$$\frac{dW_{12}}{dt} = p_1\sigma_1 H_1 + p_2\sigma_2 H_2 + \gamma_2\delta_2 I_2 W_1 + \gamma_1\delta_1 I_1 W_2 - \epsilon_0 W_{12}, \tag{3.2}$$

where, for convenience of writing, we have used $\widehat{S}(t) = S(t) + W_1(t) + W_2(t) + W_{12}(t)$, and where $N(t) = S(t) + I_1(t) + I_2(t) + W_1(t) + W_2(t) + H_1(t) + H_2(t) + W_{12}(t)$ is the total population of plant cells. Note that the total population of cells in not fixed. As a first step of the analysis, we establish well-posedness of the system (3.1).

Theorem 3.2.1 (Positivity and boundedness of solutions)**.** *The model (3.1) with initial conditions*

$$S(0) > 0, \quad I_1(0) \geq 0, \quad I_2(0) \geq 0, \quad W_1(0) \geq 0, \quad W_2(0) \geq 0,$$

$$H_1(0) \geq 0, \quad H_2(0) \geq 0, \quad W_{12}(0) \geq 0,$$

and $N(0) = N_0 < K$ is well-posed, i.e. its solutions remain non-negative and bounded for all $t \geq 0$.

Proof. Let T_2 be a period of time, such that $N(t) < K$ for $t \in [0, T_2]$, and suppose $T_1 \leq T_2$ is the first time such that $S(T_1) = 0$. This implies that

$$\dot{S}(T_1) = r(W_1 + W_2 + W_{12})[1 - (W_1 + W_2 + W_{12} + I_1 + I_2 + H_1 + H_2)/K] \geq 0,$$

hence, for any $0 \leq t \leq T_2$, we have that $S(t) \geq 0$. For the remaining variables, considering any positive time t, if for any $i = 1, 2$ we have that $I_i(t) = 0$, this implies that $\dot{I}_i(t) = a_i\lambda_i H_i \geq 0$, thus $I_i(t)$ must be non-negative for all times. Likewise, for both $W_i(t) = 0$ we obtain $\dot{W}_i(t) = I_i(\sigma_i + \delta_i S) \geq 0$ which shows that $W_i(t) \geq 0$. If $H_i(t) = 0$, we have $\dot{H}_i(t) = W_j\beta_i\lambda_i I_i \geq 0$ with $1 \leq i \neq j \leq 2$.

Finally, for $W_{12}(t) = 0$, we have that $\dot{W}_{12}(t) \geq 0$. Thus, all variables remain non-negative for $t \in [0, T_2]$.

We now prove, by contradiction, that, in fact, $N(t) < K$ for all $t \geq 0$. Assume, for a contradiction, that there is a first time $T_2 > 0$ at which the inequality $N(t) < K$ ceases to hold. Since T_2 is the first such time, $N(T_2) = K$ and $\dot{N}(T_2) \geq 0$. As has been shown earlier, all state variables are non-negative at $t = T_2$. Adding up all equations of the system (3.1) yields

$$\frac{dN}{dt} = r\hat{S}(1 - N/K) - \epsilon_1 I_1 - \epsilon_2 I_2 - \epsilon_0(W_1 + W_2) - \epsilon_1 H_1 - \epsilon_2 H_2 - \epsilon_0 W_{12}, \quad (3.3)$$

Since at $t = T_2$ we have that $N(T_2) = K$, the last equation gives $\dot{N}(T_2) < 0$, which is a contradiction, unless $I_1(T_2) = I_2(T_2) = W_1(T_2) = W_2(T_2) = H_1(T_2) = H_2(T_2) = W_{12}(T_2) = 0$. But in this exceptional case, the initial value theorem for ODEs, applied to the last 7 equations of system (3.1) with S considered as a prescribed function, yields that $I_1(t) = I_2(t) = W_1(t) = W_2(t) = H_1(t) = H_2(t) = W_{12}(t) = 0$ for all $t > T_2$ and the equation for $S(t)$ (the first equation of the system) reduces to the logistic equation $\dot{S} = rS(1 - S/K)$. Thus, for any $t \geq T_2$, we have $0 < S(t) \leq K$, which completes the proof. □

To simplify the model and reduce the number of free parameters, we non-dimensionalise the system (3.1) by introducing new dimensionless variables

$$\tau = rt, \quad u_1 = \frac{S}{K}, \quad u_2 = \frac{I_1}{K}, \quad u_3 = \frac{I_2}{K}, \quad u_4 = \frac{W_1}{K},$$

$$u_5 = \frac{W_2}{K}, \quad u_6 = \frac{H_1}{K}, \quad u_7 = \frac{H_2}{K}, \quad u_8 = \frac{W_{12}}{K},$$

and for $i = 1, 2$, parameters

$$L_i = \frac{\lambda_i}{r}, \quad d_i = \frac{K\delta_i}{r}, \quad e_i = \frac{\epsilon_i}{r}, \quad s_i = \frac{\sigma_i}{r}, \qquad e_0 = \frac{\epsilon_0}{r}.$$

This gives the following modified system

$$\begin{aligned}
\frac{du_1}{d\tau} &= \widehat{u}_1(1-\widehat{N}) - u_1\left[(L_1+d_1)\,u_2 + (L_2+d_2)\,u_3 + a_1L_1u_6 + a_2L_2u_7\right],\\
\frac{du_2}{d\tau} &= L_1\left(a_1u_6+u_2\right)u_1 - u_2\left(e_1+s_1\right),\\
\frac{du_3}{d\tau} &= L_2\left(a_2u_7+u_3\right)u_1 - u_3\left(e_2+s_2\right),\\
\frac{du_4}{d\tau} &= u_2\left(d_1u_1+s_1\right) - u_4\left[(\beta_2L_2+\gamma_2d_2)\,u_3 + \beta_2a_2L_2u_7 + e_0\right],\\
\frac{du_5}{d\tau} &= u_3\left(d_2u_1+s_2\right) - u_5\left[(\beta_1L_1+\gamma_1d_1)\,u_2 + \beta_1a_1L_1u_6 + e_0\right],\\
\frac{du_6}{d\tau} &= \beta_1L_1\left(a_1u_6+u_2\right)u_5 - u_6\left(p_1s_1+e_1\right),\\
\frac{du_7}{d\tau} &= \beta_2L_2\left(a_2u_7+u_3\right)u_4 - u_7\left(p_2s_2+e_2\right),\\
\frac{du_8}{d\tau} &= \gamma_1d_1u_2u_5 + \gamma_2d_2u_3u_4 + p_1s_1u_6 + p_2s_2u_7 - e_0u_8,
\end{aligned} \tag{3.4}$$

where $\widehat{u}_1 = u_1 + u_4 + u_5 + u_8$ and $\widehat{N} = \widehat{u}_1 + u_2 + u_3 + u_6 + u_7$.

3.3 Steady states

It is straightforward to see that independently of the values of parameters, the system (3.4) always admits a trivial steady state

$$E_0 = (0, 0, 0, 0, 0, 0, 0, 0), \tag{3.5}$$

and a disease-free steady state given by

$$E_{DF} = (1, 0, 0, 0, 0, 0, 0, 0). \tag{3.6}$$

Looking for steady states of the system (3.4) with $u_2 = 0$ and $u_{1,3} \neq 0$, gives $u_4 = u_6 = u_7 = u_8 = 0$. Substituting these values in the remaining equations of system (3.4) gives a one-virus endemic steady state with virus 2 present

$$E_2 = (u_1^*, 0, u_3^*, 0, u_5^*, 0, 0), \tag{3.7}$$

where

$$u_1^* = \frac{e_2 + s_2}{L_2}, \quad u_3^* = \frac{-c_1(u_1^*) - \sqrt{c_1^2(u_1^*) - 4c_2(u_1^*)c_0(u_1^*)}}{2c_2(u_1^*)}, \quad u_5^* = A(u_1^*)u_3^*,$$

with

$$A(u_1^*) = \frac{d_2 u_1^* + s_2}{e_0}, \quad B = L_2 + d_2, \quad c_0(u_1^*) = u_1^*(1 - u_1^*),$$

$$c_1(u_1^*) = A(u_1^*) - u_1^*[2A(u_1^*) + B + 1], \quad c_2(u_1^*) = -A(u_1^*)[A(u_1^*) + 1].$$

The steady state E_2 is biologically feasible, as long as the condition $e_2 + s_2 < L_2$

holds.

Proceeding in a similar manner, one can find the second one-virus endemic steady state E_1 corresponding to the presence of virus 1 only. This steady state is explicitly given by

$$E_1 = (\widetilde{u}_1^*, u_2^*, 0, u_4^*, 0, 0, 0), \tag{3.8}$$

where now

$$\widetilde{u}_1^* = \frac{e_1 + s_1}{L_1}, \quad u_2^* = \frac{-\widetilde{c}_1(\widetilde{u}_1^*) - \sqrt{\widetilde{c}_1^2(\widetilde{u}_1^*) - 4\widetilde{c}_2(\widetilde{u}_1^*)\widetilde{c}_0(u_1^*)}}{2\widetilde{c}_2(u_1^*)}, \quad u_4^* = \widetilde{A}(\widetilde{u}_1^*)u_2^*,$$

with

$$\widetilde{A}(\widetilde{u}_1^*) = \frac{d_1\widetilde{u}_1^* + s_1}{e_0}, \quad \widetilde{B} = L_1 + d_1, \quad \widetilde{c}_0(\widetilde{u}_1^*) = \widetilde{u}_1^*(1 - \widetilde{u}_1^*),$$

$$\widetilde{c}_1(\widetilde{u}_1^*) = \widetilde{A}(\widetilde{u}_1^*) - \widetilde{u}_1^*[2\widetilde{A}(\widetilde{u}_1^*) + \widetilde{B} + 1], \quad \widetilde{c}_2(\widetilde{u}_1^*) = -\widetilde{A}(\widetilde{u}_1^*)[\widetilde{A}(\widetilde{u}_1^*) + 1].$$

This steady state is biologically feasible whenever the condition $e_1 + s_1 < L_1$ is satisfied.

Besides the disease-free and the two one-virus endemic steady states, the system (3.4) can support one or more *syndemic* steady states characterised by the simultaneous presence of both viruses,

$$S = (u_1^*, u_2^*, u_3^*, u_4^*, u_5^*, u_6^*, u_7^*, u_8^*). \tag{3.9}$$

To find this steady state, let us introduce auxiliary variables and functions

$$u_0 = \min_{i=1,2}\left(\frac{e_i + s_i}{L_i}\right), \quad F_i(x) = -\frac{(L_i x - e_i - s_i)}{L_i a_i x}, \quad i = 1, 2,$$
$$\Delta_i(x) = \beta_i L_i (F_i(x) a_i + 1) + d_i \gamma_i, \quad G_i(x) = d_i x + s_i, \quad i = 1, 2, \tag{3.10}$$

which allow us to express all steady state variables through u_1^* in the following way:

$$u_4^* = \frac{F_2\left(u_1^*\right)\left(p_2 s_2 + e_2\right)}{\beta_2 L_2\left[a_2 F_2\left(u_1^*\right) + 1\right]}, \quad u_5^* = \frac{F_1\left(u_1^*\right)\left(p_1 s_1 + e_1\right)}{\beta_1 L_1\left[a_1 F_1\left(u_1^*\right) + 1\right]},$$

$$u_2^* = \frac{e_0 u_4^*\left[\Delta_2\left(u_1^*\right) u_5^* + G_2\left(u_1^*\right)\right]}{G_1\left(u_1^*\right) G_2\left(u_1^*\right) - \Delta_1\left(u_1^*\right)\Delta_2\left(u_1^*\right) u_4^* u_5^*}, \quad u_3^* = \frac{e_0 u_5^*\left[\Delta_1\left(u_1^*\right) u_4^* + G_1\left(u_1^*\right)\right]}{G_1\left(u_1^*\right) G_2\left(u_1^*\right) - \Delta_1\left(u_1^*\right)\Delta_2\left(u_1^*\right) u_4^* u_5^*},$$

$$u_6^* = u_2^* F_1(u_1^*), \quad u_7^* = u_3^* F_2(u_1^*),$$

$$u_8^* = \frac{d_1\gamma_1 u_2^* u_5^* + d_2\gamma_2 u_3^* u_4^* + p_1 s_1 u_6^* + p_2 s_2 u_7^*}{e_0}.$$

Substituting these expressions into

$$\hat{u}_1^*(1 - \hat{N}) - u_1^*\left[\left(L_1 + d_1\right) u_2^* + \left(L_2 + d_2\right) u_3^* + a_1 L_1 u_6^* + a_2 L_2 u_7^*\right] = 0,$$

yields a polynomial equation for u_1^*, whose roots give possible candidates for the syndemic steady state. This steady state is biologically feasible if

$$0 < u_1^* < u_0, \quad G_1\left(u_1^*\right) G_2\left(u_1^*\right) - \Delta_1\left(u_1^*\right)\Delta_2\left(u_1^*\right) u_4^* u_5^* > 0.$$

3.4 Stability Analysis

3.4.1 Trivial steady state

Linearising system (3.4) near the trivial steady state E_0 gives the following characteristic equation for eigenvalues μ:

$$(\mu - 1)\,(\mu + e_0)^3 \prod_{i=1}^{2} (\mu + e_i + s_i)(\mu + p_i s_i + e_i) = 0.$$

Since one of the roots is $\mu = 1$, this implies that the trivial steady state is always unstable and, therefore, it is impossible for all cell populations to die out.

3.4.2 Disease-free steady state

Linearisation near the disease-free steady state E_{DF} has a characteristic equation

$$(\mu + 1)\,(\mu + e_0)^3 \prod_{i=1}^{2} (p_i s_i + \mu + e_i)\,(\mu - L_i + e_i + s_i) = 0, \tag{3.11}$$

implying that the disease-free steady state E_{DF} is linearly asymptotically stable, provided $u_0 > 1$, with u_0 defined in (3.10). In epidemiology, one of the most common and efficient techniques for establishing criteria for the onset of epidemic outbreaks is the analysis of the *basic reproduction number* R_0, defined as the average number of secondary infections produced by a single infected individual in a totally susceptible population [**Die93**, **Hee96**, **Het00**, **Dri08**]. This quantity can be derived in a number of ways, e.g. using the next generation approach [**Dri08**], we define the basic reproduction number for each of the

viruses as follows

$$R_{01} = \frac{L_1}{e_1 + s_1}, \qquad R_{02} = \frac{L_2}{e_2 + s_2}, \tag{3.12}$$

and denote $R_0 = \max\{R_{01}, R_{02}\} = {u_0}^{-1}$. Then, the disease-free steady state E_{DF} is linearly asymptotically stable if $R_0 < 1$. This result means that a complete recovery from both viral infections depends on the efficacy of RNA interference from local induction, i.e the ability of the host cell to target and degrade viral RNA in order to inhibit viral multiplication, and also on whether infected cells reach their limited lifespan faster than they can spread the disease for each virus, respectively. Furthermore, since the basic reproduction number R_0 does not depend on the transmissibility ($a_{1,2}$) or susceptibility ($\beta_{1,2}$) modifiers, this implies that the interactions between the two viruses during the host co-infection cannot cause both viruses to become extinct. On the other hand, the modifiers may determine whether both viruses, or only one of them will survive.

3.4.3 Endemic steady states

Characteristic equation of linearisation near the (one virus) endemic steady state E_2 can be factorised into

$$X_1(\mu)X_2(\mu)X_3(\mu) = 0, \tag{3.13}$$

where

$$X_1(\mu) = (\mu + e_0)\,(p_2 s_2 + \mu + e_2)\,[u_3^*\,(L_2\beta_2 + d_2\gamma_2) + \mu + e_0]\,,$$

$$X_2(\mu) = \mu^2 + x_{21}\mu + x_{20}, \qquad X_3(\mu) = \mu^3 + x_{32}\mu^2 + x_{31}\mu + x_{30},$$

and

$$\begin{cases} x_{21} = s_1(p_1+1) + 2e_1 - L_1(a_1\beta_1 u_5^* + u_1^*), \\ \\ x_{20} = (p_1 s_1 + e_1)(e_1 + s_1 - L_1 u_1^*) - L_1 a_1 \beta_1 (e_1 + s_1) u_5^*, \\ \\ x_{32} = 2u_1^* + (L_2 + d_2 + 1)\,u_3^* + 2u_5^* + e_0 - 1, \\ \\ x_{31} = d_1(u_3^*)^2 + [(L_2 + d_2)[u_1^*(L_2+1) + u_5 + e_0] + d_2(u_1^* + u_5^* - 1) + e_0]\,u_3^* \\ \qquad +e_0(2u_1^* + 2u_5^* - 1), \\ \\ x_{30} = L_2 u_3^*\,[d_2 u_1^*\,(2(u_1^* + u_5^*) + u_3^* + e_0 - 1) + u_1^* e_0\,(L_2+1) + s_2\,(2u_1^* + u_3^* - 1)] \\ \qquad +L_2 u_3^* + u_5^*\,(e_0 + 2s_2)\,. \end{cases} \tag{3.14}$$

Since all system parameters are strictly positive, the roots of $X_1(\mu)$ are all real and negative. By the Routh-Hurwitz criterion we have that all roots of $X_2(\mu)$ lie in the left complex half-plane if the coefficients x_{21} and x_{20} are positive,

which translates into the requirements

$$\begin{cases} u_5^* < \dfrac{(s_1p_1+e_1)+(s_1+e_1-L_1u_1^*)}{L_1a_1\beta_1} := u_A, \quad \text{and} \\ u_5^* < \dfrac{(s_1p_1+e_1)(s_1+e_1-L_1u_1^*)}{L_1a_1\beta_1(e_1+s_1)} := u_B. \end{cases} \tag{3.15}$$

Since u_5^* must be positive, we require that $u_1^* < (s_1+e_1)/L_1$. Additionally, since $s_1+e_1-L_1u_1^* < s_1+e_1$, we have

$$\begin{cases} u_A = \dfrac{s_1p_1+e_1}{L_1a_1\beta_1} + \dfrac{s_1+e_1-L_1u_1^*}{L_1a_1\beta_1} > \dfrac{s_1p_1+e_1}{L_1a_1\beta_1}, \\ u_B = \dfrac{s_1p_1+e_1}{L_1a_1\beta_1}\dfrac{s_1+e_1-L_1u_1^*}{e_1+s_1} < \dfrac{s_1p_1+e_1}{L_1a_1\beta_1}, \end{cases} \tag{3.16}$$

implying $u_B < u_A$. Hence, the roots of $X_2(\mu)$ have a negative real part, provided

$$u_1^* < \frac{s_1+e_1}{L_1} = \widetilde{u}_1^* \quad \text{and} \quad u_5^* < u_B.$$

This also implies that a necessary condition for the stability of the endemic steady state E_2 is the intuitively natural result that the two basic reproduction numbers defined in (3.12) must satisfy $R_{02} > R_{01}$.

Applying the Routh-Hurwitz criterion to the cubic polynomial $X_3(\mu)$ gives that all roots of this polynomial have negative real parts, as long as x_{32}, x_{31} and x_{30} are positive and satisfy the condition $x_{32}x_{31} > x_{30}$. It is important to note that stability of the endemic steady state E_2 does not depend on the susceptibility and transmissibility modifiers a_2 and β_2. From a biological perspective, this suggests that the capability of the second virus to survive as a single infection is irrelevant from the point of view of its ability to infect cells that are chemically altered and are immune to the first virus. On the other

hand, the ability of viruses d_i to trigger a warning signal appears to control whether they can exclude each other or co-exist in a stable equilibrium. Hence, we have proved the following result.

Theorem 3.4.1 (Stability of the endemic steady state)**.** *For the endemic steady state* $E_2 = (u_1^*, 0, u_3^*, 0, u_5^*, 0, 0)$ *with* $u_1^* = (e_2 + s_2)/L_2$, u_3^* *and* u_5^* *given in (3.7), let* x_{30}, x_{31}, x_{32} *and* u_B *be defined by (3.14) and (3.16), respectively. Then the steady state* E_2 *is linearly asymptotically stable if and only if the following conditions hold.*

(i) $0 < u_5^* < u_B$,

(ii) $x_{30} > 0$, $x_{31} > 0$, $x_{32} > 0$,

(iii) $x_{32}x_{31} > x_{30}$.

Remark (Stability analysis of steady state E_1)**.** *The result of this* **Theorem** *can be applied to the analysis of stability of the endemic steady state* E_1 *by swapping parameter indices* 1 *with* 2*, and replacing variables* u_3^* *and* u_5^* *with* u_2^* *and* u_4^**, respectively, as a consequence of the model symmetry. Unlike some other models of multi-strain/multi-virus infections [***Gup99***, ***All03***, ***Cas96****], the complexity of the model (3.4) prevents one from expressing the conditions for stability of single-virus or co-existence equilibria in a closed form depending only on two basic reproduction numbers.*

3.4.4 Syndemic steady state

Since the syndemic steady state S cannot be found explicitly, it does not prove possible to derive analytical conditions for stability of this steady state. Hence,

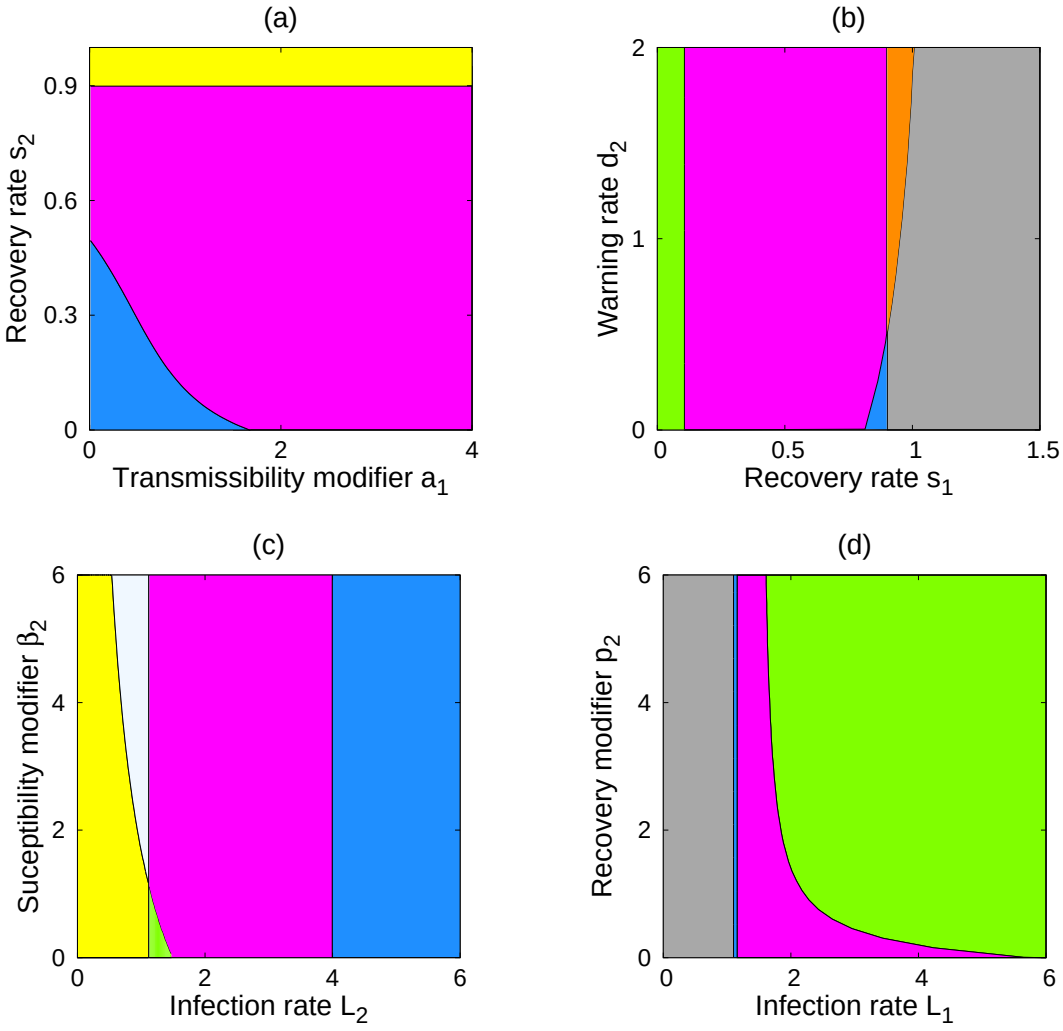

Figure 3.2: Stability of steady states of the system (3.4) with parameters from Table 3.1. Green and blue indicate regions where both endemic steady states E_1 and E_2 are feasible, but only E_1 or E_2 is stable, respectively. Magenta shows the region where all three infected steady states are feasible, but only the syndemic steady state S is stable. Yellow is the area where only E_1 is feasible and stable, whereas grey is the area where only E_2 is feasible and stable. White and orange is where the syndemic steady state is stable, whereas E_1 or E_2, respectively, is also feasible (and unstable).

Dimensionless Parameters	Biological meaning	Baseline value
$L_{1,2}$	Infection rate	1.5
$s_{1,2}$	Recovery rate	0.5
$d_{1,2}$	Propagation rate	0.05
$a_{1,2}$	Transmissibility modifier (after secondary infection)	1
$\beta_{1,2}$	Susceptibility modifier (after primary infection)	1
$\gamma_{1,2}$	Acquired secondary immunity modifier	0.5
e_0	Natural death rate	0.3
$e_{1,2}$	Infected cell death rate	0.6
$p_{1,2}$	Recovery modifier	0.2

Table 3.1: Baseline parameter values in system (3.4).

to understand how stability changes with parameters, one has to resort to numerically computing the eigenvalues of the Jacobian of the linearisation of system (3.4) near the steady state. This is presented in the next section of the thesis.

3.5 Numerical stability analysis and simulations

Due to RNAi being a very complicated multi-component process, obtaining accurate parameters values to be used in a mathematical model is extremely difficult and often impractical, as some parameters cannot currently be measured, or even when they are, there is a very wide variability in the reported values [**Mel11**, **Lia12**, **Him15**]. Parameter values that define viral properties and modifiers in the context of this study are equally problematic to obtain, as one would require virus-specific information about both the cell-to-cell and long-distance transmission of the virus. For example, in the case of the Tobacco

mosaic virus, the infection can on, average, spread from one cell to another every 3-4 hours depending on the strain of the virus and the temperature [**Kaw04**], and although this information provides some intuition about parameter values, it is not sufficient for estimating the actual infection rate.

To better understand the effects of different parameters on feasibility and stability of different steady states of the system (3.4), we use **Theorem 3.1** and numerical computation of eigenvalues to identify parameter regions associated with existence and stability of all steady states. To this end, we start with baseline parameter values given in Table 3.1 and allow some of the parameters to vary. Since model (3.4) has quite a large number of different parameters, below we present the results for only some parameter combinations that illustrate the diversity of possible scenarios, and qualitatively similar results can be obtained when other parameters are varied. Plotting the percentages of infected cells for each steady state in the same parameter space allows us to investigate possible changes in the magnitude of the infected cell population between different steady states.

Figs 3.2, 3.3 and 3.4 illustrate earlier analytical conclusions that the two endemic steady states E_1 and E_2 are only feasible and stable if the recovery/death rates of infected cells are sufficiently low. On the other hand, one expects that a virus can only survive if its infection rate is adequately high, as observed in Fig. 3.2(d) and Fig. 3.4(a). If either one of the recovery/infection rates is below or above a certain threshold, it is easy to see that the syndemic steady state disappears, and only one of the two viruses survives. However, Figs 3.2(a), (c) and 3.3(c), together with additional computations not shown here, suggest that by increasing parameters $a_{1,2}$, i.e the transmissibility modifiers, or the suscep-

tibility modifiers $b_{1,2}$, the system can generally move from one of the endemic steady states to a stable syndemic equilibrium. This suggests that the most competitive viral strain, which under different circumstances would be capable of excluding a secondary infection, might instead facilitate the survival of a secondary strain. Cells that have been chemically altered by the immune response to the more aggressive strain can now serve as ideal targets in which the second strain could proliferate. Since for the fixed values of other parameters, infection rates L_1 and L_2 are proportional to the two basic reproduction numbers, R_{01} and R_{02}, respectively, Fig. 3.4(a) is effectively equivalent to figures demonstrating the dependence of steady states on basic reproduction numbers in two-strain models of infectious diseases [**Gup96**, **And97**].

Figs 3.2(d) and 3.3(a) show that when one of the recovery modifiers $p_{1,2}$ is increased, the system can move from the syndemic to one of the endemic equilibria $E_{1,2}$, thus behaving in a qualitatively opposite way to an increase of the corresponding parameter pair $\{a_i, \beta_i\}$. This occurs when cells with acquired immunity to one of the viruses are subsequently infected with another virus but have a faster recovery. As this reduces the overall spread of the secondary infection, it will inevitably allow the primary virus to dominate and eventually be the sole survivor in the host. In Fig. 3.2(b) one observes that by increasing the dimensionless warning rate d_2 we can move from a parameter region where only the endemic steady state E_2 is feasible and stable (a grey region) to a region, where the syndemic equilibrium is also stable (an orange region). This suggests that the plant immune response to the second virus can establish conditions that are more favourable to the first virus. Thus, in the case of a double infection, it is possible for a viral infection to persevere in the presence of the host's immune

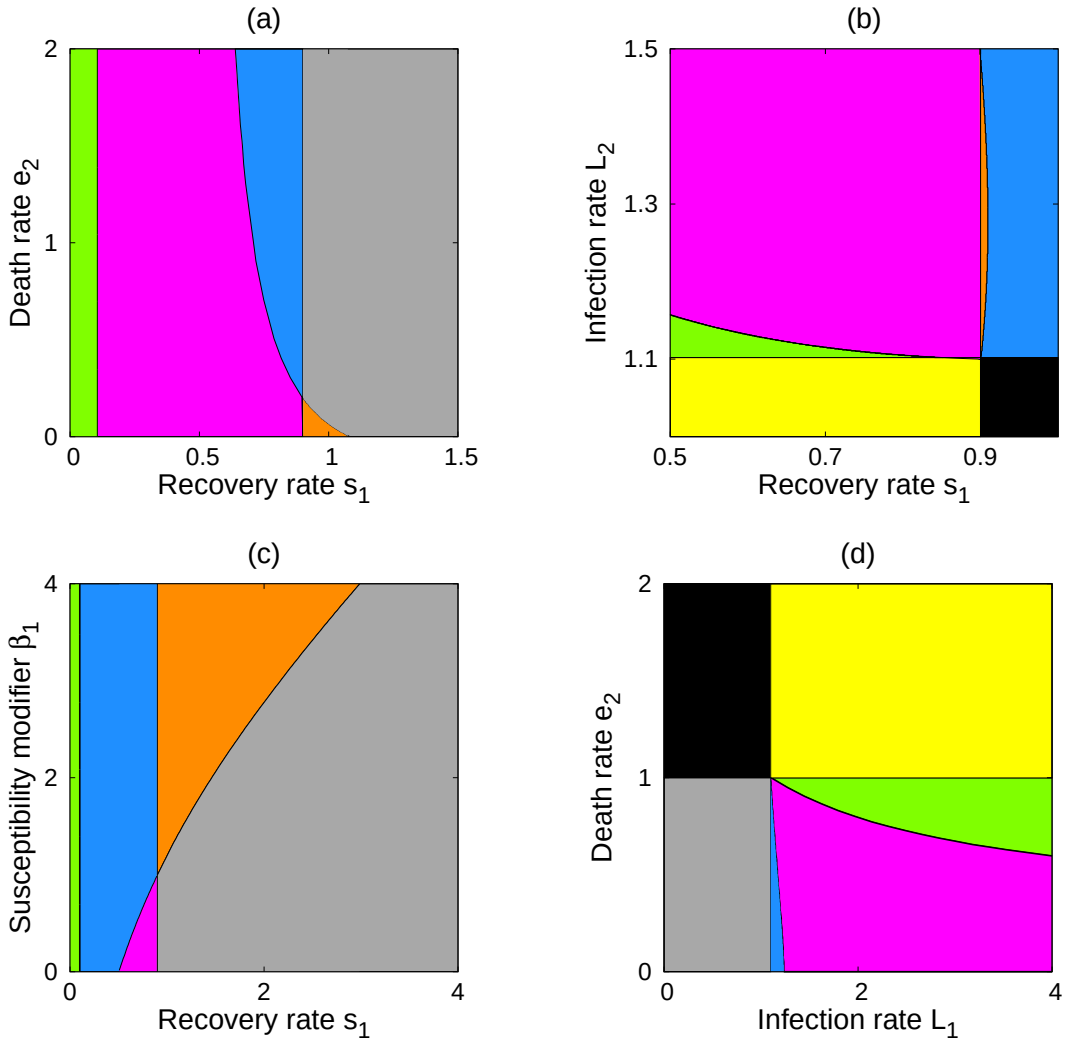

Figure 3.3: Stability of the steady states of the system (3.4) with parameters from Table 3.1. Green and blue indicate regions where both endemic steady states E_1 and E_2 are feasible, but only E_1 or E_2 is stable, respectively. Magenta shows the region where all three infected steady states are feasible, but only the syndemic steady state S is stable. Yellow is the area where only E_1 is feasible and stable, whereas grey is the area where only E_2 is feasible and stable. Orange is where the syndemic steady state is stable, and E_2 is feasible but unstable. Black is the region where only the disease-free steady state is feasible and stable.

response despite being unable to do so as a single infection. This means that the propagating component of the immune response plays a significant role in the interactions between two viruses and can dictate whether both of them can survive in a single host.

Recall that in the model (3.4), the two viruses are considered to cooperate with each other when $a_i, \beta_i > 1$, have a neutral relationship when $a_i, \beta_i = 1$, and "antagonize" each other when $a_i, \beta_i < 1$, $i = 1, 2$. One should also note the existence of other more complicated scenarios as each of a_1, a_2, β_1 and β_2 can be less than, greater than or equal to one. For example, if $a_1, \beta_1 > 1$ and $0 < a_2, \beta_2 < 1$, then, the cooperation of the two viruses will be considered to benefit mostly the first virus, thus being unequal. On the other hand, for $a_2, \beta_2 > 1$ and $a_1, \beta_1 = 0$, the relationship is completely one-sided in favour of the second virus. Figs 3.5(a) and (b) suggest that the biological interactions between different viruses may sometimes disproportionately favour one of the viruses and decrease the potency of the second infection, that is to say that one of the viruses experiences less spread during a co-infection when compared to its single-virus infected steady state. This is clearly evident in Fig. (3.5)(b): for $\beta_2 \leq 0.87$ only the first virus is present, whereas for $\beta_2 > 0.87$ the system moves into the syndemic steady state where now both viruses are able to survive, but the first virus is not as widely spread as before. One should note that this result comes at the cost of increasing the total number of infected cells, suggesting that it might not always be the preferable outcome for the plant. Similarly, Fig. (3.5)(a) shows that for small values of the transmissibility modifier a_1 combined with a higher infection rate $L_2 > L_1$ (which also implies $R_{02} > R_{01}$), only the second virus is able to survive in the host. As the value of a_1 increases,

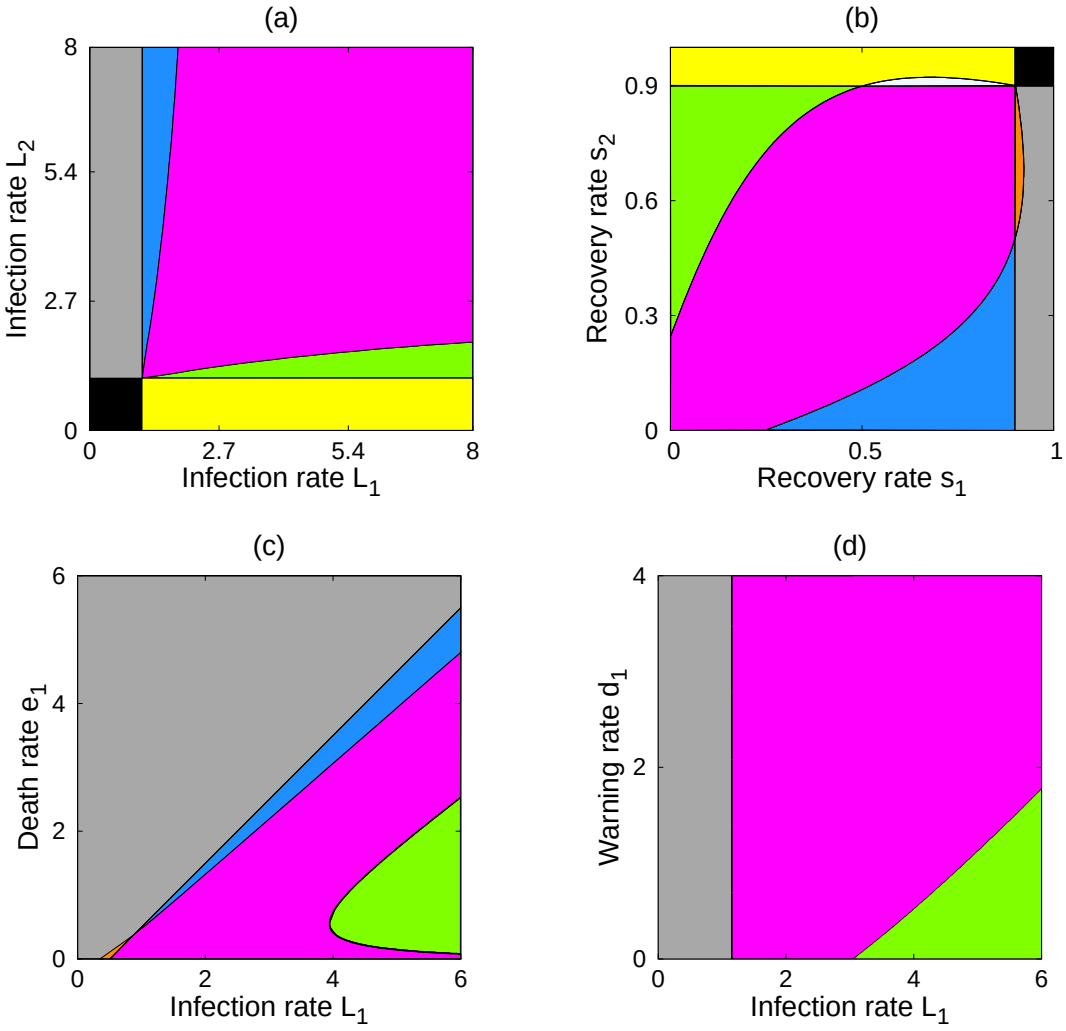

Figure 3.4: Stability of steady states of the system (3.4) with parameters from Table 3.1. Green and blue indicate regions where both endemic steady states E_1 and E_2 are feasible, but only E_1 or E_2 is stable, respectively. Magenta shows the region where all three infected steady states are feasible, but only the syndemic steady state S is stable. Yellow is the area where only E_1 is feasible and stable, whereas grey is the area where only E_2 is feasible and stable. White and orange is where the syndemic steady state is stable, whereas E_1 or E_2, respectively, is also feasible (and unstable). Black is the region where only the disease-free steady state is feasible and stable.

the picture changes, and the system moves to a syndemic steady state, where not only both of the viruses are able to survive, but given sufficiently high value of a_1, the first virus can become dominant. This also suggests that increasing a_i is qualitatively interchangeable with increasing β_j for $j \neq i$. Figs 3.5(c) and (d) show how depending on the level of cooperation between the two viruses, i.e for sufficiently high values of a_1 and a_2, it can be beneficial for the viruses to co-exist, as they can both infect a bigger biomass of the host compared to their respective one-virus steady states, possibly resulting in a chronic condition that is more severe. These results show that sufficient levels of mutual cooperation between two viruses promote their virulence and ensure that neither of them becomes eradicated, which eventually leads to a persistent double infection with parameter values determining the magnitude of each infection.

If the cooperation between the two viruses is unequal or one-sided, it is possible that the least benefited virus will experience less spread compared to its single-virus infected steady state. To investigate scenarios where both viruses "antagonize" each other, we solve the system at $a_i, \beta_i = 0.5$, $i = 1, 2$. One result is given in Fig. (3.6)(a), and it shows that increasing β_2 decreases the presence of the first virus, but similarly to our previous results it increases the overall level of infection. The most interesting case is shown in Fig. (3.6)(b), where adequately increasing the warning rate d_2, not only the percentage of cells infected with the second virus goes down, but also the total number of infected cells is reduced. One also observes in this Figure that although the number of cells infected with the first virus is slowly increasing, it is still at a much lower level than what it was in the absence of the second virus, i.e, compared

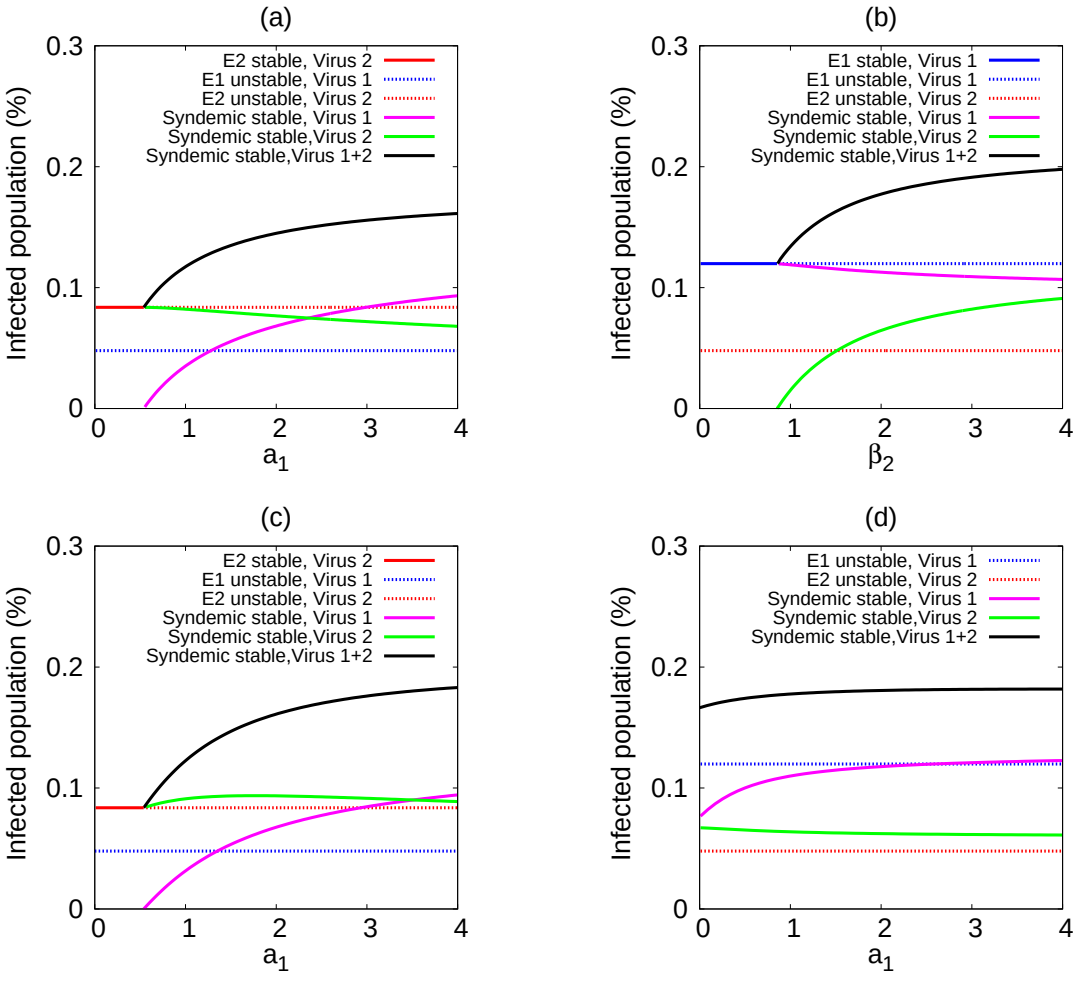

Figure 3.5: Stability of endemic and syndemic steady states of the system (3.4) with parameter values from Table 3.1. Stable (unstable) steady states are indicated by solid (dotted) lines for single-virus endemic steady states E_1 (blue) and E_2 (red). The percentage of cells at the syndemic steady state is illustrated for virus 1 (magenta), virus 2 (green), and the total infected population (black). (a) $L_1 < L_2 = 2$. (b) $L_2 < L_1 = 3$. (c) $L_1 < L_2 = 2$ and $a_2 = 2$. (d) $L_2 < L_1 = 3$, $a_2 = 2$ and $\beta_1 = 1.5$.

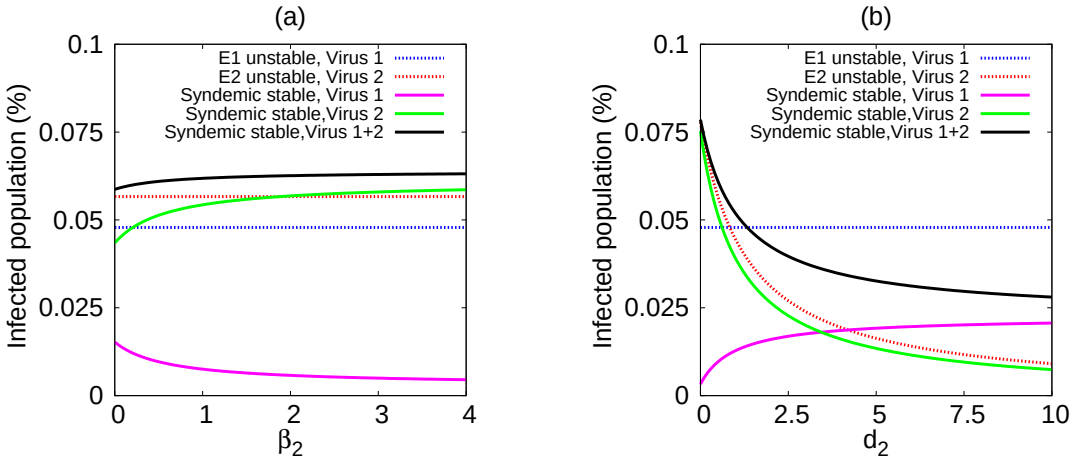

Figure 3.6: Stability of endemic and syndemic steady states of the system (3.4) with $L_1 < L_2 = 1.6$ and the other parameter values given in Table 3.1. (a) $a_{1,2} = \beta_1 = 0.5$. (b) $a_{1,2} = \beta_{1,2} = 0.5$. Stable (unstable) steady states are indicated by solid (dotted) lines for single-virus endemic steady states E_1 (blue) and E_2 (red). The percentage of cells at the syndemic steady state is illustrated for virus 1 (magenta), virus 2 (green), and the total infected population (black).

to the steady state E_1 which is now unstable. This situation represents an ideal scenario, where inoculating the target plant with a less harmful virus or viral strain can offer partial protection against another specific virus or strain, thus potentially minimizing damage to the host.

To demonstrate different kinds of dynamics that can be exhibited by the model, we have solved the system (3.4) numerically for different combinations of parameters, and the results are presented in Fig. 3.7. Fig.e 3.7(a) shows the solution of the model that approaches the stable syndemic steady state, with all compartments having positive values. As mentioned earlier, from a biological perspective this represents the cases where interactions between the two viruses facilitate the survival of both viral species within the same host. Figs 3.7(b) and (c) illustrate situations where one of the viruses survives, while the other one is eradicated by the plant immune system, and Fig. 3.7(d) demonstrates the case where the plant makes a full recovery.

3.6 Chapter conclusions

In this chapter we have derived and analysed a mathematical model of biological interactions between two viruses and a single plant host, with particular account for RNA interference. Our results have shown that RNA interference can provide a mechanism for cross-protection, and a co-infection can either increase or decrease the overall potency of individual infections, illustrating how cross-protection or cross-enhancement can occur between the two viruses. The framework we developed can be directly applicable to analysis of RNAi-mediated interactions for many combinations of plant viruses, with examples including

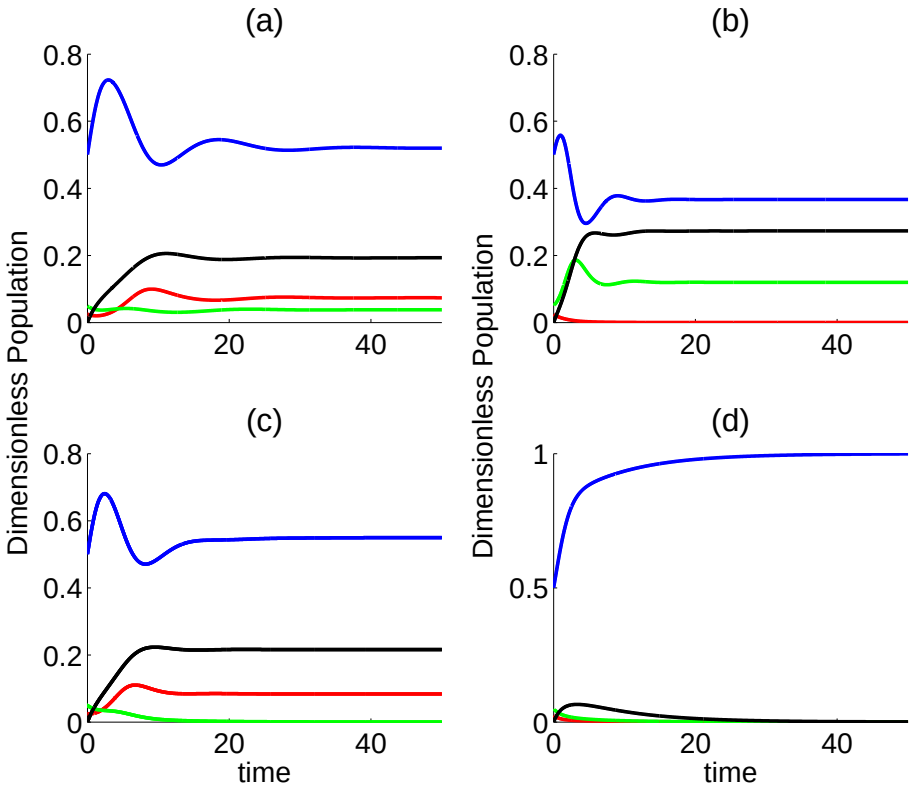

Figure 3.7: Numerical simulations of the model (3.4) with parameter values from Table 3.1. Colours represent dimensionless populations of susceptible cells (blue), cells infected with the first (red) and second (green) virus, the total population of cells with immunity to one or both viruses (black). (a) Stable co-existence of viruses: $a_1 = 3$. (b) Stable single-virus state E_2: $L_1 = 1$ and $L_2 = 3$. (c) Stable single-virus state E_1: $L_1 = 2$ and $p_2 = 3$. (d) Stable disease-free steady state E_{DF}: $s_1 = 1$ and $L_2 = 1$.

co-infections with *Soybean mosaic virus* and *Alfalfa mosaic virus* [**Mal09**], as well as *Abutilon mosaic virus* and *Cucumber mosaic virus* [**Weg07**]. The model can also be used to offer insight into how one could control viral diseases through cross-protection and, by extension, through gene and antiviral therapy, where genetically modified viruses are introduced to the host. Unlike the wild type strains, these modified viruses can be engineered to deliver specific therapeutic siRNA, which through the process of RNA interference would trigger an immune response, thus acting as a powerful vaccination strategy [**Sil02**, **Cap04**, **Soi07**].

To achieve greater biological realism, we have assumed that the new plant growth depends on the availability of healthy cells which can be impeded once the plant becomes infected. Stability analysis of the steady states has demonstrated the significance of different parameters of the model and showed how they dictate the dynamical behaviour exhibited by the system.

One should note that in the current model it is impossible for all cell populations to die, as there will always be some new growth taking place to replace the parts of the plant that are lost either naturally or due to infections. This is true despite the growth penalty introduced by allocating some of the resources to infected parts of the plant. Even if a plant were to experience a severe case of stunting, it would be highly unlikely that every healthy cell would become infected and therefore, lead to the death of the plant. Although our model cannot capture this scenario, realistically, such events do occur quite rarely in nature depending also on the environmental and host conditions at the time of infection [**Sut99**, **Ger06**].

Stability of the disease-free equilibrium and the feasibility of the two single-

virus endemic steady states depend on the two basic reproduction numbers R_{01} and R_{02}. In the model these quantities are represented as functions of only the rates of infection, recovery and death of infected cells for each strain, but they are not affected by the propagating component of the immune response. This suggests that a faster mobile signal can at best help the plant to recover faster (as determined by the above-mentioned factors), but, by itself it is not sufficient for a recovery. However, this picture changes when the stability of the syndemic steady state is considered. The results show that the warning signal plays a significant role in determining whether both viruses can persist simultaneously, and as such, it controls situations where the plant is able to support some constant level of both infections. Due to the nature of the RNA warning (silencing) signal, the immunological relation of the two viruses is paramount in determining the outcome of a double infection. That is to say that viruses of similar genomes are most likely to trigger the same immunological response by the plant. If the two viruses are sufficiently immunologically related, then the viral dsRNA produced during their viral replication will contain a number of identical segments which will be used to initialize the RNA interference process. As such, the immune response trigged by a primary infection with a less virulent strain could induce a sufficient response against a secondary strain. In such a case our results shown that the least harmful of the two viruses becomes dominant, and the plant experiences a degree of cross-protection which may sometimes result in the increased total population of infected cells.

Analysis of the model has demonstrated that the total population of infected cells during a co-infection can sometimes, but not always, be higher than during a single infection, for which there are two possible explanations. One possibility

is that the two different infections simply increase the overall rate of infection. Another aspect is that the two viruses only have to compete for susceptible cells, as there is a source of cells that might be exclusively available to each of the viruses, i.e. cells that have acquired immunity to one virus may be less or more susceptible to the other virus. Our results have shown that when two viruses "antagonize" each other, i.e. $a_i, \beta_i < 1$, for sufficiently high warning rates, not only can one minimize the spread of a specific virus, but the overall infection can also be reduced. Hence, depending on the virulence of the two strains, one might choose to either avoid the introduction of a secondary viruses, or instead use it in order to produce the more favourable outcome.

If the two viruses are immunologically unrelated and co-infecting the same plant, they can indirectly promote each other by inadvertently making cells they can no longer infect more susceptible to the other virus. Hence, despite the fact that both viruses are effectively competing for the same resource, there is always some exclusive source of potential cells in which the infection could survive, with the potency of individual infections strongly dependent on the interaction between the two viruses. Another important result is that the syndemic steady state can potentially be stable in parameter regions where only one of the endemic steady states is feasible, implying that a secondary virus can only survive when another infection is present.

Chapter 4

Intracellular RNA interference

4.1 Introduction

In this chapter we consider a mathematical model of RNAi with particular emphasis on time delays associated with two aspects of primed amplification: binding of siRNA to aberrant RNA, and binding of siRNA to mRNA, both of which result in the expanded production of dsRNA responsible for RNA silencing. Analytical and numerical stability analyses are performed to identify regions of stability of different steady states and to determine conditions on parameters that lead to instability. Our results will show that while the original model without time delays exhibits a bi-stability due to the presence of a hysteresis loop, under the influence of time delays, one of the two steady states with the smallest or highest concentration of mRNA can actually lose its stability via a Hopf bifurcation. This leads to the co-existence of a stable steady state and a stable periodic orbit, which has a profound effect on the dynamics of the system.

4.2 Model derivation

To analyse the dynamics of RNAi with primed amplification, following Groenenboom *et al.* [**Gro05**] we consider the populations of mRNA, dsRNA, siRNA and garbage (aberrant) RNA, to be denoted by $M(t)$, $D(t)$, $S(t)$ and $G(t)$, respectively. It is assumed that mRNA is constantly transcribed by each transgene at rate h, with n_1 being the number of transgenic copies, and is degraded at the rate d_m. For simplicity, it will be assumed that each transgene produces the same amount of mRNA. Some dsRNA is synthesized directly from mRNA through the activity of RdRp at a rate p. The available dsRNA is cleaved by a dicer enzyme into n_2 siRNA molecules at a rate a. In this model it is assumed that siRNA is involved into forming two distinct complexes that use the siRNA as a guide to identify and associate with different categories of RNA strands to initiate the dsRNA synthesis. The first is the RISC complex responsible for degrading mRNA into garbage RNA, which decays naturally at a rate $d_g > d_m$. For simplicity, the RISC population is not explicitly included in the model, but it is rather assumed that siRNA directly associates with mRNA at a rate b_1. The second complex guided by siRNA binds mRNA and aberrant (garbage) RNA, and subsequently is primed by RdRp to synthesize additional dsRNA (primed amplification). To avoid unnecessary complexity, the second complex will also be represented implicitly by assuming that siRNA directly associates with mRNA and garbage RNA for the purpose of dsRNA synthesis at the rates b_2 and b_3, respectively. At this point, we include two distinct time delays τ_1 and τ_2 to represent the delays inherent in the production of dsRNA from mRNA and garbage RNA, respectively. With these assumptions, the system describing

the dynamics of different RNA populations takes the form

$$\begin{aligned}
\frac{dM}{dt} &= n_1 h - d_m M(t) - pM(t) - b_1 S(t)M(t) - b_2 S(t)M(t), \\
\frac{dD}{dt} &= pM(t) - aD(t) + b_2 S(t-\tau_1)M(t-\tau_1) + b_3 S(t-\tau_2)G(t-\tau_2), \\
\frac{dS}{dt} &= n_2 aD(t) - d_s S(t) - b_1 S(t)M(t) - b_2 S(t)M(t) - b_3 S(t)G(t), \\
\frac{dG}{dt} &= n_3 b_1 S(t)M(t) - d_g G(t) - b_3 S(t)G(t),
\end{aligned} \tag{4.1}$$

with the initial conditions

$$\begin{aligned}
&M(s) = M_0(s) \geq 0, \quad s \in [-\tau_1, 0], \quad G(s) = G_0(s) \geq 0, \quad s \in [-\tau_2, 0], \\
&S(s) = S_0(s) \geq 0, \quad s \in [-\tau, 0], \quad \tau = \max\{\tau_1, \tau_2\}, \quad D(0) \geq 0.
\end{aligned} \tag{4.2}$$

Before proceeding with the analysis of the model (4.1), we have to establish that this system is well-posed, i.e. its solutions are non-negative and bounded.

Theorem 4.2.1 (Positivity of solutions)**.** *Solutions $M(t)$, $D(t)$, $S(t)$, $G(t)$ of the system (4.1) with the initial conditions (4.2), are non-negative for all $t \geq 0$.*

This result can be proven using standard techniques, or, alternatively, it follows from Theorem 5.2.1 in [**Smi95**] (see Theorem A.0.2). As a next step, we look at boundedness of solutions.

Theorem 4.2.2 (Boundedness of solutions)**.** *Suppose there exists a time $T > 0$, such that the solution $D(t)$ of the model (4.1) satisfies the condition $D(t) \leq \widehat{D}$*

for all $t \geq T$ with $\widehat{D} > 0$. Then, the solutions $M(t)$, $S(t)$, $G(t)$ of the model (4.1) are bounded for all $t \geq T$.

Proof. Suppose $t \geq T$. Then, the third equation of the system (4.1) can be recast in the form

$$\frac{dS}{dt} \leq n_2 a\widehat{D} - d_s S(t).$$

By the comparison theorem (see Theorem A.0.1) one then has

$$S(t) \leq \frac{n_2 a\widehat{D}}{d_s}\left(1 - e^{-d_s t}\right) + S(0)e^{-d_s t} \leq \widehat{S} = \frac{n_2 a\widehat{D}}{d_s} + S(0),$$

which implies that $S(t)$ is bounded for $t \geq T$. Using the non-negativity of solutions, one can rewrite the first equation of the system (4.1) in the form

$$\frac{dM}{dt} \leq n_1 h - (d_m + p)M(t) \quad \Longrightarrow \quad M(t) \leq \widehat{M} = \frac{n_1 h}{d_m + p} + M(0),$$

which shows that $M(t)$ is also bounded for $t \geq T$. Finally, the last equation of (4.1) can now be rewritten as follows

$$\frac{dG}{dt} \leq n_3 b_1 \widehat{S}\widehat{M} - d_g G(t) \quad \Longrightarrow \quad G(t) \leq \widehat{G} = \frac{n_3 b_1 \widehat{S}\widehat{M}}{d_g} + G(0).$$

Hence, one concludes the existence of upper bounds $\widehat{S}$, $\widehat{M}$ and $\widehat{G}$, such that $S(t) \leq \widehat{S}$, $M(t) \leq \widehat{M}$ and $G(t) \leq \widehat{G}$ for all $t \geq T$, which concludes the proof.

■

Parameter	Biological meaning	Value	Units
d_m	mRNA decay rate	0.14	hr^{-1} **(half life 5h)**
d_s	siRNA decay rate	2	hr^{-1} **(half life 21 min)**
d_g	Garbage RNA decay rate	2.8	hr^{-1} **(half life 15 min)**
h	mRNA transcription rate	160	hr^{-1} $cell^{-1}$
p	Rate of dsRNA synthesis from RNA	0.002	hr^{-1}
a	Rate of dsRNA cleavage by dicer	2	hr^{-1}
b_1	Rate of RISC-mRNA complex formation	8×10^{-4}	$cell\ mol^{-1}\ hr^{-1}$
b_2	Rate of RdRp-mRNA complex formation	8×10^{-5}	$cell\ mol^{-1}\ hr^{-1}$
b_3	Rate of RdRp-garbage complex formation	9×10^{-4}	$cell\ mol^{-1}\ hr^{-1}$
n_1	Transgene copy number	1	
n_2	Yield of siRNA per cleaved dsRNA	10	
n_3	Yield of garbage RNA from degraded mRNA	1	
τ_1	Delay in dsRNA synthesis from mRNA	0	
τ_2	Delay in dsRNA synthesis from aberrant RNA	0	

Table 4.1: Baseline parameter values for the system (4.1).The majority of the parameter values are taken from [**Gro05**].

4.3 Steady states and their feasibility

Steady states of the system (4.1) are given by non-negative roots of the following system of algebraic equations

$$\begin{aligned} n_1 h - d_m M - pM - b_1 SM - b_2 SM &= 0, \\ pM - aD + b_2 SM + b_3 SG &= 0, \\ n_2 aD - d_s S - b_1 SM - b_2 SM - b_3 SG &= 0, \\ n_3 b_1 SM - d_g G - b_3 SG &= 0. \end{aligned} \tag{4.3}$$

It is straightforward to see that the system (4.3) does not admit solutions with $M = 0$, as this would immediately violate the first equation due to the presence

of the constant transcription of mRNA. Substituting $S = 0$ into the third equation implies $D = 0$, and due to the second equation this then implies $M = 0$, which is impossible. Hence, there can be no steady states with either D or S being zero. Similarly, if $G = 0$, the last equation implies $SM = 0$ which again is not possible. Thus, the system can only exhibit steady states where all components are non-zero.

Let us introduce the following auxiliary parameters

$$b = b_1 + b_2, \qquad \hat{h} = n_1 h. \tag{4.4}$$

Assuming $S^* \geq 0$, one can solve the first equation of (4.3) to obtain

$$M^* = M(S^*) = \frac{\hat{h}}{p + d_m + bS^*} > 0. \tag{4.5}$$

Adding the second and the third equations of the system (4.3) gives

$$D^* = D(S^*) = \frac{bd_s S^{*2} + (\hat{h}b_1 + pd_s + d_m d_s)S^* - ph}{a[p + d_m + bS^*](n_2 - 1)}. \tag{4.6}$$

One should note that for $S^* \geq 0$ and $n_2 \geq 1$, $D^* \geq 0$ if and only if the following condition holds

$$bd_s S^{*2} + (b_1 h\hat{h} + d_m d_s + d_s p)_z S^* - hp > 0, \tag{4.7}$$

which implies that S^* must satisfy

$$S^* \geq S_{\min} = \frac{-z + \sqrt{4\, bd_s ph + z^2}}{2bd_s}, \text{where } z = b_1 h\hat{h} + d_m d_s + d_s p. \tag{4.8}$$

From the last equation of the system (4.3) and using the expression for M from (4.5), we obtain

$$G^* = G(S^*) = \frac{\hat{h} n_3 b_1 S^*}{(p + d_m + bS^*)(b_3 S^* + d_g)} > 0. \tag{4.9}$$

Substituting these values back into the third equation of the system (4.3), one obtains the following cubic equation for S^*

$$Q(S^*) = \alpha_3 S^{*3} + \alpha_2 S^{*2} + \alpha_1 S^* + \alpha_0 = 0, \tag{4.10}$$

where

$$\begin{aligned}
&\alpha_0 = -\hat{h} p d_g n_2 < 0, \quad \alpha_3 = b b_3 d_s > 0, \\
&\alpha_1 = \hat{h}[d_g b - n_2(p b_3 + d_g b_2)] + d_g d_s (p + d_m), \\
&\alpha_2 = \hat{h}[b_1 b_3 (1 + n_3 - n_2 n_3) + b_2 b_3 (1 - n_2)] + b_3 d_s (p + d_m) + b d_g d_s.
\end{aligned}$$

Due to the fact that $\alpha_0 < 0$ and $\alpha_3 > 0$, the cubic $Q(S^*)$ has at least one positive real root for any $n_i \geq 1,\ i = 1, 2, 3$. In fact, by using the Descartes's rule of signs one can deduce that this cubic has exactly one positive and two negative roots, with the exception of $\alpha_2 < 0$ and $\alpha_1 > 0$, when it admits three positive roots. Hence, to identify which of these three roots are real, we need to determine the extrema of $Q(S^*)$. Differentiating $Q(S^*)$ with respect to S^* and setting the resulting expression to zero, we find that the local minimum of $Q(S^*)$ is given by

$$\widetilde{S} = \frac{2|\alpha_2| + \left[4\alpha_2^2 - 12\alpha_3\alpha_1\right]^{1/2}}{6\alpha_3} > 0. \tag{4.11}$$

Let us introduce a set $\mathcal{S} = \{S : Q(S) = 0, S \in \mathbb{R}_+\} \cap \{S \geq S_{min}\}$ of all positive real roots of $Q(S^*)$, which are also greater than S_{min}. We then have the following result.

Theorem 4.3.1 (Number of feasible steady states)**.** *Let M^*, D^*, G^*, $Q(S^*)$, S_{min}, $\widetilde{S}$ and $\mathcal{S}$ be defined as above. Given any $S^* \in \mathcal{S}$ with $|\mathcal{S}| = k$, the system (4.1) admits the steady states $E_j = (M^*, D^*, S^*, G^*)$, $j = 1, ..., k$. There is only a single feasible steady state if either of the following conditions holds:*

(i) $\alpha_2 > 0$,

(ii) $\alpha_{2,1} < 0$,

(iii) $\alpha_1 > 0$, $\alpha_2 < 0$ *and* $Q(\widetilde{S}) > 0$,

and up to three feasible steady states if $Q(\widetilde{S}) \leq 0$, $\alpha_2^2 > 3\alpha_3\alpha_1$, $\alpha_1 > 0$ *and* $\alpha_2 < 0$.

4.4 Stability analysis

Linearisation of the delayed system (4.1) around the steady state $E = (M^*, D^*, S^*, R^*)$ yields the following characteristic equation

$$P(\lambda) = p_4\lambda^4 + p_3\lambda^3 + p_2\lambda^2 + p_1\lambda + p_0 = 0, \tag{4.12}$$

where the coefficients p_i, which are functions of λ, are defined by

$$p_0 = p_{03}S^3 + p_{02}S^2 + p_{01}S + p_{10}, p_1 = p_{13}S^3 + p_{12}S^2 + p_{11}S + p_{10}, p_4 = MS,$$

$$p_2 = p_{22}S^2 + p_{21}S + p_{20}, \quad p_3 = b_3MS^2 + \left[(a + d_g)\, M + n_1h\right] S + an_2DM,$$

with

$$p_{20} = an_2D[n_1h + M(a + d_g)], \quad p_{22} = n_1hb_3 + M(ab_3 - b^2M),$$

$$p_{21} = -ab_2n_2T_1M^2 + [(b_3d_g - ab_3n_2T_2)\,G + ab_3n_2D + ad_g]\,M + (a + d_g)\,n_1h,$$

and

$$p_{10} = an_2D[ad_gM + n_1h(a + d_g)], \quad p_{13} = -M^2bb_3\,(b_1n_3 + b)\,,$$

$$\begin{aligned} p_{11} = {} & n_2a(bp - b_2d_gT_1)M^2 + a[n_2(ab_3D - n_1hb_2T_1) + b_3d_gG(1 - 2n_2T_2)]M \\ & + n_1h[an_2b_3(D - T_2G) + d_g(a + b_3G)], \end{aligned}$$

$$p_{12} = ahb_3n_1 + \left[ab_2n_2T_1(b - b_3) - b^2(a + d_g)\right]M^2 - ab_3{}^2n_2T_2GM,$$

$$p_{00} = n_1n_2ahd_gD, \quad p_{03} = -bb_3M^2[n_3b_1(1 - n_2T_2) + b - b_2n_2T_1],$$

$$p_{01} = an_1n_2h[ab_3D - d_g(2b_3T_2G + b_2T_1M)] + ad_g(n_2pbM^2 + n_1hb_3G),$$

$$p_{02} = bM^2(pn_2b_3 + n_2b_2d_gT_1 - bd_g) - n_1n_2hb_3(b_2T_1M + b_3T_2G),$$

and for convenience of notation we note that $(M, D, S, R) = (M^*, D^*, S^*, R^*)$ and introduced auxiliary parameters $T_i = e^{-\lambda\tau_i}$, $i = 1, 2$. In the case of instantaneous primed amplification, i.e. for $T_{1,2} = 1$ in (4.12), any steady state (M^*, S^*, D^*, G^*) defined in **Theorem 4.3.1** is linearly asymptotically stable, if the appropriate Routh-Hurwitz conditions are satisfied, i.e if $p_0, \ldots, p_4 > 0$, $p_3p_2 > p_1p_4$, and $p_3p_2p_1 > p_4p_1^2 + p_3^2p_0$.

4.4.1 Primed amplification with small delays

First we consider the situation where primed amplification delays are small $\tau_i \ll 1$, which means one can use the approximation $T_i = e^{-\lambda\tau_i} \approx 1 - \lambda\tau_i$. This allows us to rewrite the characteristic equation as a simple quartic

$$R(\lambda, \tau_1, \tau_2) = \lambda^4 + r_3\lambda^3 + r_2\lambda^2 + r_1\lambda + r_0 = 0, \tag{4.13}$$

where the coefficients are given by

$$\begin{aligned}
r_0 &= ab_1b_3n_3[b(n_2-1)MS - n_2\hat{h}] + r_{01}M^2SG^{-1} + r_{02}G^{-1} + r_{03}GM^{-1},\\
r_1 &= r_{11}M^2 + r_{12}M + r_{13}S + r_{14} - ab_3d_g(n_2-1)G + a\hat{h}n_2(b_1n_3DG^{-1} - b_2),\\
r_2 &= r_{21}S + r_{22}M + r_{23}G - a\hat{h}(n_2\tau_2b_3G + 1)M^{-1} + an_2D(aM + \hat{h})M^{-1},\\
r_3 &= ab_3n_2\tau_2G + \tau_1ab_2n_2M + n_3b_1SMG^{-1} + an_2DS^{-1} + a\hat{h}M^{-1},
\end{aligned}$$

with

$$\begin{aligned}
r_{01} &= abb_1n_3[pn_2 + (b_2n_2 - b)S], \quad r_{02} = a\hat{h}b_1n_2n_3(aD - b_2SM),\\
r_{03} &= a\hat{h}b_3d_g(1-n_2),
\end{aligned}$$

and

$$r_{11} = -n_3 b_1 S\left(Sabb_2 n_2 \tau_1 + Sb^2 + ab_2 n_2\right) G^{-1},$$

$$r_{12} = -bb_1 b_3 n_3 \left(an_2\tau_2 + 1\right) S^2 + \left[bb_2 an_2(-\hat{h} b_1 \tau_1 b_2 n_3 G^{-1} - b_1 b_3 n_3 - ab^2)\right] S$$
$$+an_2\left(ab_1 n_3 DG^{-1} + bp\right), \quad r_{13} = a\hat{h} b_1 n_3 (n_2\tau_2 b_3 + G^{-1}),$$

$$r_{14} = \hat{h}(a^2 n_2 DM^{-1}S^{-1} + b_3 d_g GM^{-1}) - an_2\hat{h} b_3(1 - d_g\tau_2)GM^{-1},$$

$$r_{21} = ab_1 n_2 n_3 M\left(\tau_1 b_2 MG^{-1} + \tau_2 b_3\right) + \left(ab_1 n_3 G^{-1} - \tau_1 abb_2 n_2 - b^2\right)M + b_1 n_3 \hat{h} G^{-1},$$

$$r_{22} = ab_1 n_2 n_3 DG^{-1} - ab_2 n_2, \qquad r_{23} = b_3\left(ad_g n_2\tau_2 - an_2 + d_g\right) G.$$

Using the Routh-Hurwitz criteria and the Hopf bifurcation theorem we deduce that a Hopf bifurcation occurs for $\tau_1 = \tau_1^*$, when the following conditions are satisfied

$$\begin{aligned} &r_n > 0, \text{ for all } n = 0, ..., 3, \\ &r_3 r_2 > r_1, \\ &r_3 r_2 r_1 = r_1^2 + r_3^2 r_0. \end{aligned} \tag{4.14}$$

Introducing an auxiliary parameter $q^2 = r_1/r_3$, the third condition in (4.14) can be rewritten in the form

$$r_0 = r_2\left(\frac{r_1}{r_3}\right) - \left(\frac{r_1}{r_3}\right)^2 = q^2(r_2 - q^2),$$

and, hence, the characteristic equation (4.13) at the Hopf bifurcation point turns into

$$\lambda^4 + r_3\lambda^3 + r_2\lambda^2 + q^2 r_3\lambda + q^2(r_2 - q^2) = 0. \tag{4.15}$$

It is known that any 4th-order polynomial with purely imaginary roots can be written in the form

$$(x^2 + \delta)(x^2 + \beta x + \gamma) = x^4 + \beta x^3 + (\delta + \gamma)x^2 + \delta\beta x + \delta\gamma. \tag{4.16}$$

Comparing this expression with (4.13) and identifying specific coefficients as $\delta = q^2 > 0$, $\beta = r_3 > 0$ and $\gamma = r_2 - q^2 > 0$, it follows that the roots of R are given by

$$\begin{aligned} &\lambda_{1,2}(\tau_1^*) = \pm i\sqrt{\delta} = \pm iq, \\ &\lambda_{3,4}(\tau_1^*) = -r_3 \pm \left[r_3^2 - 4(r_2 - q^2)\right]^{1/2}. \end{aligned} \tag{4.17}$$

Differentiating equation (4.15) with respect to τ_1 yields

$$\frac{d\lambda}{d\tau_1} = -\frac{r_3'\lambda^3 + r_2'\lambda^2 + r_1'\lambda}{4\lambda^3 + 3r_3\lambda^2 + 2r_2\lambda + q^2 r_3}, \tag{4.18}$$

where

$$\begin{aligned} r_1' &= -abb_1b_2n_2n_3MS\left(MS + \hat{h}b_2\right)G^{-1}, \\ r_2' &= ab_2n_2SM(b_1n_3MG^{-1} - 1), \quad r_3' = ab_2n_2M. \end{aligned} \tag{4.19}$$

Evaluating this derivative at $\tau_1 = \tau_1^*$, for which $\lambda_{1,2}(\tau_1^*) = \pm iq$, gives

$$\frac{d\lambda_{1,2}(\tau_1^*)}{d\tau_1} = \frac{r_2'q^2 \pm iq(r_3'q^2 - r_1')}{-2q^2r_3 \pm 2iq(r_2 - 2q^2)} = \frac{A \pm iB}{C \pm iD} = \frac{(AC + BD) \pm i(BC - AD)}{C^2 + D^2}. \tag{4.20}$$

Hence, we obtain

$$\frac{d\,\mathrm{Re}[\lambda_{1,2}(\tau_1^*)]}{d\tau_1} = \frac{AC + BD}{C^2 + D^2} = \frac{2q^3Z(\tau_2)}{C^2 + D^2}, \tag{4.21}$$

where

$$Z(\tau_2) = (r_3'q^2 - r_1')(r_2 - 2q^2) - qr_2'r_3, \tag{4.22}$$

and, therefore,

$$\mathrm{sign}\left(\frac{d\,\mathrm{Re}[\lambda(\tau_1^*)]}{d\tau_1}\right) = \mathrm{sign}[Z(\tau_2)].$$

This gives the following result.

Theorem 4.4.1 (Critical time delay for Hopf Bifurcation when delays are sufficiently small.)**.** *Suppose $\tau_{1,2} \ll 1$ and $Z(\tau_2)$ is given by (4.22). Let the coefficients of the characteristic equation (4.15) satisfy $r_n > 0$, $n = 0, ..., 3$, $r_3r_2 > r_1$ and $r_3r_2r_1 > r_1^2 + r_3^2r_0$. If $Z(\tau_2) > 0$, then the steady state E of the system (4.1) undergoes a Hopf bifurcation at $\tau_1 = \tau_1^*$.*

Remark (Hopf bifurcation criteria for steady state E)**.** *A similar argument can be used to establish Hopf bifurcation of the steady state E for a fixed value of τ_1 and some critical value of the time delay $\tau_2 = \tau_2^*$.*

4.4.2 Single primed amplification delay

As a next case, we consider a situation where one of the primed amplification time delays is negligibly small compared to other timescales of the model, so that that part of the amplification pathway can be considered to take place instantaneously. Formally, this can be represented by $\tau_n > 0$ for some $n = 1, 2$, with $\tau_m = 0$ for $m \neq n$. In this case, analysis of the distribution of roots of the characteristic equation follows the methodology of [**Rua01**]. The first step is to rewrite the characteristic equation (4.12) in the form

$$\lambda^4+\alpha\lambda^3+(\beta_1 T_1+\beta_2 T_2+\beta_3)\lambda^2+(\gamma_1 T_1+\gamma_2 T_2+\gamma_3)\lambda+(\delta_1 T_1+\delta_2 T_2+\delta_3) = 0, \quad (4.23)$$

where

$$\alpha = b_1 n_3 MSG^{-1} + an_2 DS^{-1} + a + \hat{h}M^{-1},$$

$$\beta_1 = -ab_2 n_2 M, \qquad \beta_2 = -an_2 b_3 G,$$

$$\beta_3 = \frac{ab_1 n_3 (n_2 D + S)M}{G} + \frac{an_2 (aM + \hat{h})D}{MS} + \frac{\hat{h}(b_1 n_3 SM + aG)}{MG} - b^2 SM + b_3 d_g G,$$

$$\gamma_1 = ab_2 n_2 [(bG - b_1 n_3)SMG^{-1} - \hat{h}], \gamma_2 = -an_2 b_3 [b_1 n_3 SM + (d_g + \hat{h}M^{-1})G],$$

$$\begin{aligned}\gamma_3 = {} & bb_1 n_3 MS^2 (b_3 + bMG^{-1}) + an_2 D[b_1 n_3 G^{-1}(a + \hat{h}) + a\hat{h}G^{-1}M^{-1}] \\ & + \hat{h}(ab_1 n_3 SG^{-1} + b_3 d_g GM^{-1}) + a[b_3 d_g G + M(b^2 S + bpn_2)],\end{aligned}$$

$$\delta_1 = ab_1 b_2 n_2 n_3 MS(bSM - \hat{h})G^{-1}, \quad \delta_2 = an_2 b_3 [b_1 n_3 S(bMS - \hat{h}) - \hat{h} d_g GM^{-1}],$$

$$\delta_3 = abb_1 n_3 MS[pn_2 MG^{-1} - S(b_3 + bMG^{-1})] + a\hat{h}(ab_1 n_2 n_3 G^{-1} + b_3 d_g GM^{-1}).$$

If one of the delays τ_m is zero, we have

$$\lambda^4 + \alpha\lambda^3 + (\beta_n T_n + \hat{\beta}_m)\lambda^2 + (\gamma_n T_n + \hat{\gamma}_m)\lambda + (\delta_n T_n + \hat{\delta}_m) = 0, \tag{4.24}$$

where

$$\hat{\beta}_m = \beta_m + \beta_3, \;\; \hat{\gamma}_m = \gamma_m + \gamma_3, \;\; \hat{\delta}_m = \delta_m + \delta_3.$$

To investigate whether this equation can have purely imaginary roots, we substitute $\lambda = i\omega$ with some $\omega > 0$ and separate real and imaginary parts, which

yields the following system of equations

$$\begin{aligned}\omega\gamma_n \sin(\omega\tau_n) + (\delta_n - \omega^2\beta_n)\cos(\omega\tau_n) &= \omega^2(\hat{\beta}_m - \omega^2) - \hat{\delta}_m,\\ \omega\gamma_n \cos(\omega\tau_n) - (\delta_n - \omega^2\beta_n)\sin(\omega\tau_n) &= \omega(\alpha\omega^2 - \hat{\gamma}_m).\end{aligned} \tag{4.25}$$

Squaring and adding these two equations gives the equation for the Hopf frequency ω

$$h(v) = v^4 + c_3v^3 + c_2v^2 + c_1v + c_0 = 0, \qquad v = \omega^2, \tag{4.26}$$

with

$$c_0 = \hat{\delta}_m^2 - \delta_n^2, \quad c_1 = 2(\beta_n\delta_n - \hat{\beta}_m\hat{\delta}_m) + \hat{\gamma}_m^2 - \gamma_n^2,$$

$$c_2 = 2(\hat{\delta}_m - \alpha\hat{\gamma}_m) + \hat{\beta}_m^2 - \beta_n^2, \quad c_3 = \alpha^2 - 2\hat{\beta}_m.$$

Without loss of generality, let us assume that the equation (4.26) has four distinct positive roots denoted by v_1, v_2, v_3 and v_4. This implies that the equation (4.24) in turn has four purely imaginary roots $\lambda = i\omega_k$, $k = 1, ..., 4$, where

$$\omega_1 = \sqrt{v_1}, \qquad \omega_2 = \sqrt{v_2}, \qquad \omega_3 = \sqrt{v_3}, \qquad \omega_4 = \sqrt{v_4}. \tag{4.27}$$

With the help of auxiliary parameters

$$F_1 = w\omega\gamma_n, F_2 = \delta_n - w^2\beta_n, H_1 = w^2(\hat{\beta}_m - w^2) - \hat{\delta}_m, H_2 = w(aw^2 - \hat{\gamma}_m),$$

one can rewrite the system (4.25) in the form

$$\begin{aligned} F_1 \sin(w\tau_n) + F_2 \cos(w\tau_n) &= H_1, \\ F_1 \cos(w\tau_n) - F_2 \sin(w\tau_n) &= H_2. \end{aligned} \tag{4.28}$$

From this system we obtain

$$\tan(w\tau_n) = \frac{F_1 H_1 - F_2 H_2}{H_1 F_2 + H_2 F_1}, \tag{4.29}$$

which gives the values of the critical time τ_n for each $k = 1, ..., 4$, and any $j \in \mathbb{N}$ as

$$\tau_{n,k}^{(j)} = \frac{1}{\omega_k}\Bigg[(j-1)\pi + \arctan\left(\frac{(\alpha\beta_n - \gamma_n)\omega_k^5 + (\hat{\beta}_m\gamma_n - \alpha\delta_n - \hat{\gamma}_m\beta_n)\omega_k^3 + (\hat{\gamma}_m\delta_n - \hat{\delta}_m\gamma_n)}{\beta_n\omega_k^6 + (\alpha\gamma_n - \hat{\beta}_m\beta_n - \delta_n)\omega_k^4 + (\hat{\beta}_m\delta_n + \hat{\delta}_m\beta_n - \hat{\gamma}_m\gamma_n)\omega_k^2 - \hat{\delta}_m\delta_n}\right)\Bigg]. \tag{4.30}$$

This allows us to define the following:

$$\tau_n^* = \tau_{n,k_0}^{(j_0)} = \min_{1\le k\le 4,\, j\ge 1}\{\tau_{n,k}^{(j)}\}, \quad \omega_0 = \omega_{k_0}. \tag{4.31}$$

In order to establish whether the steady state E_j, $j = 1, 2, 3$, actually undergoes a Hopf bifurcation at $\tau_n = \tau_n^*$, one has to compute the sign of $d[\mathrm{Re}\,\lambda(\tau_n^*)]/d\tau_n$. Differentiating the equation (4.24) with respect to τ_n yields

$$\left(\frac{d\lambda}{d\tau_n}\right)^{-1} = \frac{(4\lambda^3 + 3\alpha\lambda^2 + 2\hat{\beta}_m\lambda + \hat{\gamma}_m)e^{\lambda\tau_n} + 2\beta_n\lambda + \gamma_n}{\lambda(\beta_n\lambda^2 + \gamma_n\lambda + \delta_n)} - \frac{\tau_n}{\lambda}.$$

Introducing the notation $U = \omega_0^2[\omega_0^2\gamma_n^2 + (\delta_n - \beta_n\omega_0^2)^2]$, it is clear that $U > 0$ for all $\omega_0 > 0$, and

$$\left(\frac{d\,\mathrm{Re}\,\lambda(\tau_n^*)}{d\tau_n}\right)^{-1} = \frac{1}{U}\left[\underbrace{A\cos(w_0\tau_n) + B\sin(w_0\tau_n)}_{:=\Gamma} + 2\beta_n w_0^2(\delta_i - \beta_n w_0^2) - \gamma_n^2 w_0^2\right], \tag{4.32}$$

where

$$A = 2\omega_0^2(\hat{\beta}_m - 2\omega_0^2)F_2 + \omega_0(3\alpha\omega_0^2 - \hat{\gamma}_m)F_1,$$

$$B = -\omega_0(3\alpha\omega_0^2 - \hat{\gamma}_m)F_2 + 2\omega_0^2(\hat{\beta}_m - 2\omega_0^2)F_1,$$

$$\Gamma = 2\omega_0^2(\hat{\beta}_m - 2\omega_0^2)H_1 + \omega_0(3\alpha\omega_0^2 - \hat{\gamma}_m)H_2.$$

Consequently, with $v_0 = {w_0}^2$ one can write $d[\mathrm{Re}\,\lambda(\tau_n^*)]/d\tau_n$ as follows

$$\begin{aligned}\left(\frac{d\,\mathrm{Re}\,\lambda(\tau_n^*)}{d\tau_n}\right)^{-1} &= \frac{1}{U}\left[4{w_0}^8 + 3c_3{w_0}^6 + 2c_2{w_0}^4 + c_1{w_0}^2\right] \\ &= \frac{1}{U}\left[4{v_0}^4 + 3c_3{v_0}^3 + 2c_2{v_0}^2 + c_1v_0\right] = \frac{v_0}{U}h'(v_0),\end{aligned} \tag{4.33}$$

where $h(v)$ is defined in (4.26). Since $v_0 = {w_0}^2 > 0$, this implies

$$\mathrm{sign}\left(\frac{d\,\mathrm{Re}\,\lambda({\tau_n}^*)}{d\tau_n}\right) = \mathrm{sign}\left[\left(\frac{d\,\mathrm{Re}\,\lambda({\tau_n}^*)}{d\tau_n}\right)^{-1}\right]$$

$$= \mathrm{sign}\left[\frac{v_0h'(v_0)}{U}\right] = \mathrm{sign}\left[h'(v_0)\right].$$

We can therefore conclude the following result.

Theorem 4.4.2. *Let the coefficients of the characteristic equation at the steady state E_j, $j = 1, 2, 3$ with $\tau_{1,2} = 0$, be given by (4.12). Suppose these coefficients satisfy the Routh-Hurwitz criteria, namely, $p_0, \ldots, p_4 > 0$, $p_3 p_2 > p_1 p_4$, and $p_3 p_2 p_1 > p_4 p_1^2 + p_3^2 p_0$. Additionally, let ω_0 and τ_n^*, $n = 1, 2$ be defined as in (4.31) with $h'(\omega_0^2) > 0$ where $\tau_m = 0$ for $m \neq n$. Then, the steady state E_j of the system (4.1) is stable for $\tau_n < \tau_n^*$, unstable for $\tau_n > \tau_n^*$ and undergoes a Hopf bifurcation at $\tau_n = \tau_n^*$.*

Remark (Required condition for Theorem 4.4.2)**.** *The theorem above only holds if the quartic (4.26) has at least one positive real root, e.g this is guaranteed in the special case for $c_0 < 0$. However, when $c_0 \geq 0$, it is impractical to talk about the analytical distribution of roots. Hence, one would have to compute the roots numerically in order to verify the assumptions needed to apply the theorem.*

4.4.3 Garbage- and mRNA-associated amplification delays are non-zero

Let us now consider the most complex situation where both time delays τ_1 and τ_2 associated with the primed amplification are positive. In this case the characteristic equation (4.12) can be rearranged into the following equation

$$\sigma(\lambda) = \sigma_0(\lambda) + \sigma_1(\lambda) e^{-\lambda \tau_1} + \sigma_2(\lambda) e^{-\lambda \tau_2} = 0, \tag{4.34}$$

where

$$\sigma_0 = [\sigma_{01}(\lambda + d_g) + \sigma_{02}](\lambda + a) + abpn_2SM^2(\lambda + d_g),$$

$$\sigma_1 = ab_2n_2MS(b_3S + \lambda + d_g)(bMS - \lambda M - \hat{h}),$$

$$\sigma_2 = -ab_3n_2S\left[-bb_1n_3M^2S^2 + (b_3S + \lambda + 2\,d_g)\,(\lambda M + \hat{h})G\right],$$

$$\sigma_{01} = -S^2M^2 + \left(Da\lambda\, n_2 + S\lambda^2\right)M + \hat{h}\lambda S + a\hat{h}n_2D,$$

$$\sigma_{02} = -bb_3(b_1n_3 + b)M^2 + b_3(an_2D + d_gG)(\lambda M + \hat{h})S + b_3\lambda(\lambda M + \hat{h}S)S^2.$$

To analyse the distribution of roots of the equation (4.34) we follow the methodology introduced by Gu *et al.* [**Gu05**]. Let T denote the *stability crossing curves* which is the set of all the *crossing points* $(\tau_1, \tau_2) \in \mathbb{R}^2_+$, for which the characteristic polynomial $\sigma(\lambda)$ has at least one purely imaginary root. Introducing the parametrisation

$$\delta_j(\lambda) = \frac{\sigma_j(\lambda)}{\sigma_0(\lambda)}, \qquad j = 1, 2, \tag{4.35}$$

the equation (4.34) transforms into

$$\delta(\lambda, \tau_1, \tau_2) = 1 + \delta_1(\lambda)e^{-\lambda\tau_1} + \delta_2(\lambda)e^{-\lambda\tau_2} = 0. \tag{4.36}$$

It is important to note that this parametrisation is only valid as long as σ_0 does not have any imaginary zeros. Hence, by Proposition 3.1 in [**Gu05**], for each $\omega \neq 0$, $\lambda = i\omega$ is a solution of $\sigma(\lambda, \tau_1, \tau_2) = 0$ for some $(\tau_1, \tau_2) \in \mathbb{R}^2_+$ if and only if

(i) Given $\sigma_0(i\omega) \neq 0$,

$$\begin{aligned} |\delta_1(i\omega)| + |\delta_2(i\omega)| &\geq 1, \\ -1 \leq |\delta_1(i\omega)| - |\delta_2(i\omega)| &\leq 1. \end{aligned} \tag{4.37}$$

(ii) Given $\sigma_0(i\omega) = 0$,

$$|\sigma_1(i\omega)| = |\sigma_2(i\omega)|. \tag{4.38}$$

Let Ω denote the *crossing set*, i.e the set of all $\omega > 0$ which satisfy the conditions (i),(ii) above. This set consists of N intervals with a finite length. Moreover, if the intervals are ordered such that the left-end point of Ω_k is an increasing function of k, $k = 1, 2, ..., N$, then we have that

$$\Omega = \bigcup_{k=1}^{N} \Omega_k. \tag{4.39}$$

Thus, for any given $\omega \in \Omega$ satisfying $\sigma_j(i\omega) \neq 0$, $j = 0, 1, 2$, the critical time delay pairs satisfying $\sigma(\lambda, \tau_1, \tau_2) = 0$ with $\lambda = i\omega$ are given by

$$\begin{aligned} &(\tau_1^*, \tau_2^*) \in \mathcal{T} = \{\mathcal{T}_\omega | \omega \in \Omega\}, \\ &\mathcal{T}_\omega = \left(\bigcup_{u \geq u_0^+, v \geq v_0^+} \mathcal{T}_{\omega,u,v}^+ \right) \cup \left(\bigcup_{u \geq u_0^-, v \geq v_0^-} \mathcal{T}_{\omega,u,v}^- \right), \end{aligned} \tag{4.40}$$

where

$$\mathcal{T}_{\omega,u,v}^{\pm} = \left\{ (\tau_1^{u\pm}, \tau_2^{v\pm}) \right\}, \tag{4.41}$$

with

$$\tau_1 = \tau_1^{u\pm}(\omega) = \frac{\text{Arg}[\delta_1(i\omega)] + (2u-1)\pi \pm \theta_1}{\omega} \geq 0, \quad u = u_0^{\pm}, u_0^{\pm}+1, u_0^{\pm}+2, ...$$

$$\tau_2 = \tau_2^{v\pm}(\omega) = \frac{\text{Arg}[\delta_2(i\omega)] + (2v-1)\pi \mp \theta_2}{\omega} \geq 0, \quad v = v_0^{\pm}, v_0^{\pm}+1, v_0^{\pm}+2, ... \tag{4.42}$$

and the angles $\theta_{1,2} \in [0, \pi]$ are computed as follows

$$\begin{aligned} \theta_1 &= \arccos\left(\frac{1 + |\delta_1(i\omega)|^2 - |\delta_2(i\omega)|^2}{2|\delta_1(i\omega)|}\right), \\ \theta_2 &= \arccos\left(\frac{1 + |\delta_2(i\omega)|^2 - |\delta_1(i\omega)|^2}{2|\delta_2(i\omega)|}\right), \end{aligned} \tag{4.43}$$

and $u_0^{\pm}$ and $v_0^{\pm}$ are the smallest possible integers for which the corresponding delays $\tau_1^{u_0^{\pm}\pm}$, $\tau_2^{v_0^{\pm}\pm}$ are non-negative. These stability crossing curves are illustrated in Figure 4.7.

4.5 Numerical stability analysis and simulations

In order to understand the effects of different parameters on feasibility and stability of different steady states, and, investigate the role of the time delays associated with primed amplification, we have used a pseudospectral method implemented in a traceDDE suite for MATLAB [**Bre06**] to numerically compute the eigenvalues of the characteristic equation (4.34). Since RNA interference is a very complex multi-component process, many parameter values are case-specific and hard to obtain experimentally [**Mel11**, **Lia12**, **Him15**], hence rather than focus on a specific set of parameters, we perform an extensive

bifurcation analysis to illustrate all the different types of dynamical behavior that the model (4.1) can exhibit.

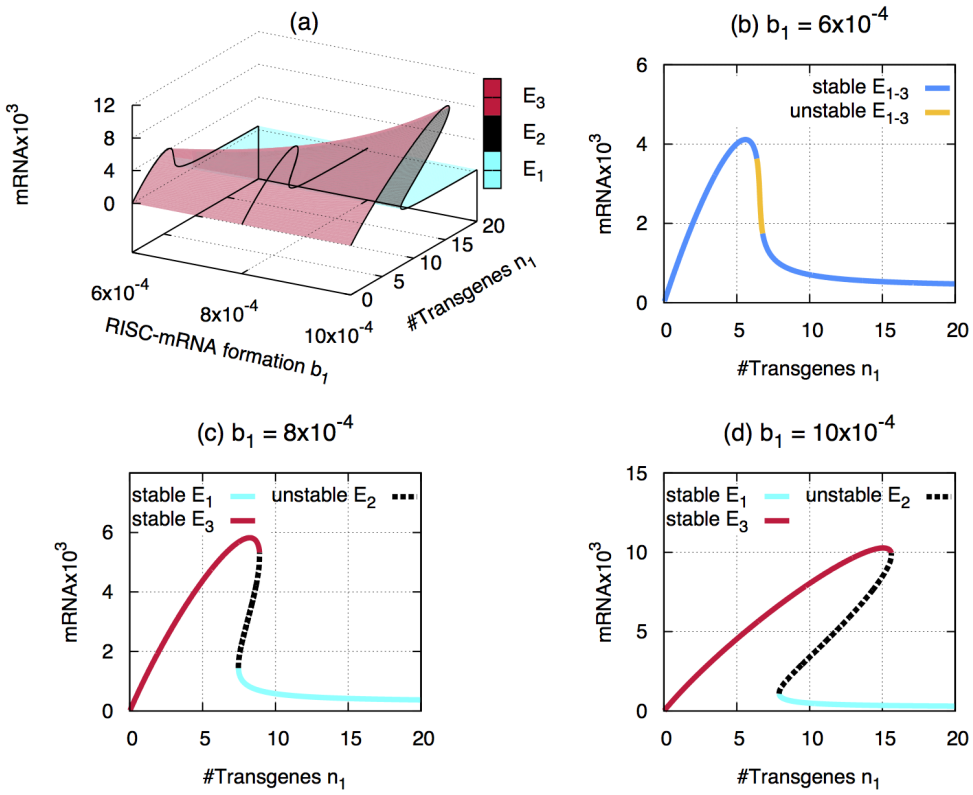

Figure 4.1: Stability of the steady states E_1, E_2 and E_3 depending on the rate b_1 and the number of transgenes n_1, with other parameter values taken from Table 4.1.

Fig. 4.1(b) and Figs. 4.4(a)-(b) show that if the rate b_1, at which the RISC-mRNA complex is formed, is sufficiently small, then only a single steady state E_{1-3} is feasible, and it is stable for small or high numbers of transgenes, and unstable for intermediate values of n_1. As the value of b_1 increases, the system acquires an additional feasible steady state E_2 with an intermediate level of mRNA, which is always unstable, thus creating a region of bi-stability, as

shown in Figs. 4.1(c) and (d). In fact, the range of values of transgenes n_1, for which the bi-stability is observed, itself increases with b_1, which means that if the RISC complexes are more efficient in cleaving mRNA, it is possible to have the stable states with high and low values of mRNA for higher and lower numbers of transgenes. A very interesting and counter-intuitive observation from Figs. 4.1(c) and (d) is that the actual values of the steady state mRNA concentration are also growing with b_1. One possible explanation for this is that the reduced availability of mRNA means that a smaller amount of it can be directly used to synthesize dsRNA, as described by the $pM(t)$ term in the second equation of (4.1), and more mRNA is directly degraded into the garbage RNA, thus generating a smaller feedback loop in the model for sufficient silencing to occur.

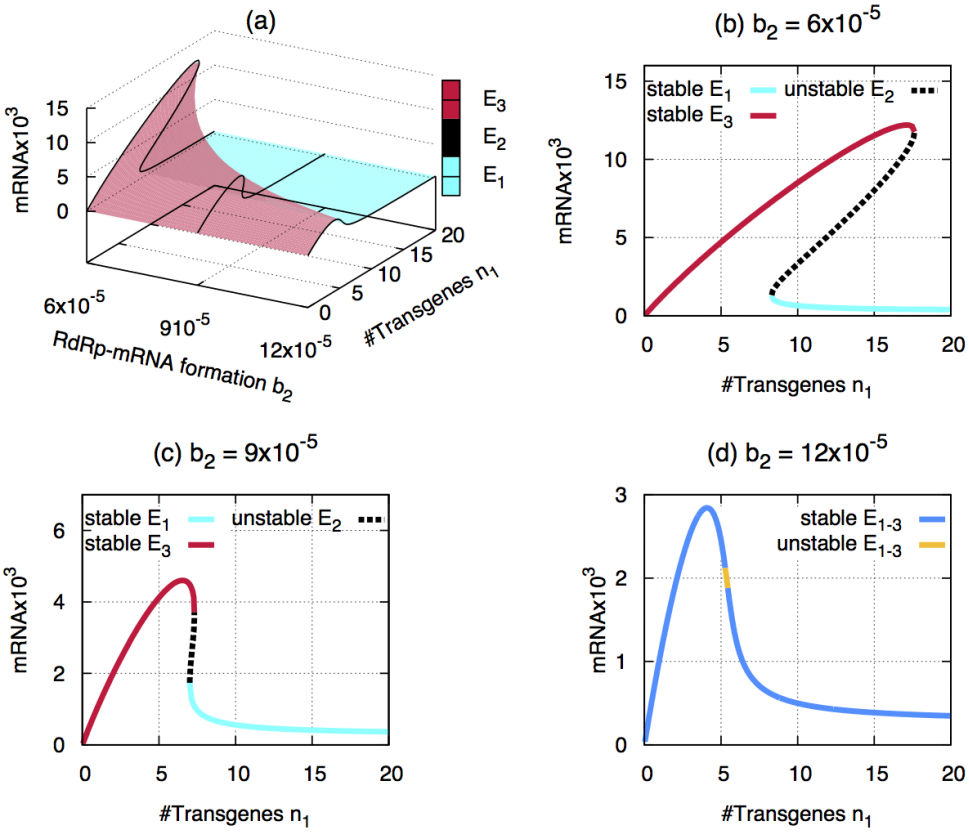

Figure 4.2: Stability of the steady states E_1, E_2 and E_3 depending on the rate b_2 and the number of transgenes n_1, with other parameter values from Table 4.1.

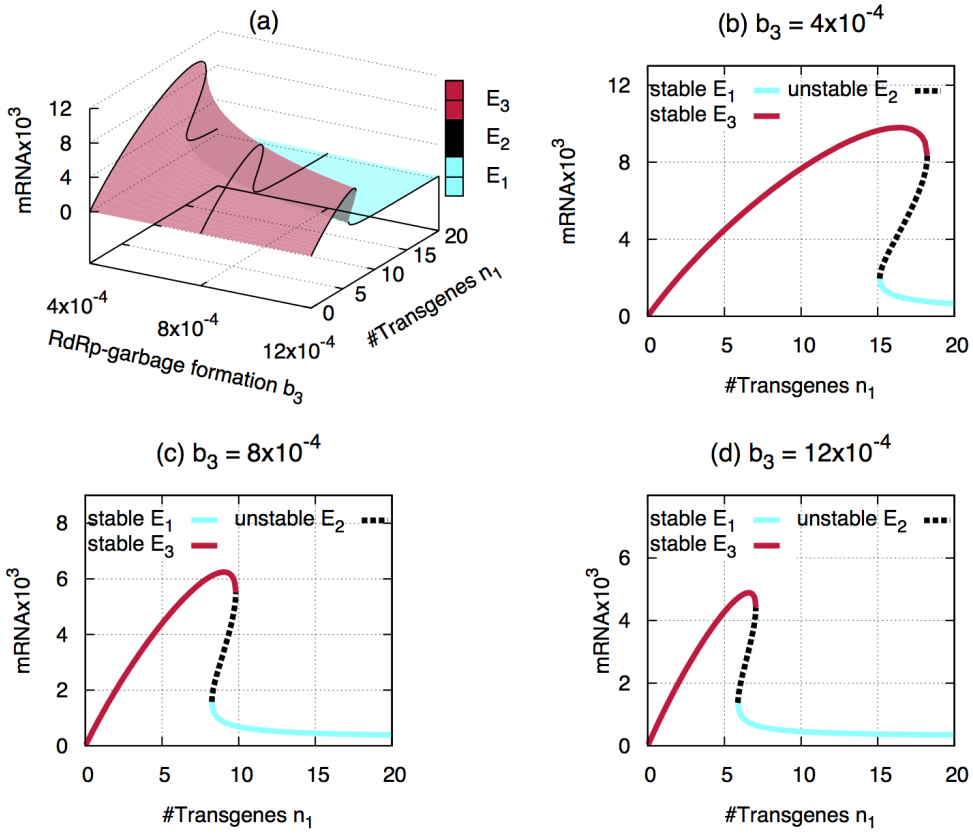

Figure 4.3: Stability of the steady states E_1, E_2 and E_3 depending on the rate b_3 and the number of transgenes n_1, with other parameter values from Table 4.1.

When one considers the effect of varying the rate b_2 of forming RdRp-mRNA complexes, the behaviour is qualitatively different in that increasing b_2 leads to the reduction in the size of the bi-stability region, and for sufficiently high values of b_2, the intermediate steady state E_2 completely disappears, and the system possesses a single feasible steady state E_{1-3}, which is stable for low and high numbers of transgenes, and unstable for intermediate values of n_1, as shown in Figs. 4.2 and 4.4(c)-(d). Increasing the rate b_2 leads to a decrease in the maximum values that can be attained by the mRNA concentration.

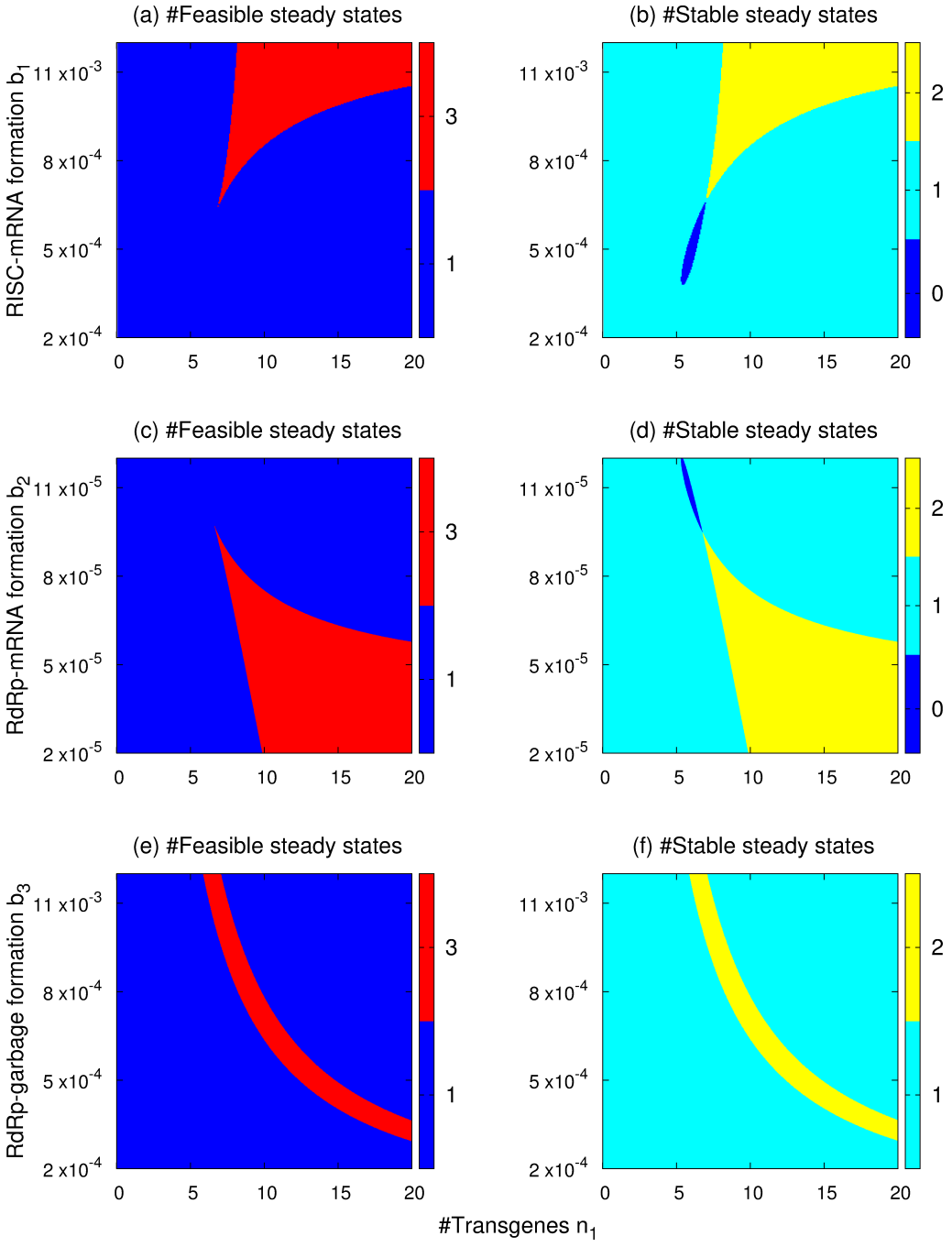

Figure 4.4: Regions of feasibility and stability of different steady with parameter values from Table 4.1.

Similar behaviour is observed in Fig. 4.3, where the rate b_3 of forming RdRP-garbage complexes is varied. Increasing this rate b_3 results in a reduced region of bi-stability and smaller values of the maximum mRNA concentration, but at the same time, it does not result in the complete disappearance of the bi-stability region, as was the case when the rate b_2 was varied. This behaviour is better observed in Fig. 4.4(e)-(f).

Comparing the influence of the rate p, at which dsRNA is synthesised directly from the mRNA to the number of siRNA n_2 produced by Dicer per cleaved dsRNA, one can notice that for sufficiently small n_2 and p, only the steady state E_3 is feasible and stable, and therefore, the strength of RNA silencing is severely limited, with a relatively high concentration of mRNA surviving, as illustrated in Figs. 4.5(a)-(b). This lies in agreement with experimental observations in which plants that carry a mutation in RdRp cannot synthesize trigger-dsRNA directly from mRNA and thus, fail to induce transgene induced silencing [**Dal00**], but like mammals who do not carry RdRp, might experience transient silencing [**Cap01**]. Increasing p reduces the range of n_2 values, for which bi-stability occurs, and eventually it leads to the complete disappearance of the intermediate steady state E_2. For higher value of p, the state E_{1-3} can exhibit instability in a small range of n_2 values, and for even higher rates of dsRNA production, this steady state is always stable, thus signifying that gene silencing has been achieved. From a biological perspective, this should be expected, as by increasing p, more mRNA can be used for dsRNA synthesis, which is then used for the production of siRNA, which in turn amplifies the process even further. This is consistent with experimental observations which show that strains of the fungus *Neurospora crassa*, which overexpress RdRp, are

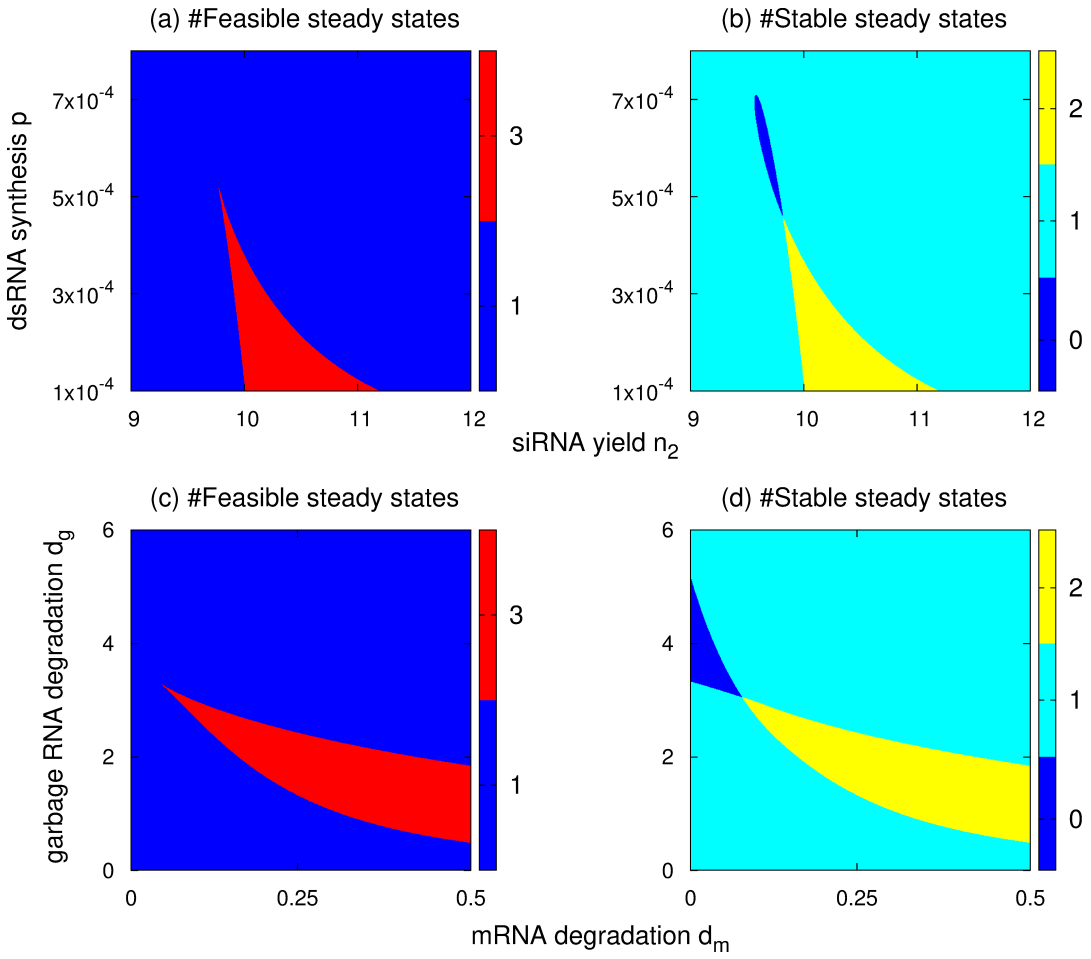

Figure 4.5: Regions of feasibility and stability of different steady with parameter values from Table 4.1.

able to progressively carry fewer transgenes without reverting back to their wild type. As such, even a single transgene is sufficient to induce gene silencing and therefore preserve the phenotypic stability of the species. [**For04**]. When one considers the relative effects of the degradation rates of mRNA d_m and garbage RNA d_g, it becomes clear that if the mRNA decays quite slowly, while garbage RNA decays fast, in a certain range of d_g values the system does not converge to any steady states but rather exhibits a limit cycle, as shown in Figs. 4.5(a)-(b). As the rate of mRNA degradation is increased, this reduces the range of possible d_g values where periodic behaviour is observed, until it eventually disappears completely. It is important to note that higher values of d_g correspond to E_3, and lower values correspond to E_1, which suggests that decreasing the rate d_g of garbage RNA degradation results in more of it being available for additional dsRNA synthesis, which subsequently results in a more efficient gene silencing.

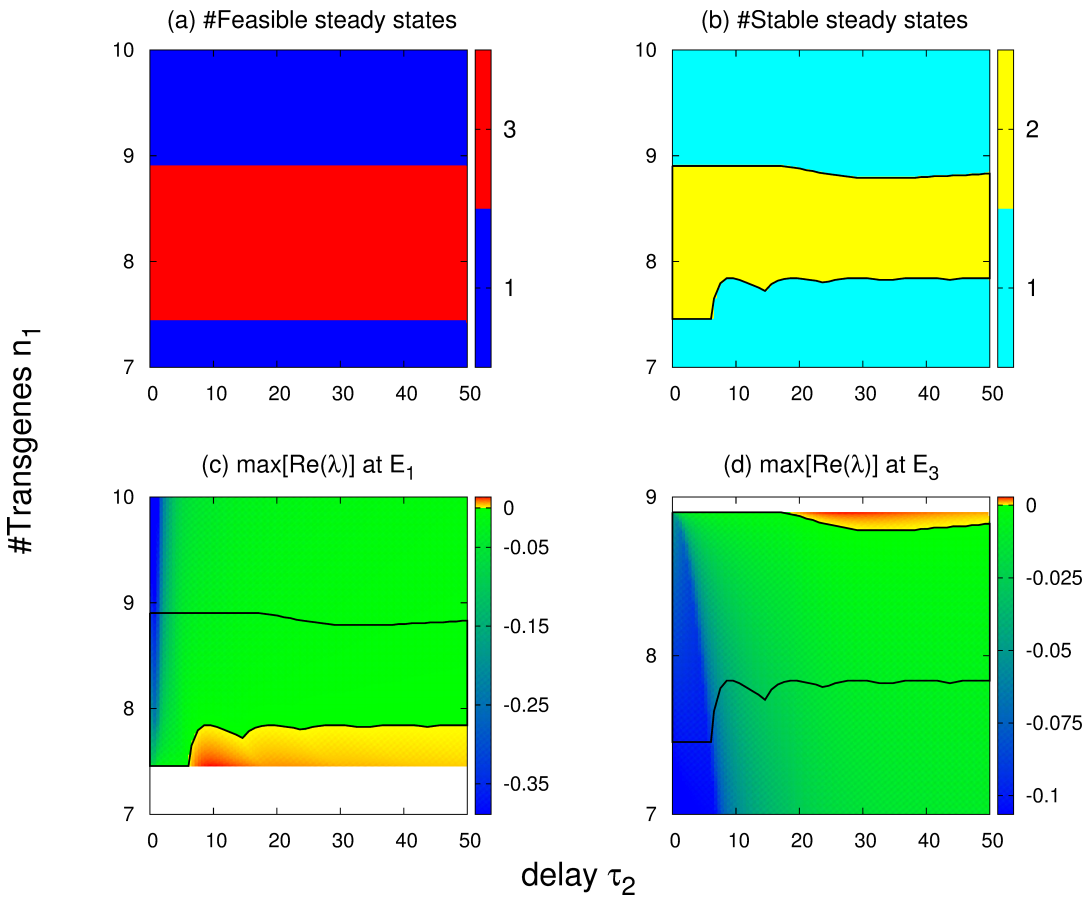

Figure 4.6: The top row shows the number of feasible (a) and stable (b) steady states depending on the time delay τ_2 and the number of transgenes n_1, with $\tau_1 = 1$, and the rest of the parameter values taken from Table 4.1. The bottom row shows max[Re(λ)] for the steady states E_1 (c) and E_3 (d) with a low and high concentration of mRNA, respectively, while the steady state E_2, which has a medium mRNA concentration, is unstable everywhere.

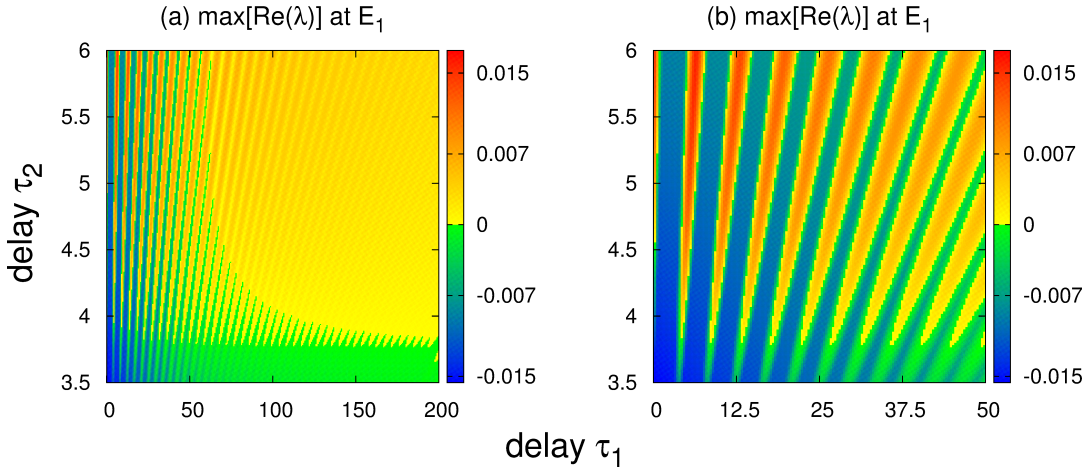

Figure 4.7: Colour code denotes max[Re(λ)] for the steady state E_1 with a low concentration of mRNA depending on the two time delays τ_1 and τ_2 associated with primed amplification, with the rest of the parameter values taken from Table 4.1. In the regions where E_1 is stable, the system is actually bi-stable, as the steady state E_3 with a high mRNA concentration is also stable.

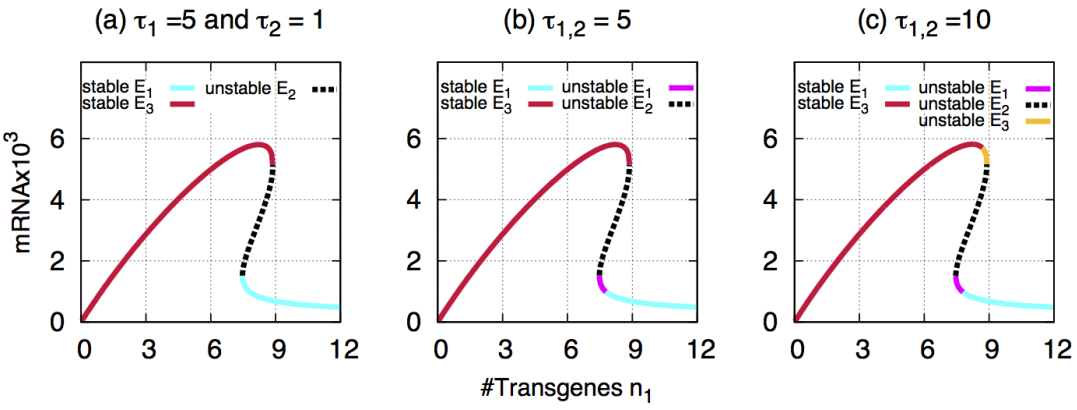

Figure 4.8: Stability of the three steady states E_1, E_2 and E_3 with parameter values from Table 4.1. The red and cyan lines denote the transgenic range where the steady states with a low (E_1) and high (E_3) levels of mRNA are stable, respectively. The black line signifies the steady state E_2 with a medium concentration of mRNA which is always unstable. The violet and light-brown lines denote the regions where the steady states E_1 and E_3 are unstable, respectively.

Fig. 4.6 shows how the region where the system (4.1) is bi-stable depends on the number of transgenes and the time delay τ_2, associated with a delayed production of dsRNA from aberrant RNA, when the delay associated with production of dsRNA from mRNA is fixed at $\tau_1 = 1$. This figure shows that when $\tau_2 = 0$, the system is bi-stable in the approximate range $7.5 \leq n_1 \leq 8.9$, and for sufficiently small τ_2 up until $\tau_2 \leq 7$, the behaviour of the system remains largely unchanged, whereas for $\tau_2 > 7$ and sufficiently small number of transgenes, the silenced steady state E_1 loses stability. This stability can be regained for some higher values of τ_2, but then it will be lost again. Steady states E_1 with higher values of n_1 are not affected by the variations in τ_2 and remain stable throughout the bi-stability region. In a similar way, the steady state E_3 can

also lose its stability, but unlike E_1, this happens for high values of transgenes, and the range of n_1 values where instability happens is smaller than for E_1. These results suggest that the time delays associated with primed amplification can result in a destabilisation of the steady states E_1 and E_3, thus disrupting gene silencing. When both time delays are varied, as shown in Figs. 4.7 and 4.8, the steady state E_3 without sufficient silencing is always stable, whereas increasing τ_1 and/or τ_2 causes the silenced steady state E_1 to switch between being stable or unstable. We note that the boundaries of the stability crossing curves demonstrated in Figure 4.7 are analytically described by (4.42). Fig. 4.8 illustrates that whilst the time delays do not affect the shape of the hysteresis curve, they can cause some extra parts of it to become unstable, which happens for smaller values of the time delay to E_1 only, and for higher values of the time delays to E_3 as well. A possible interpretation of this result is that the feedback loop in the model is highly sensitive to the speed of dsRNA production from its constituent parts. When the dsRNA synthesis is hindered by the time delays, the production cannot maintain the required consistent pace and, as a result, one of the steady states loses stability, which gives birth to stable periodic solutions.

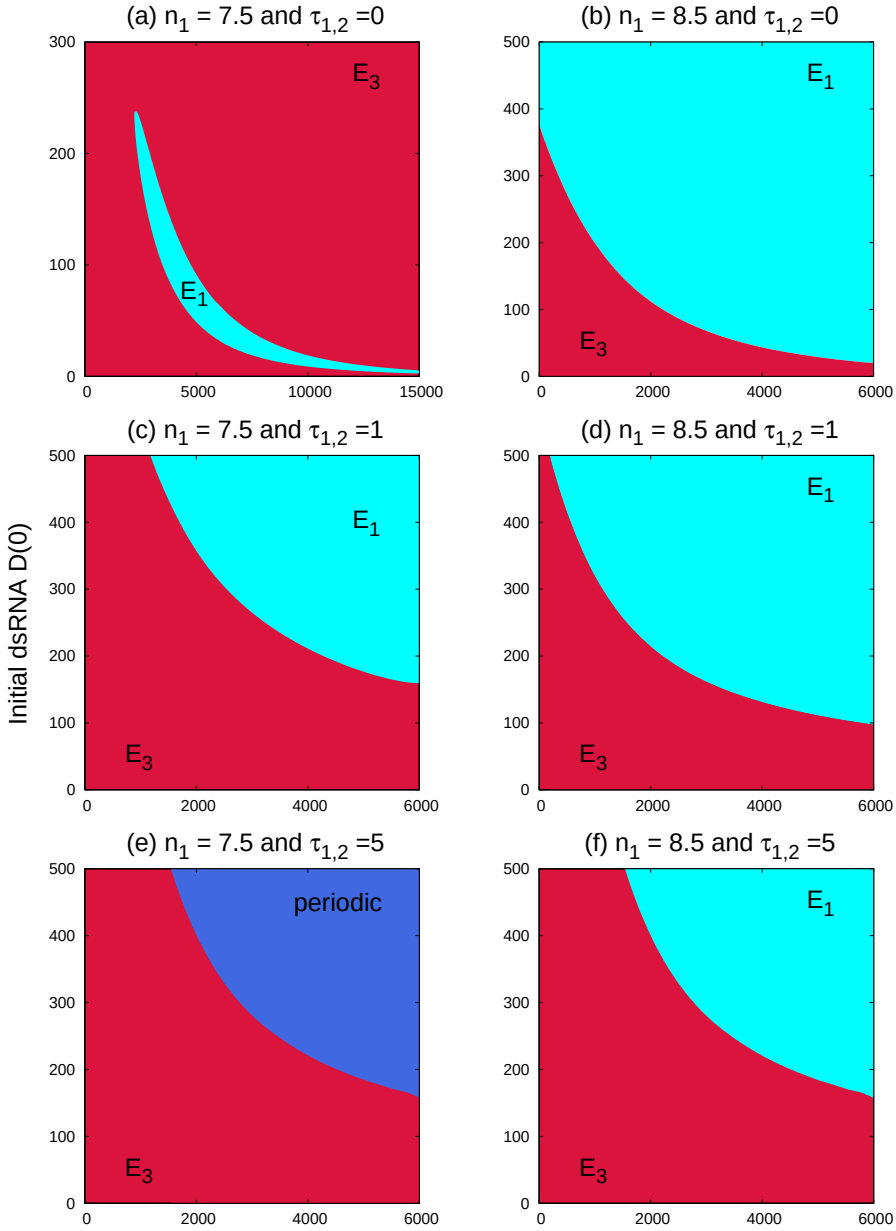

Figure 4.9: Basins of attraction of different steady stated depending on the initial dosage of dsRNA and garbage RNA within the host cell. The red and cyan regions are where the system converges to the steady state with a high, E_3, and low, E_1, levels of mRNA, respectively. In the dark-blue region the system exhibits periodic oscillations around the steady state E_1.

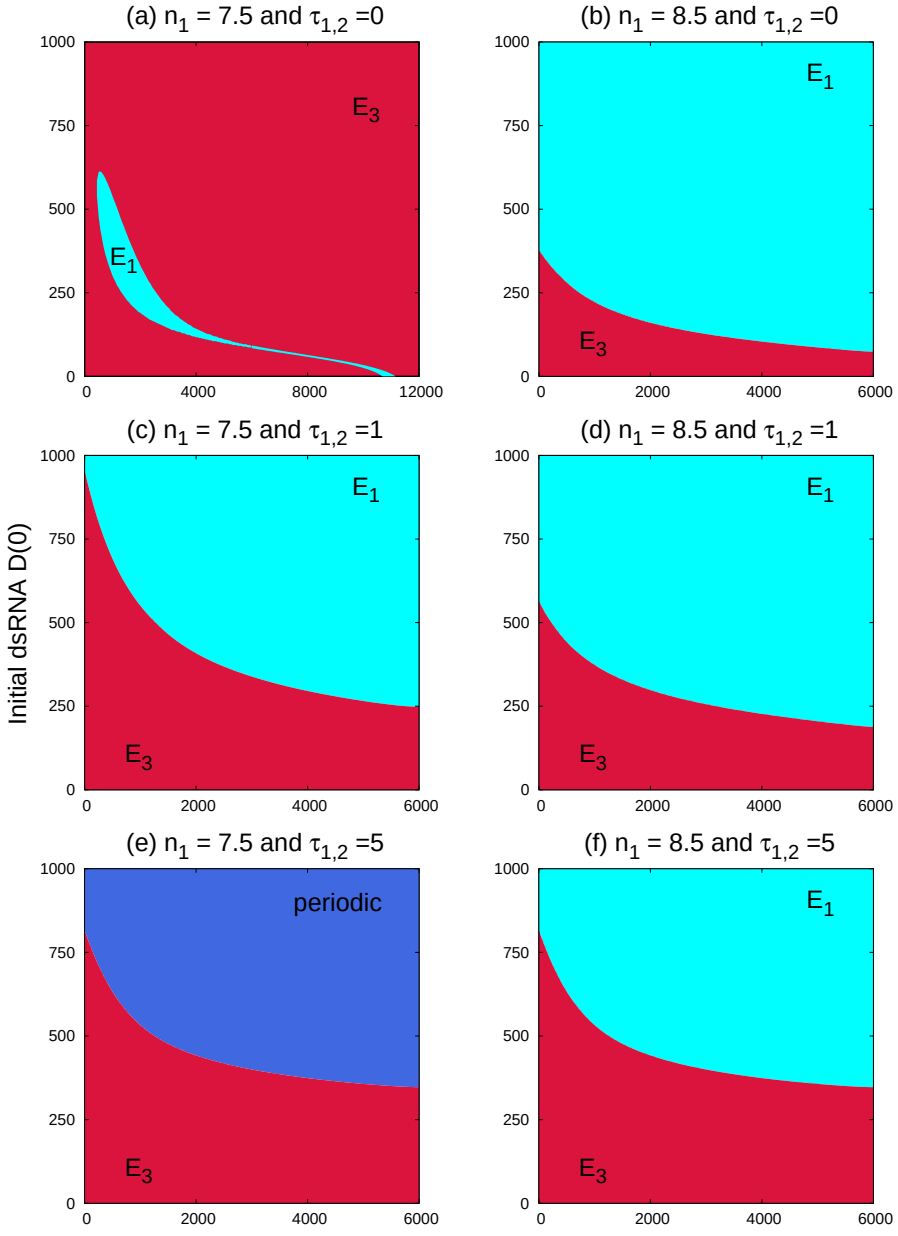

Figure 4.10: Basins of attraction of different steady stated depending on the initial dosage of dsRNA and initial mRNA within the host cell. The red and cyan regions are where the system converges to the steady state with a high, E_3, and low, E_1, levels of mRNA, respectively. In the dark-blue region the system exhibits periodic oscillations around the steady state E_1.

Figs 4.9 and 4.10 illustrate how the initial dosages of the dsRNA $D(0)$, garbage RNA $G(0)$ and mRNA $M(0)$ affect the behaviour of the model. Starting with the smaller number of transgenes, for which the system (4.1) is bi-stable we see that in Figs. 4.9(a),(b) and Figs. 4.10(a),(b), when the delays τ_1 and τ_2 are both set to zero, the system mostly converges to the steady state E_3 with a relatively high concentration of mRNA for smaller numbers of transgenes n_1, and to the steady state E_1 with a lower concentration of mRNA for higher numbers of transgenes n_1. As the time delays associated with the primed amplification increase, this increases the basin of attraction of E_1 for smaller n_1, and the basin of attraction of E_3 for higher n_1, as shown in Figs. 4.9,4.10(c) and Figs. 4.9,4.10(d), respectively. These figures suggest that for sufficiently high dosage of dsRNA and initial garbage RNA or mRNA being present in the cell, the system achieves a stable steady state where gene silencing is sustained. For higher values of the time delays, there is a qualitative difference in behaviour between lower and higher numbers of transgenes. For lower numbers of transgenes, the system exhibits a bi-stability between a stable steady state E_3 with a high concentration of mRNA and a periodic orbit around the now unstable steady state E_1. On the other hand, for higher values of n_1, there is still a bi-stability between E_1 and E_3. Whilst in this case, the system may appear not to be as sensitive to the effects of time delays in the primed amplification pathway, it is still evident that in the presence of time delays one generally requires a higher initial dosage of dsRNA to achieve sustained silencing. Furthermore, in the narrow range of n_1 values, where the steady state E_3 is destabilised by the time delays, numerical simulations show that the system always moves towards a stable steady state E_1 rather than oscillate around E_3, thus suggesting that

the Hopf bifurcation of this steady state is subcritical.

To illustrate the dynamics of the system (4.1) in different dynamical regimes, we have solved this system numerically, and the results are presented in Fig. 4.11. Figures (a) and (b) demonstrate the regime of bi-stability shown in Figs. 4.9,4.10(e), where under the presence of both time delays and depending on the initial conditions, the system either approaches the default stable steady state E_3 under a low dsRNA dosage, or tends to a periodic orbit around the silenced steady state E_1 despite a high dsRNA dosage Figure. (c) corresponds to a situation where the number of transgenes is sufficiently high, and the steady state E_3 is destabilised by the time delays, in which case the system approaches a silenced steady state E_1. It is interesting to note that prior to settling on the silenced state E_1, the system exhibits a prolonged period of oscillations around this state - a phenomenon very similar to the one observed in models of autoimmune dynamics [**Bly12**, **Bly15**], where the system can also show oscillations and then settle on some chronic steady state. This behaviour highlights an important issue that during experiments one has to be able to robustly distinguish between genuine sustained oscillations and long-term transient oscillations that eventually settle on a steady state.

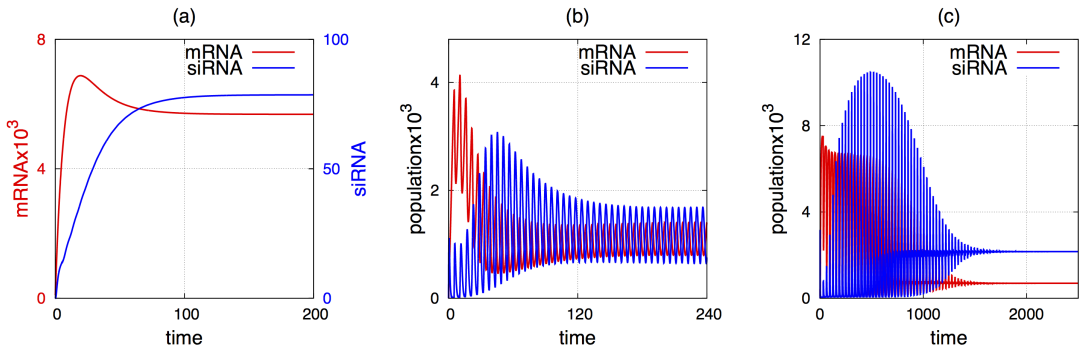

Figure 4.11: Numerical solutions of the model (4.1). (a) Stable steady state E_3 for $\tau_1 = \tau_2 = 5$, $n_1 = 7.5$. (b) Periodic oscillations around the steady state E_1 for $\tau_1 = \tau_2 = 5$, $n_1 = 7.5$. (c) Transient oscillations settling on a stable steady state E_1 for $\tau_1 = 1$, $\tau_2 = 30$ and $n_1 = 8.87$. Other parameter values are taken from Table 4.1.

4.6 Chapter conclusions

In this chapter we have considered a model of RNA interference with two primed amplification pathways associated with the production of dsRNA from siRNA and two separate RdRp-carrying complexes formed by targeting mRNA and garbage RNA. For better biological realism, we have explicitly included distinct time delays for each of these pathways to account for delays inherent in dsRNA synthesis. The system is shown to exhibit up to three biologically feasible steady states, with a relatively low (E_1), medium (E_2), or high (E_3) concentration of mRNA.

Stability analysis of the model has shed light on the relative importance of different system parameters. For sufficiently small levels of host mRNA, the system has a single stable steady state E_3, whose mRNA concentration is growing with the number of transgenes n_1. Experimental observations suggest

that the amount of transcribed mRNA is an important factor in the ability of transcripts to trigger silencing. Production of mRNA can generally be enhanced in two ways; either the target transgene is under control of a 35S promoter with a double enhancer so that the gene is transcribed at a higher rate [**Elm96**] or, that there are enough transgenic copies to maintain an adequate production of mRNA to trigger silencing. In our model, the trangenic number n_1 and the transcription rate of mRNA h are qualitatively interchangeable. As the number of transgenes increases, there is a range of transgenic copies for which the system is bi-stable, exhibiting steady states with a high (E_3) and low (E_1) mRNA concentrations, where E_1 describes a silenced state. For higher values of n_1, only the steady state E_1 is feasible and stable, suggesting that a sustained state of gene silencing is achieved. From a biological perspective, it is very interesting and important to note that in the bi-stable region, it is not only the parameters, but also the initial conditions that determine whether RNA silencing occurs. This implies that the dosage of dsRNA, which initialises the RNA interference mechanism, as well as the current levels of mRNA and garbage RNA within the cell, determine the evolution of the system. In the absence of time delays, a high dosage of dsRNA and an initial concentration of mRNA or garbage RNA results in a silenced steady state.

In the case when the delays associated with the primed amplification are non-zero, our analysis shows that for specific range of τ_1 and τ_2, both steady states E_1 or E_3 can lose stability in the bistable region. Once again, not only the parameters, but also the initial conditions control whether the system will converge to the remaining stable state or will oscillate around the unstable steady state. Additionally, under the presence of time delays, one generally requires

an even higher initial dosage of dsRNA to achieve sustained silencing compared to the non-delayed model. Interestingly, oscillations can only happen around the silenced steady state E_1, and when the steady state E_3 loses its stability, the system just moves towards a stable steady state E_1. Oscillations around E_1 biologically correspond to switching between higher and lower concentrations of mRNA, implying that at certain moments during time evolution, the exogenous mRNA is silenced, and at other times it is not affected by the RNAi. It follows that this switching behaviour might have case-specific implications for the phenotypic stability of a species which most likely depends on the amplitude of the oscillations around the silenced steady state. The biological significance of this result lies in the fact that there are cases where even a high dosage of dsRNA will not always result into a silenced steady state. Thus, the augmented model exhibits an enriched dynamical behavior compared to its predecessor which otherwise can only be replicated by different extensions to the core pathway, like the RNase model also developed in [**Gro05**], which assumes the presence of a specific siRNA degrading RNase with saturating kinetics.

Chapter 5

Discussion

5.1 Summary and conclusions

This thesis is concerned with the role of RNA interference as a vital defence component of the plant immune system and a gene regulator. In the context of plant immune dynamics, we have used an extended SIR framework to develop two new single-host mathematical models; a model of plant immune response against a single virus, and a model of plant-virus interactions between two competing viruses. To better understand the role of RNAi in gene regulation, we have augmented a well-known model of RNAi[**Gro05**] with time delays that also includes two amplification pathways. For all three models we have identified the equilibrium points for which we performed extensive bifurcation analysis, both analytically and numerically, to obtain feasibility and stability boundaries for different sets of parameter space. For the two models with time delays we derived conditions for a Hopf bifurcation and investigated whether the systems could exhibit periodic solutions. In addition to the stability analysis, each sys-

tem was solved numerically to illustrate different types of dynamical behaviour and to verify that results are qualitatively consistent with both theoretical and field observations.

In the first part ot the thesis, we introduced the biological intricacies of RNA interference and offered a basic mathematical background for the dynamics of infectious diseases, and a basic model of RNAi (Chapter 1). In Chapter 2, we derived a time-delayed model of plant immune response in order to investigate how RNA interference offers protection against a virus. This model includes two time delays to account for intrinsic delays in the propagating component of RNAi and a maturation time for undifferentiated/proliferating cells. It was shown that the system is biologically feasible, and, when it satisfies some basic assumptions regarding initial conditions, the solutions remain bounded. The model (2.3) has up to three possible steady states, a *trivial*, a *disease-free* and a single *endemic* steady state. We obtained feasibility criteria for these steady states and showed that the endemic steady state only becomes feasible in the parameter space where the disease-free steady state is unstable, which itself depends on the maturity delay. We then investigated the stability of the endemic steady state for different maturation times and speeds of the propagating warning signal and, when it was analytically possible, derived the critical time delays for which this steady state undergoes a Hopf-bifurcation. This was complemented with numerical stability analysis for different regimes of parameter space and simulations which show that the system is capable of exhibiting the three main phenotypes of plants, as classified by their immune response, namely susceptible, resistant and the recovery phenotype.

Our results suggest that the maturation time of undifferentiated cells can

play a very important role in the spread of the infection as it represents how fast the newly developed part of the plant becomes accessible to the virus. Plants which belong to either the resistant or recovery phenotype are most likely characterized by a successful localized immune response at the infection sites. On the other hand, the strength of the warning signal, propagating from infected sites to non-infected parts of the plant, only controls the pace of recovery but is not by itself sufficient for complete host recovery thus, it can at most determine whether a slow or fast recovery phenotype will be observed. Similarly, if both the localized immunity response and the systemic signal are sufficiently strong, the plant exhibits the resistant phenotype characterized by the successful isolation of the virus to the initial infected sites and a subsequently rapid recovery. When both the localized and systemic immune response are sufficiently weak, the plant will be completely susceptible, resulting in a severe host infection but it will, however, not be overwhelmed to the point where death becomes possible. As such, the main result from this chapter is the significance of the maturation time of undifferentiated cells acting as an intrinsic temporary immunity period that plays a fundamental role in determining the long-term behaviour of the system. This lies in contrast to the limited impact of the speed of the propagating warning signal.

In Chapter 3 we developed a model of plant immune response against two viruses in order to examine how RNAi mediates the interactions betweens competing viruses and to explore how situations of viral synergism and antagonism might arise. We proved that the system (3.1) is well-posed and has the following possible equilibria: a *trivial*, a *disease-free*, two *single-virus endemic* equilibria, and it can also support one or more *syndemic* steady states. Since the first

four equilibria can be found explicitly, we investigated their biological feasibility and derived the basic reproduction numbers R_{01}, R_{02} for each of the two viruses respectively. This allowed us to define the basic reproduction number $R_0 = \max\{R_{01}, R_{02}\}$, such that for $R_0 < 1$, the disease-free steady state is stable. By using the Routh-Hurwitz criteria we obtained stability conditions for the two single-virus endemic steady states and performed extensive numerical bifurcation analysis to identify stable regimes for all the different steady states. The Chapter includes numerical simulations that are qualitatively consistent with examples of cross-protection or cross-enhancement. It was shown that if the propagating signal rates, triggered by the presence of two immunologically related viruses, were sufficiently high, one could not only minimize the spread of one of the viruses, but also reduce the overall infection. Additionally, the results indicated specific cases in which one virus could only exist under the presence of a second strain, which has important implications for the pathology of plants and viral evolutionary dynamics. Generally speaking, analysis of the second model has demonstrated that the total population of infected cells during a co-infection can sometimes, but not always, exceed the levels compared to individual infections for which we offered two possible explanations: either the two different infections simply increase the overall rate of infection, or the cells that have acquired immunity against one of the viruses may be less or more susceptible to the other virus. Our results have shown that when two viruses "antagonize" each other, i.e $a_i, \beta_i < 1$, for sufficiently high warning rates, not only can one minimize the spread of a specific virus, but the overall infection can also be reduced which enables different control strategies. As such, one might choose to intentionally infect a healthy plant with the appropriate viral

strain in order to trigger a pre-emptive immune response that can be used as a safeguard against a more harmful strain.

Similarly, if two viruses are immunologically unrelated, they can indirectly promote each other by inadvertently making each other's exclusive source of cells more susceptible to the other virus. This effectively bypasses some of the resource competition and allows for partial spatial exclusion and therefore, the occupation of a partially different niche, thus enabling the possibility of co-existence with the potency of individual infections strongly dependent on the immunological relation between the two viruses. Another important result is that the syndemic steady state can potentially be stable in the parameter regions where only one of the endemic steady states is feasible, implying that a secondary virus can only survive when another infection is present. Unlike the results obtained from single infections (including Chapter 2), when the syndemic steady state is considered, our results show that the warning signal plays a crucial role in determining whether both viruses can co-exist. If the two viruses are sufficiently related in such a way that the immune response trigged by one of the viruses negatively affects the other, then one of the two viruses becomes dominant, and the plant experiences a degree of cross-protection which, may however, in some cases elevate the total level of infection.

In Chapter 4 we performed a thorough mathematical analysis of a time-delayed model of RNAi. This allowed us to investigate the significance of the two intrinsic delays associated with signal amplification in which siRNA primes dsRNA-synthesis by either directly targeting mRNA or garbage RNA. It was shown that if the population of dsRNA is bounded by some upper threshold, given the right initial conditions the remaining solutions of the system will not

only stay positive but will also remain bounded throughout the time evolution. The model (4.1) exhibits up to three non-trivial steady states. When all these steady states are feasible, they can be classified according to the concentration of mRNA, namely E_1 (low), E_2 (medium), E_3 (high), which also signifies whether the long-term behaviour of the system has reached a silenced, partially-silenced state, or that no silencing has occurred, respectively. We then investigated the stability of different steady states for various choices of parameters and cases where one or both the amplification delays are small. When the time delays in the system are small enough to be ignored, we used the Routh-Hurwitz criterion to obtain stability conditions for the three steady states. In the case where the time delays are present, we made use of the bifurcation theorem to obtain the values of the critical time delays, and, used stability crossing curves to identify the stability boundaries for these steady states. We computed bifurcation diagrams which showed that the system is bi-stable in different parameter regimes. Furthermore, by calculating the basins of attraction of each steady state, we found that sustained silencing can only occur for particular initial dosages of trigger dsRNA. We also performed numerical stability analysis to determine how system parameters affect the long-term behaviour of the system and, included numerical examples with different outcomes that are qualitatively consistent with absent or sustained silencing.

As the production of mRNA is increased due to an increasing number of transgenes, there is a range of transgenic copies n_1 for which the system becomes bi-stable, exhibiting steady states with a high (E_3) and low (E_1) mRNA concentrations. For higher values of n_1, only the steady state E_1 is feasible and stable, suggesting that the targeted transgenes can be suppressed indefinitely.

Since the system is also bi-stable for different regions of parameter space, it implies that the dosage of trigger dsRNA, as well as the current levels of mRNA and garbage RNA within the cell, determine the strength of silencing. When dsRNA synthesis is unaffected by delays, we observe that a high initial dosage of dsRNA and mRNA or garbage RNA results in a silenced steady state as the feedback loop feeds the system with sufficient dsRNA to sustain the process.

In the case when the primed amplification is affected by time delays, our analysis shows that for specific range of τ_1 and τ_2, both steady states E_1 or E_3 can lose stability in the bi-stable region. Numerical simulations of the model have shown that it is possible for the system to either converge to the remaining stable state, or oscillate around the unstable steady state depending on the initial conditions. It is interesting to note however, that these oscillations can only happen around the silenced steady state E_1, and when the steady state E_3 loses its stability, the system just moves towards a stable steady state E_1. Oscillations around E_1 biologically correspond to a continuous switching between higher and lower concentrations of mRNA, implying periodic intervals in which the silencing is weak. At the moment there is no clear indication of how the cells could be affected by this behaviour. Hence, a follow-up question is whether this could offer partial protection against the self-inflicted response to an erroneous identification of target mRNA, and whether periodic silencing can, to some extent, minimise the damage to the host cell and limit morphogenetic changes.

5.2 Future work

The work in this thesis has, demonstrated the significance of time delays in models of RNA interference. We note that in the second chapter we have seen that the time delay associated with maturation period of undifferentiated/proliferating cells can play a very important role in controlling the spread of the infection. It is therefore an interesting and practically important question whether that model can be further improved by including some more realistic distribution of maturation periods in the way it was done while modelling different distributions of temporary immunity [**Bly10**, **Kyr14**], latency and incubation [**Ber95**, **Mcc10**], or infectious periods [**Rob07**, **Zha08**].

Similarly, the results presented in the third chapter can be extended to explicitly include the time delays associated with plant maturation time, and with delayed propagation of the RNAi signal, as it was done for the first model. Another interesting phenomenon to consider is the possibility of cells being occupied by two viruses simultaneously, which would allow for a wider spectrum of interactions between the viruses and their host. This could include superinfection of individual cells, viral interference or recombination events that can give rise to additional strains [**Fle96**, **Sil11**, **Per15**].

Another issue is that the time delays considered in the third model are assumed to be discrete, and hence it would be very insightful and relevant, from a biological perspective, to investigate how stability results for this model would change in the case where the time delays obey certain distributions. Recent results suggest that distributed delays can in some instances increase [**Kyr13**, **Kyr14**], and in others reduce [**Rah15**] parameter regions where oscillations are suppressed. Our future research will look into the effects of distributed time

delays on primed amplification in RNAi.

Additionally, it would be interesting and important to investigate how the plant immune system responds to viral infections when spatial dynamics are considered. Within such framework, one could study whether diffusion of virus particles and the spread of siRNA can result in the formation of spatial patterns arising from travelling waves. This would provide useful insights for the development of optimal techniques for using RNA interference to control viral infections.

Bibliography

[Agi12] Agius, C., Eamens, A. L., Millar, A. A., Watson, J. M., & Wang, M.-B. (2012). RNA silencing and antiviral defense in plants. Methods in Molecular Biology (Clifton, N.J.), 894, 17–38.

[All03] Allen, L. J. S., Langlais, M., & Phillips, C. J. (2003). The dynamics of two viral infections in a single host population with applications to hantavirus. Mathematical Biosciences, 186(2), 191–217.

[And66] Andronov, A. A., Vitt, A. A., & Khaikin, S. E. (1966). Theory of oscillators. Translated from the Russian by F. Immirzi; translation edited and abridged by W. Fishwick (Pergamon Press, Oxford, 1966).

[AlT11] Al-Taleb, M. M., Hassawi, D. S., & Abu-Romman, S. M. (2011). Production of virus free potato plants using meristem culture from cultivars grown under Jordanian environment. The American-Eurasian Journal of Agricultural & Environmental Sciences, 11(4), 467–472.

[And97] Andreasen, V., Lin, J., & Levin, S. A. (1997). The dynamics of cocirculating influenza strains conferring partial cross-immunity. Journal of mathematical biology, 35(7), 825–842.

[Arc04] Arciero, J. C., Jackson, T. L., & Kirschner, D. E. (2004). A mathematical model of tumor-immune evasion and siRNA treatment. Discrete and Continuous Dynamical Systems Series B, 4(1), 39–58.

[Ari04] Arino, J., Cooke, K. L., van den Driessche, P., & Velasco-Hernández, J. X. (2004). An Epidemiology Model That Includes a Leaky Vaccine with a General Waning Function. Discrete and Continuous Dynamical Systems - Series B, 4(2), 479–495.

[Bar06] Bartlett, D. W., & Davis, M. E. (2006). Insights into the kinetics of siRNA-mediated gene silencing from live-cell and live-animal bioluminescent imaging. Nucleic acids research, 34(1), 322–333.

[Bea99] Beachy, R. N. (1999). Coat–protein–mediated resistance to tobacco mosaic virus: discovery mechanisms and exploitation. Philosophical Transactions of the Royal Society of London B: Biological Sciences, 354(1383), 659–664.

[Ben97] Bendahmane, M., Fitchen, J. H., Zhang, G., & Beachy, R. N. (1997). Studies of coat protein-mediated resistance to tobacco mosaic tobamovirus: correlation between assembly of mutant coat proteins and resistance. Journal of virology, 71(10), 7942–7950.

[Ber95] Beretta, E., & Takeuchi, Y. (1995). Global stability of an SIR epidemic model with time delays. Journal of mathematical biology, 33(3), 250–260.

[Ber01a] Beretta, E., & Kuang, Y. (2001). Modeling and analysis of a marine bacteriophage infection with latency period. Nonlinear Analysis: Real World Applications, 2(1), 35–74.

[Ber01b] Bernstein, E., Caudy, A. A., Hammond, S. M., & Hannon, G. J. (2001). Role for a bidentate ribonuclease in the initiation step of RNA interference. Nature, 409(6818), 363–366.

[Ber02] Beretta, E., & Kuang, Y. (2002). Geometric Stability Switch Criteria in Delay Differential Systems with Delay Dependent Parameters. SIAM Journal on Mathematical Analysis, 33(5), 1144—1165.

[Ber03] Bergstrom, C. T., McKittrick, E., & Antia, R. (2003). Mathematical models of RNA silencing: unidirectional amplification limits accidental self-directed reactions. Proceedings of the National Academy of Sciences, 100(20), 11511–11516.

[Ber07] Berger, S., Sinha, A. K., & Roitsch, T. (2007). Plant physiology meets phytopathology: plant primary metabolism and plant–pathogen interactions. Journal of experimental botany, 58(15-16), 4019–4026.

[Ber14] Bergua, M., Zwart, M. P., El-Mohtar, C., Shilts, T., Elena, S. F., & Folimonova, S. Y. (2014). A viral protein mediates superinfection exclusion at the whole-organism level but is not required for exclusion at the cellular level. Journal of virology, 88(19), 11327–11338.

[Bly08] Blyuss, K. B., Kyrychko, Y. N., Hövel, P., & Schöll, E. (2008). Control of unstable steady states in neutral time-delayed systems. The European Physical Journal B, 65(4), 571–576.

[Bly10] Blyuss, K. B., & Kyrychko, Y. N. (2010). Stability and bifurcations in an epidemic model with varying immunity period. Bulletin of mathematical biology, 72(2), 490–505.

[Bly12] Blyuss, K. B., & Nicholson, L. B. (2012). The role of tunable activation thresholds in the dynamics of autoimmunity. Journal of theoretical biology, 308, 45–55.

[Bly15] Blyuss, K. B., & Nicholson, L. B. (2015). Understanding the roles of activation threshold and infections in the dynamics of autoimmune disease. Journal of theoretical biology, 375, 13–20.

[Bra12] Brauer, F., & Castillo-Chavez, C. (2012). Mathematical Models for Communicable Diseases.

[Bre06] Breda, D., Maset, S., & Vermiglio, R. (2006). Pseudospectral approximation of eigenvalues of derivative operators with non-local boundary conditions. Applied numerical mathematics, 56(3), 318–331.

[Buc04] Buckee, C. O. F., Koelle, K., Mustard, M. J., & Gupta, S. (2004). The effects of host contact network structure on pathogen diversity and strain structure. Proceedings of the National Academy of Sciences of the USA, 101(29), 10839–10844.

[Buc10] Buckee, C.O., & Gupta, S., (2010). A network approach to understanding pathogen population structure, in Sintchenko, V. (Ed.), Infectious Disease Informatics. Springer New York, 167–185.

[Bur03] Burdon, J. J., & Thrall, P. H. (2003). The fitness costs to plants of resistance to pathogens. Genome biology, 4(9), 1.

[Burg11] Burgyán, J., & Havelda, Z. (2011). Viral suppressors of RNA silencing. Trends in plant science, 16(5), 265–272.

[Cam61] Campbell, A. (1961). Conditions for the existence of bacteriophage. Evolution,15(2), 153–165.

[Can08] Cañizares, M. C., Navas-Castillo, J., & Moriones, E. (2008). Multiple suppressors of RNA silencing encoded by both genomic RNAs of the crinivirus, Tomato chlorosis virus. Virology, 379(1), 168–174.

[Cap01] Caplen, N. J., Parrish, S., Imani, F., Fire, A., & Morgan, R. A. (2001). Specific inhibition of gene expression by small double-stranded RNAs in invertebrate and vertebrate systems. Proceedings of the National Academy of Sciences, 98(17), 9742–9747.

[Cap04] Caplen, N. J. (2004). Gene therapy progress and prospects. Downregulating gene expression: the impact of RNA interference. Gene therapy, 11(16), 1241–1248.

[Cas96] Castillo-Chavez, C., Huang, W., & Li, J. (1996). Competitive exclusion in gonorrhea models and other sexually transmitted diseases. SIAM Journal on Applied Mathematics, 56(2), 494-508.

[Cis04] Cisternas, J., Gear, C. W., Levin, S., & Kevrekidis, I. G. (2004). Equation-free modelling of evolving diseases: coarse-grained computations with individual-based models. Proceedings of the Royal Society of London A: Mathematical, Physical and Engineering Sciences, The Royal Society, 460(2050), 2761–2779

[Ciu07] Ciupe, S. M., Ribeiro, R. M., Nelson, P. W., & Perelson, A. S. (2007). Modeling the mechanisms of acute hepatitis B virus infection. Journal of theoretical biology, 247(1), 23–35.

[Cha94] Chan, M. S., & Jeger, M. J. (1994). An analytical model of plant virus disease dynamics with roguing and replanting. Journal of Applied Ecology, 31(3), 413-427.

[Coo99] Cooke, K., van den Driessche, P., & Zou, X. (1999). Interaction of maturation delay and nonlinear birth in population and epidemic models. Journal of Mathematical Biology, 39(4), 332—352.

[Cos13] Costa, A. T., Bravo, J. P., Makiyama, R. K., Nunes, A. V., & Maia, I. G. (2013). Viral counter defense X antiviral immunity in plants: mechanisms for survival. Current Issues in Molecular Virology, Viral Genetics and Biotechnological Applications, 10(5772), 56253.

[Cuc11] Cuccato, G., Polynikis, A., Siciliano, V., Graziano, M., di Bernardo, M., & di Bernardo, D. (2011). Modeling RNA interference in mammalian cells. BMC Systems Biology, 5(1), 1.

[Dal00] Dalmay, T., Hamilton, A., Rudd, S., Angell, S., & Baulcombe, D. C. (2000). An RNA-dependent RNA polymerase gene in Arabidopsis is required for posttranscriptional gene silencing mediated by a transgene but not by a virus. Cell, 101(5), 543–553.

[Die93] Dietz, K. (1993). The estimation of the basic reproduction number for infectious diseases. Statistical methods in medical research, 2(1), 23–41.

[Dri77] Driver, R.D. (1977). Ordinary and Delay Differential Equations, 20. New York, NY: Springer New York.

[Dri08] Van den Driessche, P., & Watmough, J. (2008). Further notes on the basic reproduction number. Mathematical Epidemiology, 1945, 159–178.

[Ehn97] Ehness, R., Ecker, M., Godt, D. E., & Roitsch, T. (1997). Glucose and stress independently regulate source and sink metabolism and defense mechanisms via signal transduction pathways involving protein phosphorylation. The Plant Cell, 9(10), 1825–1841.

[Elb01] Elbashir, S. M., Lendeckel, W., & Tuschl, T. (2001). RNA interference is mediated by 21-and 22-nucleotide RNAs. Genes & development, 15(2), 188–200.

[Elm96] Elmayan, T., & Vaucheret, H. (1996). Expression of single copies of a strongly expressed 35S transgene can be silenced post–transcriptionally. The Plant Journal, 9(6), 787-797.

[Esc00] Escobar, M. A., & Dandekar, A. M. (2003). Post-transcriptional gene silencing in plants. Non-coding RNAs: Molecular Biology and Molecular Medicine. J. Barciszewski and VA Erdmann (Eds), 129–140.

[Fer03] Ferguson, N. M., Galvani, A. P., & Bush, R. M. (2003). Ecological and immunological determinants of influenza evolution. Nature, 422(6930), 428–433.

[Fer04] Ferreira, M. U., da Silva Nunes, M., & Wunderlich, G. (2004). Antigenic diversity and immune evasion by malaria parasites. Clinical and diagnostic laboratory immunology, 11(6), 987–995.

[Fir98] Fire, A., Xu, S., Montgomery, M. K., Kostas, S. A., Driver, S. E., & Mello, C. C. (1998). Potent and specific genetic interference by double-stranded RNA in Caenorhabditis elegans. Nature, 391(6669), 806–811.

[Fit06] Fit06 Fitt, B. D. L., Huang, Y.-J., van den Bosch, F., & West, J. S. (2006). Coexistence of related pathogen species on arable crops in space and time. Annual Review of Phytopathology, 44, 163—82.

[Fle96] Fleischmann, W. R. (1996). Viral Genetics. Medical Microbiology. University of Texas Medical Branch at Galveston.

[For04] Forrest, E. C., Cogoni, C., & Macino, G. (2004). The RNA-dependent RNA polymerase, QDE-1, is a rate-limiting factor in post-transcriptional gene silencing in Neurospora crassa. Nucleic acids research, 32(7), 2123-2128.

[Fos02] Foster, T.M., Lough, T.J., Emerson, S.J., Lee, R.H., Bowman, J.L., Forster, R.L.S., & Lucas, W.J. (2002). A surveillance system regulates selective entry of RNA into the shoot apex. Plant Cell 14(7), 1497–1508.

[Fra02] Frank, S. A. (2002). Immunology and evolution of infectious disease. Princeton University Press.

[Fra77] Frazer, B. D. (1977). Plant virus epidemiology and computer simulation of aphid populations. Aphids as Virus Vectors, 413–31.

[Fri07] Fritig, B., Kauffmann, S., Dumas, B., Geoffroy, P., Kopp, M., & Legrand, M. (2007). Mechanism of the hypersensitivity reaction of plants. Ciba Foundation Symposium 133, Plant Resistance to Virus, 92–108.

[Gaa06] García-Andrés, S., Monci, F., Navas-Castillo, J., & Moriones, E. (2006). Begomovirus genetic diversity in the native plant reservoir Solanum nigrum: Evidence for the presence of a new virus species of recombinant nature. Virology, 350(2), 433–442.

[Gao06] Gao, S., Chen, L., Nieto, J. J., & Torres, A. (2006). Analysis of a delayed epidemic model with pulse vaccination and saturation incidence. Vaccine, 24(35), 6037–6045.

[Gal06] Gal-On, A., & Shiboleth, Y. M. (2006). Cross-protection. Natural resistance mechanisms of plants to viruses, 261–288.

[Ger06] Gergerich, R. C., & Dolja, V. V. (2006). Introduction to plant viruses, the invisible foe. The Plant Health Instructor.

[Gio02] Giordano, E., Rendina, R., Peluso, I., & Furia, M., (2002). RNAi triggered by symmetrically transcribed transgenes in *Drosophila melanogaster*. Genetics 160 (2), 637–648.

[Gom02] Gomes, M. G. M., Medley, G. F., & Nokes, D. J. (2002). On the determinants of population structure in antigenically diverse pathogens. Proceedings of the Royal Society of London B: Biological Sciences, 269(1488), 227–233.

[Gou05] Gourley, S. A., & Kuang, Y. (2004). A delay reaction-diffusion model of the spread of bacteriophage infection. SIAM Journal on Applied Mathematics, 65(2), 550–566.

[Gro05] Groenenboom, M. A., Marée, A. F., & Hogeweg, P. (2005). The RNA silencing pathway: the bits and pieces that matter. PLoS Computational Biology, 1(2), e21.

[Gro08a] Groenenboom, M. A., & Hogeweg, P. (2008). RNA silencing can explain chlorotic infection patterns on plant leaves. BMC systems biology, 2(1), 1.

[Gro08b] Groenenboom, M. A., & Hogeweg, P. (2008). The dynamics and efficacy of antiviral RNA silencing: A model study. BMC systems biology, 2(1), 1.

[Gu05] Gu, K., Niculescu, S. I., & Chen, J. (2005). On stability crossing curves for general systems with two delays. Journal of mathematical analysis and applications, 311(1), 231–253.

[Guo95] Guo, S., & Kemphues, K. J. (1995). par-1, a gene required for establishing polarity in C. elegans embryos, encodes a putative Ser/Thr kinase that is asymmetrically distributed. Cell, 81(4), 611–620.

[Gup94] Gupta, S., Trenholme, K., Anderson, R. M., & Day, K. P. (1994). Antigenic diversity and the transmission dynamics of Plasmodium falciparum. Science-AAAS-Weekly Paper Edition-including Guide to Scientific Information, 263(5149), 961–962.

[Gup96] Gupta, S., Maiden, M. C., Feavers, I. M., Nee, S., May, R. M., & Anderson, R. M. (1996). The maintenance of strain structure in populations of recombining infectious agents. Nature Medicine, 2(4), 437–442.

[Gup99] Gupta, S., Maiden, M. C., Feavers, I. M., Nee, S., May, R. M., & Anderson, R. M. (1996). The maintenance of strain structure in populations of recombining infectious agents. Nature Medicine, 2(4), 437-442.

[Gog02] Gog, J. R., & Grenfell, B. T. (2002). Dynamics and selection of many-strain pathogens. Proceedings of the National Academy of Sciences, 99(26), 17209–17214.

[Gou04] Gourley, S. A., & Kuang, Y. (2004). A stage structured predator-prey model and its dependence on maturation delay and death rate. Journal of Mathematical Biology, 49(2), 188-–200.

[Gut74] Gutierrez, A. P., Havenstein, D. E., Nix, H. A., & Moore, P. A. (1974). The ecology of Aphis craccivora Koch and subterranean clover stunt virus in south-east Australia. II. A model of cowpea aphid populations in temperate pastures. Journal of Applied Ecology,11(1) 1–20.

[Hal71] Hale, J. K. (1971). Functional Differential Equations.

[Hal93] Hale, J. K., & Lunel, S. M. V. (1993). Introduction to Functional Differential Equations (Vol. 99). New York, NY: Springer New York.

[Ham00] Hammond, S.M., Bernstein, E., Beach, D., & Hannon, G.J., (2000). An RNA-directed nuclease mediates post-transcriptional gene silencing in *Drosophila* cells. Nature 404, 293–296.

[Han02] Hannon, G.J., (2002). RNA interference. Nature 418, 244–251.

[Han04] He, L., & Hannon, G. J. (2004). MicroRNAs: small RNAs with a big role in gene regulation. Nature Reviews Genetics, 5(7), 522–531.

[Hee96] Heesterbeek, J. A. P., & Dietz, K. (1996). The concept of R_0 in epidemic theory. Statistica Neerlandica, 50(1), 89–110.

[Hei99] Heinen, M. (1999). Analytical growth equations and their Genstat 5 equivalents. Netherlands Journal of Agricultural Science, 47, 67–89.

[Het00] Hethcote, H. W. (2000). The mathematics of infectious diseases. SIAM review, 42(4), 599–653.

[Him15] Himber, C., & Dunoyer, P. (2015). The tracking of intercellular small RNA movement. Plasmodesmata: Methods and Protocols, 275–281.

[Hir98] Hinrichs, J., Berger, S., & Shaw, J. G. (1998). A hypersensitive response-like mechanism is involved in resistance of potato plants bearing the Ry (sto) gene to the potyviruses potato virus Y and tobacco etch virus. Journal of general virology, 79(1), 167–176.

[Hop42] Hopf, E., (1942). Abzweigung einer periodischen Lösung von einer stationären Lösung eines Differentialsystems, Berichten der Mathematisch-Physischen Klasse der Sächsischen Akademie der Wissenschaften zu Leipzig XCIV, 1-22 . An English translation, with comments, is included as Section 5 in [Mar76].

[Hua10] Huang, G., Takeuchi, Y., Ma, W., & Wei, D. (2010). Global Stability for Delay SIR and SEIR Epidemic Models with Nonlinear Incidence Rate. Bulletin of Mathematical Biology, 72(5), 1192–1207.

[Irw00] Irwin, M. E., Ruesink, W. G., Isard, S. A., & Kampmeier, G. E. (2000). Mitigating epidemics caused by non-persistently transmitted aphid-borne viruses: the role of the pliant environment. Virus research, 71(1), 185–211.

[Jus10] Just, W., Pelster, A., Schanz, M., & Schöll, E. (2010). Delayed complex systems: an overview. Philosophical Transactions. Series A, Mathematical, Physical, and Engineering Sciences, 368(1911), 303—304.

[Jeg04] Jeger, M. J., Holt, J., Van Den Bosch, F., & Madden, L. V. (2004). Epidemiology of insect-transmitted plant viruses: Modelling disease dynamics and control interventions. Physiological Entomology, 29(3), 291–304.

[Jeg11] Jeger, M. J., Van den Bosch, F., & Madden, L. V. (2011). Modelling virus-and host-limitation in vectored plant disease epidemics. Virus research, 159(2), 215–222.

[Jon06] Jones, J. D., & Dangl, J. L. (2006). The plant immune system. Nature, 444(7117), 323–329.

[Kat04] Katoh, N., Yui, M., Sato, S., Shirai, T., Yuasa, H., & Hagimori, M. (2004). Production of virus-free plants from virus-infected sweet pepper by in vitro grafting. Scientia horticulturae, 100(1), 1-6.

[Kaw04] Kawakami, S., Watanabe, Y., & Beachy, R. N. (2004). Tobacco mosaic virus infection spreads cell to cell as intact replication complexes. Proceedings of the National Academy of Sciences of the USA, 101(16), 6291–6296.

[Kee08] Keeling, M. J., & Rohani, P. (2008). Modeling infectious diseases in humans and animals. Princeton University Press.

[Ker27] Kermack, W. O., & McKendrick, A. G. (1927). A Contribution to the Mathematical Theory of Epidemics. Proceedings of the Royal Society A: Mathematical, Physical and Engineering Sciences, 115(772), 700–721.

[Ket01] Ketting, R. F., Fischer, S. E., Bernstein, E., Sijen, T., Hannon, G. J., & Plasterk, R. H. (2001). Dicer functions in RNA interference and in synthesis of small RNA involved in developmental timing in *C. elegans*. Genes & development, 15(20), 2654–2659.

[Kir78] Kirtani, K., Sasaba, T., (1978). An experimental validation of the systems model for the prediction of rice dwarf virus infection. Applied Entomology and Zoology, 13(3), 209–214.

[Kry07] Kryazhimskiy, S., Dieckmann, U., Levin, S. A., & Dushoff, J. (2007). On state-space reduction in multi-strain pathogen models, with an application to antigenic drift in influenza A. PLoS Computational Biology, 3(8), e159.

[Kun14] Kuntz, M. (2014). Is it possible to overcome the GMO controversy? Some Elements for a philosophical perspective. Plant Biotechnology, 107–111.

[Kyr05] Kyrychko, Y. N., & Blyuss, K. B. (2005). Global properties of a delayed SIR model with temporary immunity and nonlinear incidence rate. Nonlinear Analysis: Real World Applications, 6(3), 495-–507.

[Kyr13] Kyrychko, Y.N., Blyuss, K.B., Schöll, E., (2013). Amplitude and phase dynamics in oscillators with distributed-delay coupling. Philosophical Transactions of the Royal Society A, 371 (1999), 20120466.

[Kyr14] Kyrychko, Y.N., Blyuss, K.B., Schöll, E., (2014). Synchronization of networks of oscillators with distributed delay coupling. Chaos: An Interdisciplinary Journal of Nonlinear Science, 24(4), 043117.

[Lal04] Lalonde, S., Wipf, D., & Frommer, W. B. (2004). Transport mechanisms for organic forms of carbon and nitrogen between source and sink. Annual Reviews, Plant Biology, 55, 341-372.

[Lee05] Lee, Y. M., Tscherne, D. M., Yun, S. I., Frolov, I., & Rice, C. M. (2005). Dual mechanisms of pestiviral superinfection exclusion at entry and RNA replication. Journal of virology, 79(6), 3231–3242.

[Lev04] Levin, S. A., Dushoff, J., & Plotkin, J. B. (2004). Evolution and persistence of influenza A and other diseases. Mathematical biosciences, 188(1), 17–28.

[Lia12] Liang, D., White, R.G., & Waterhouse, P.M., (2012). Gene silencing in *Arabidopsis* spreads from the root to the shoot, through a gating bar-

rier, by template-dependent, nonvascular, cell-to-cell movement. Plant physiology, 159(3), 984–1000.

[Lip01] Lipardi, C., Wei, Q., & Paterson, B. M. (2001). RNAi as random degradative PCR: siRNA primers convert mRNA into dsRNAs that are degraded to generate new siRNAs. Cell, 107(3), 297-307.

[Lip07] Lipsitch, M., & O'Hagan, J. J. (2007). Patterns of antigenic diversity and the mechanisms that maintain them. Journal of the Royal Society Interface, 4(16), 787–802.

[Lla00] Llave, C., Kasschau, K. D., & Carrington, J. C. (2000). Virus-encoded suppressor of post-transcriptional gene silencing targets a maintenance step in the silencing pathway. Proceedings of the National Academy of Sciences, 97(24), 13401–13406.

[Mad00] Madden, L.V., Jeger, M.J., & van den Bosch, F. (2000) A theoretical assessment of the effects of vector-virus transmission mechanism on plant virus disease epidemics. Phytopathology, 90, 576–594.

[Mak02] Makeyev, E. V., & Bamford, D. H. (2002). Cellular RNA-dependent RNA polymerase involved in posttranscriptional gene silencing has two distinct activity modes. Molecular cell, 10(6), 1417–1427.

[Man13] Mandadi, K. K., & Scholthof, K. B. G. (2013). Plant immune responses against viruses: how does a virus cause disease?. The Plant Cell, 25(5), 1489–1505.

[Mal09] Malapi-Nelson, M., Wen, R. H., Ownley, B. H., & Hajimorad, M. R. (2009). Co-infection of soybean with Soybean mosaic virus and Alfalfa

mosaic virus results in disease synergism and alteration in accumulation level of both viruses. Plant Disease, 93(12), 1259–1264.

[Mar12] Marsden, J. E., & McCracken, M. (1976). The Hopf Bifurcation and Its Applications.Springer-Verlag, New York, 1976.

[Mat92] Matthews, R.E.F. (1992). Fundamentals of Plant Virology.

[Mau10] Mauck, K. E., De Moraes, C. M., & Mescher, M. C. (2010). Deceptive chemical signals induced by a plant virus attract insect vectors to inferior hosts. Proceedings of the National Academy of Sciences, 107(8), 3600–3605.

[Mcc10] McCluskey, C.C., 2010. Global stability of an SIR epidemic model with delay and general nonlinear incidence. Mathematical Biosciences and Engineering. 7(4), 837–850.

[Mel11] Melnyk, C. W., Molnar, A., & Baulcombe, D. C. (2011). Intercellular and systemic movement of RNA silencing signals. The EMBO journal, 30(17), 3553–3563.

[Min42] Minorsky, N. (1942). Self-excited oscillations in dynamical systems possessing retarded actions. ASME Journal of Applied Mechanics, 9, 65–71.

[Mit02] Mitsuhara, I., Shirasawa-Seo, N., Iwai, T., Nakamura, S., Honkura, R., & Ohashi, Y. (2002). Release from post-transcriptional gene silencing by cell proliferation in transgenic tobacco plants: possible mechanism for noninheritance of the silencing. Genetics, 160(1), 343–352.

[Mol11] Molnar, A., Melnyk, C., & Baulcombe, D. C. (2011). Silencing signals in plants: a long journey for small RNAs. Genome biology, 12(1), 1.

[Mor13] Moreno-Delafuente, A., Garzo, E., Moreno, A., & Fereres, A. (2013). A plant virus manipulates the behavior of its whitefly vector to enhance its transmission efficiency and spread. PLoS One, 8(4), e61543.

[Nap90] Napoli, C., Lemieux, C., & Jorgensen, R. (1990). Introduction of a Chimeric Chalcone Synthase Gene into Petunia Results in Reversible Co-Suppression of Homologous Genes in trans. The Plant Cell, 2(4), 279–289.

[Nik07] Nikolov, S., & Petrov, V. (2007). Time delay model of RNA silencing. Journal of Mechanics in Medicine and Biology, 7(03), 297–314.

[Nik09] Nikolov, S., Lai, X., Wolkenhauer, O., & Vera, J. (2009). Time delay and protein modulation analysis in a model of RNA silencing. Communications of SIWN Journal, 6, 111–117.

[Nor73] Norkin, S. B. (1973). Introduction to the theory and application of differential equations with deviating arguments, 105.

[Opa98] Opalka, N., Brugidou, C., Bonneau, C., Nicole, M., Beachy, R. N., Yeager, M., & Fauquet, C. (1998). Movement of *rice yellow mottle virus* between xylem cells through pit membranes. Proceedings of the National Academy of Sciences, 95(6), 3323–3328.

[Pak12] Pak, J., Maniar, J. M., Mello, C. C., & Fire, A. (2012). Protection from feed-forward amplification in an amplified RNAi mechanism. Cell, 151(4), 885–899.

[Pal97] Palauqui, J.-C., Elmayan, T., Pollien, J.-M., & Vaucheret, H., (1997). Systemic acquired silencing: transgene-specific post-transcriptional silencing is transmitted by grafting from silenced stocks to non-silenced scions. The EMBO Journal 16 (15), 4738–4745.

[Pai12] Paine, C. E., Marthews, T. R., Vogt, D. R., Purves, D., Rees, M., Hector, A., & Turnbull, L. A. (2012). How to fit nonlinear plant growth models and calculate growth rates: an update for ecologists. Methods in Ecology and Evolution, 3(2), 245–256.

[Pen01] Pennazio, S., Roggero, P., & Conti, M. (2001). A history of plant virology. Cross protection. The new microbiologica, 24(1), 99–114.

[Per99] Perelson, A. S., & Nelson, P. W. (1999). Mathematical analysis of HIV-1 dynamics in vivo. SIAM review, 41(1), 3–44.

[Per02] Perelson, A. S. (2002). Modelling viral and immune system dynamics. Nature Reviews Immunology, 2(1), 28–36.

[Pér15] Pérez-Losada, M., Arenas, M., Galán, J. C., Palero, F., & González-Candelas, F. (2015). Recombination in viruses: mechanisms, methods of study, and evolutionary consequences. Infection, Genetics and Evolution, 30, 296-307.

[Poi92] Poincaré, H. (1892). Les Méthodes Nouvelles de ka Mécanique Céleste Vol. 1, Gauthier-Villars, Paris.

[Pru97] Pruss, G., Ge, X., Shi, X. M., Carrington, J. C., & Vance, V. B. (1997). Plant viral synergism: the potyviral genome encodes a broad-range

pathogenicity enhancer that transactivates replication of heterologous viruses. The Plant Cell, 9(6), 859–868.

[Pum13] Pumplin, N., & Voinnet, O. (2013). RNA silencing suppression by plant pathogens: defence, counter-defence and counter-counter-defence. Nature Reviews Microbiology, 11(11), 745–760.

[Pur05] Purcell, A.H., Almeida, R.P.P., (2005). Insects as vectors of disease agents. Encyclopedia of plant and crop science, 5.

[Raa04] Raab, R. M., & Stephanopoulos, G. (2004). Dynamics of gene silencing by RNA interference. Biotechnology and Bioengineering, 88(1), 121–132.

[Rah15] Rahman, B., Blyuss, K. B., & Kyrychko, Y. N. (2015). Dynamics of neural systems with discrete and distributed time delays. SIAM Journal on Applied Dynamical Systems, 14(4), 2069–2095.

[Raj08] Raja, P., Sanville, B. C., Buchmann, R. C., & Bisaro, D. M. (2008). Viral genome methylation as an epigenetic defense against geminiviruses. Journal of virology, 82(18), 8997–9007.

[Rat99] Ratcliff, F. G., MacFarlane, S. A., & Baulcombe, D. C. (1999). Gene silencing without DNA: RNA-mediated cross-protection between viruses. The Plant Cell, 11(7), 1207–1215.

[Rec09] Recker, M., Blyuss, K. B., Simmons, C. P., Hien, T. T., Wills, B., Farrar, J., & Gupta, S. (2009). Immunological serotype interactions and their effect on the epidemiological pattern of dengue. Proceedings of the Royal Society of London B: Biological Sciences.

[Red12] Reddy, R. C., Dong, W., Njock, T., Rey, M. E. C., & Fondong, V. N. (2012). Molecular interaction between two *cassava geminiviruses* exhibiting cross-protection. Virus research, 163(1), 169–177..

[Ric03] Richard, J.-P. (2003). Time-delay systems: an overview of some recent advances and open problems. Automatica, 39(10), 1667–1694.

[Rob07] Roberts, M. G., & Heesterbeek, J. A. P. (2007). Model-consistent estimation of the basic reproduction number from the incidence of an emerging infection. Journal of mathematical biology, 55(5-6), 803–816.

[Rod11] Rodrigo, G., Carrera, J., Jaramillo, A., & Elena, S. F. (2011). Optimal viral strategies for bypassing RNA silencing. Journal of The Royal Society Interface, 8(55), 257–268.

[Roj14] Rojas, C. M., Senthil-Kumar, M., Tzin, V., & Mysore, K. (2014). Regulation of primary plant metabolism during plant-pathogen interactions and its contribution to plant defense. Frontiers in plant science, 5(17).

[Rom92] Romano, N., & Macino, G. (1992). Quelling: transient inactivation of gene expression in Neurospora crassa by transformation with homologous sequences. Molecular microbiology, 6(22), 3343–3353.

[Roo05] Roossinck, M. J. (2005). Symbiosis versus competition in plant virus evolution. Nature Reviews Microbiology, 3(12), 917–924.

[Rot04] Roth, B. M., Pruss, G. J., & Vance, V. B. (2004). Plant viral suppressors of RNA silencing. Virus research, 102(1), 97–108.

[Rua01] Ruan, S., & Wei, J. (2001). On the zeros of a third degree exponential polynomial with applications to a delayed model for the control of testosterone secretion. Mathematical Medicine and Biology, 18(1), 41–52.

[Sav12] Savary, S., Ficke, A., Aubertot, J. N., & Hollier, C. (2012). Crop losses due to diseases and their implications for global food production losses and food security. Food Security, 4(4), 519–537.

[Sil02] Silva, J. M., Hammond, S. M., & Hannon, G. J. (2002). RNA interference: a promising approach to antiviral therapy?. Trends in molecular medicine, 8(11), 505–508.

[Sij00] Sijen, T., & Kooter, J. M. (2000). Post-transcriptional gene-silencing: RNAs on the attack or on the defense?. Bioessays, 22(6), 520–531.

[Sij01] Sijen, T., Fleenor, J., Simmer, F., Thijssen, K. L., Parrish, S., Timmons, L., ... & Fire, A. (2001). On the role of RNA amplification in dsRNA-triggered gene silencing. Cell, 107(4), 465-476.

[Smi03] Smith, H. L., & De Leenheer, P. (2003). Virus dynamics: a global analysis. SIAM Journal on Applied Mathematics, 63(4), 1313–1327.

[Son00] Sonoda, S., & Nishiguchi, M. (2000). Delayed activation of post-transcriptional gene silencing and de novo transgene methylation in plants with the coat protein gene of sweet potato feathery mottle potyvirus. Plant Science, 156(2), 137–144.

[Sch13] Schultz, J. C., Appel, H. M., Ferrieri, A., & Arnold, T. M. (2013). Flexible resource allocation during plant defense responses. Frontiers in plant science, 4(324).

[Sha13] Sharma, N., Sahu, P. P., Puranik, S., & Prasad, M. (2013). Recent advances in plant–virus interaction with emphasis on small interfering RNAs (siRNAs). Molecular biotechnology, 55(1), 63–77.

[SiL11] Simon-Loriere, E., & Holmes, E. C. (2011). Why do RNA viruses recombine? Nature Reviews Microbiology, 9(8), 617–626.

[Smi95] Smith, H.L., (1995). Monotone dynamical systems: an introduction to the theory of competitive and cooperative systems, 41. American Mathematical Society.

[Smi11] Smith, H., (2011). An introduction to delay differential equations with applications to life sciences, 57. Springer Science & Business Media.

[Sof07] Soifer, H. S., Rossi, J. J., & Sætrom, P. (2007). MicroRNAs in disease and potential therapeutic applications. Molecular Therapy, 15(12), 2070–2079.

[Sto62] Stokes, A. (1962). A Floquet theory for functional differential equation. Proceedings of The National Academy of Sciences, 48(8), 1330–1334.

[Str05] Strange, R.N., Scott, P.R., (2005). Plant disease: a threat to global food security. Annual Reviews, Phytopathology, 43, 83–116.

[Sut99] Sutic, D. D., Ford, R. E., & Tosic, M. T. (1999). Handbook of plant virus diseases. CRC Press.

[Tak04] Takeshita, M., Shigemune, N., Kikuhara, K., Furuya, N., & Takanami, Y. (2004). Spatial analysis for exclusive interactions between subgroups I and II of *Cucumber mosaic virus* in cowpea. Virology, 328(1), 45–51.

[Tak05] Takeshita, M. (2005). Molecular biological study of host specificity and cross-protection of *Cucumber mosaic virus*. Journal of General Plant Pathology, 71(6), 459–459.

[Tas13] Taşkin, H., Baktemur, G., Kurul, M., & Büyükalaca, S., (2013). Use of tissue culture techniques for producing virus-free plant in garlic and their identification through real-time PCR. The Scientific World Journal, 781282.

[Ten01] Tenllado, F., & Díaz-Ruízâ J.R., (2001). Double-stranded RNA-mediated interference with plant virus infection. Journal of virology, 75(24), 12288–12297.

[Tia03] Tian, D., Traw, M. B., Chen, J. Q., Kreitman, M., & Bergelson, J. (2003). Fitness costs of R-gene-mediated resistance in Arabidopsis thaliana. Nature, 423(6935), 74–77.

[Tri10] Tridane, A., & Kuang, Y. (2010). Modeling the interaction of cytotoxic T lymphocytes and influenza virus infected epithelial cells. Mathematical Biosciences and Engineering, 7(1), 171–185.

[Van96] van den Bosch, F., & de Roos, A. M. (1996). The dynamics of infectious diseases in orchards with roguing and replanting as control strategy. Journal of Mathematical Biology, 35(2), 129–157.

[Vau01] Vaucheret, H., Béclin, C., & Fagard, M., (2001). Post-transcriptional gene silencing in plants. Journal of cell science, 114(17), 3083–3091.

[Yua14] Yuan, Y., & Bélair, J. (2014). Threshold dynamics in an SEIRS model with latency and temporary immunity. Journal of mathematical biology, 69(4), 875–904.

[Zha00a] Zhang, X. S., Holt, J., & Colvin, J. (2000). A general model of plant-virus disease infection incorporating vector aggregation. Plant Pathology, 49(4), 435–444.

[Zha00b] Zhang, X. S., Holt, J., & Colvin, J. (2000). Mathematical models of host plant infection by helper-dependent virus complexes: Why are helper viruses always avirulent?. Phytopathology, 90(1), 85–93.

[Zha01] Zhang, X. S., & Holt, J. (2001). Mathematical models of cross protection in the epidemiology of plant-virus diseases. Phytopathology, 91(10), 924–934.

[Zha08] Zhang, F., Li, Z. Z., & Zhang, F. (2008). Global stability of an SIR epidemic model with constant infectious period. Applied Mathematics and Computation, 199(1), 285–291.

[Zha10] Zhang, J.-Z., Wang, J.-J., & Su, T.-X. (2010). Bifurcation analysis of a delayed SIR model. International Conference on Computer Application and System Modeling 2010, 12, 593-596.

[Zha12a] Zhang, T., Meng, X., Song, Y., & Li, Z., (2012). Dynamical analysis of delayed plant disease models with continuous or impulsive cultural control strategies. Abstract and Applied Analysis. 2012, 1–25.

[Zha12b] Zhang, C., & Ruvkun, G. (2012). New insights into siRNA amplification and RNAi. RNA biology, 9(8), 1045-1049.

[Zho12] Zhou, C., & Zhou, Y. (2012). Strategies for viral cross protection in plants. Antiviral Resistance in Plants: Methods and Protocols, 894, 69–81.

[Zve12] Zvereva, A. S., & Pooggin, M. M. (2012). Silencing and innate immunity in plant defense against viral and non-viral pathogens. Viruses, 4(11), 2578–2597.

[Wan15] Wan, J., Cabanillas, D. G., Zheng, H., & Laliberté, J. F. (2015). *Turnip mosaic virus* moves systemically through both phloem and xylem as membrane-associated complexes. Plant physiology, 167(4), 1374–1388.

[Was00] Wassenegger, M., 2000. RNA-directed DNA methylation. Plant Molecular Biology 43, 203–220.

[Wat99] Waterhouse, P. M., Smith, N. A., & Wang, M. B. (1999). Virus resistance and gene silencing: killing the messenger. Trends in plant science, 4(11), 452–457.

[Wat01] Waterhouse, P. M., Wang, M. B., & Lough, T. (2001). Gene silencing as an adaptive defence against viruses. Nature, 411(6839), 834–842.

[Weg07] Wege, C., & Siegmund, D. (2007). Synergism of a DNA and an RNA virus: enhanced tissue infiltration of the *begomovirus Abutilon mosaic virus* (AbMV) mediated by *Cucumber mosaic virus* (CMV). Virology, 357(1), 10–28.

[Wei08] Wei, C., & Chen, L. (2008). A Delayed Epidemic Model with Pulse Vaccination. Discrete Dynamics in Nature and Society, 2008, 1-12.

[Wod02] Wodarz, D., Christensen, J.P.,& Thomsen, A.R., (2002). The importance of lytic and nonlytic immune responses in viral infections. Trends in Immunology, 23(4), 194–200.

Appendix A

Auxiliary results

Theorem A.0.1 (Comparison theorem for differential equations)**.**

Suppose

$$\dot{y}(t) \leq a - by(t), \qquad y(0) = y_0, \tag{A.1}$$

it follows that

$$\limsup_{t \to +\infty} y(t) \leq \frac{a}{b},$$

where $a \in \mathbb{R}$, and b is a positive constant.

Proof. Multiply both sides of (A.1) with the integrating factor e^{bt}. Solving this inequality yields $y(t) \leq \frac{a}{b} + (y_0 - a/b)e^{-bt}$, and

$$\lim_{t \to +\infty} ce^{-bt} \to 0,$$

which concludes the proof. □

Theorem A.0.2 (Positivity of solutions for non-autonomous systems, Theorem 5.2.1 in [**Smi95**])**.**

Define the Banach space $C = \mathrm{C}([-\tau_{\max}, 0], \mathbb{C}^{\mathrm{n}})$ *which contains the cone* $C_+ = \{\phi \in C : \phi(\theta) \geq 0, -\tau_{max} \leq \theta \leq 0)\}$.

Consider the system

$$y'(t) = f(y, y_t)$$

where $f : \mathbb{R} \times \mathrm{D} \to \mathbb{R}^n$ *is continuous,* $D \subset C$ *is open and* f *is Lipschitz in its second argument on each compact subset of* $\mathbb{R} \times \mathrm{D}$ *so that initial value problems associated with the system above have unique solutions and that* $C_+ \cap \mathrm{D}$ *is non-empty.*

Assume that whenever $\phi \in \mathrm{D}$ *satisfies* $\phi \geq 0$, $\phi_i = 0$ *for some* i *and* $t \in \mathbb{R}$, *then* $f_i(t, \phi) \geq 0$. *If* $\phi \in \mathbb{D}$ *satisfies* $\phi \geq 0$ *and* $t_0 \in \mathbb{R}$, *then* $y(t, t_0, \phi) \geq 0$ *for all* $t \geq t_0$ *in its maximal interval of existence.*

Proposition A.0.3 (Boundedness of solutions of the delayed logistic equation, Proposition 5.13 in [**Smi11**])**.**

Every orbit of the discrete-delay logistic equation given by

$$N'(t) = N(t)[1 - N(t - \tau)], \qquad t \geq 0,$$

with initial data $\phi : [-\tau, 0] \to \mathbb{R}$ *and* $\phi \geq 0$ *is bounded. Additionally, for each such* ϕ, *there exists* $T > 0$ *such that*

$$0 \leq N(t, \phi) \leq e^{\tau}, \qquad t > T.$$